The Design and Construction of a High Bandwidth Proportional Fuel Injection System for Liquid Fuel Active Combustion Control

by
Ernest E. Lagimoniere, Jr.

Thesis submitted to the Faculty of the Virginia
Polytechnic and State University as partial fulfillment of
the requirements for the degree of

Master of Science
in
Mechanical Engineering

Approved:

_____
William R. Saunders

_____ _____
Uri Vandsburger Donald J. Leo

August 21, 2000

Blacksburg, Virginia

Keywords: Thermo-acoustic Instabilities, Active Combustion Control, Fuel Modulation, Proportional Fuel Injection, Piezo-ceramic actuator

The Design and Construction of a High Bandwidth Proportional Fuel Injection System for Liquid Fuel Active Combustion Control

Ernest E. Lagimoniere, Jr.
Virginia Polytechnic Institute and State University
Advisor: Dr. William R. Saunders, Chair

Abstract:

This last decade experienced a sudden increase of interest in the control of thermo-acoustic instabilities, in particular through the use of fuel modulation techniques. The primary goal of this research was to design, construct and characterize a high bandwidth proportional fuel injection system, which could be used to study the effect of specific levels of fuel modulation on the combustion process and the reduction of thermo-acoustic instabilities. A fuel injection system, incorporating the use of a closed loop piston and check valve, was designed to modulate the primary fuel supply of an atmospheric liquid-fueled swirl stabilized combustor operating at a mean volumetric fuel flow rate of 0.4 GPH. The ability of the fuel injection system to modulate the fuel was examined by measuring the fuel line pressure and the flow rate produced during operation. The authority of this modulation over the combustion process was investigated by examining the effect of fuel modulation on the combustor pressure and the heat release of the flame. Sinusoidal operation of the fuel injection system demonstrated: a bandwidth greater that 800 Hz, significant open loop authority (averaging 12 dB) with regards to the combustor pressure, significant open loop authority (averaging 33 dB) with regards to the unsteady heat release rate and an approximate 8 dB reduction of the combustor pressure oscillation present at 100 Hz, using a phase shift controller. It is possible to scale the closed loop piston and check valve configuration used to create the fuel injection system discussed in this work to realistic combustor operating conditions for further active combustion control studies.

Acknowledgements

I would like to warmly thank all the people who have helped me with this work:

I would like to specifically thank the senior design class that worked side by side with me on this project for its first year.

The entire VACCG group has at some point offered advice or assistance to me, for which I am very grateful. I would, however, specifically like to thank Denzil who was always willing to help me better understand and work on his combustor rig.

I would also like to thank Matt, Anna, Noah and Aaron for their help, discussion and company. They are all quality people and it has been enjoyable and rewarding to work with them.

I would like to thank Dr. Saunders for not letting me squeak out of here without putting up a fight. His positive attitude and high expectations gave me a better appreciation for this work and his character.

I would especially like to thank my wife and daughter for giving me the motivation to complete this project. They are my light and their smiles make my life worthwhile.

I cannot forget to thank my parents, whose love and support have encouraged me through the years and who always pushed me to do my best.

Most importantly, I would like to thank my Father in heaven who has given me my life and holds me in his hand.

Table of Contents

List of Figures

List of Tables

Nomenclature

R	Rayleigh index
P	pressure
q	heat release
Q	volumetric flow rate
t	time
T	period
$\%_{Qpeak}$	percent modulation (see Section 1.3)
V	volume, voltage
ω	frequency (rad/s)
f	frequency (Hz)
x	displacement
F	force
k	mechanical stiffness
i	current
C	capacitance
m	mass
ζ	damping ratio
K	compensator
K_p	proportional gain
Δ	change
$\frac{d\bullet}{dt}$	time rate of change of $\bullet$
$\frac{\delta\bullet}{\delta\circ}$	partial derivative of $\bullet$ with respect to $\circ$

Glossary of Super and Subscripts

Q_{ss}	steady state volumetric flow rate
Q_{peak}	peak volumetric flow rate
Q_{trough}	trough volumetric flow rate
V_{strain}	strain related voltage
V_{noise}	noise related voltage
V_i	voltage proportional to current
x_{max}	maximum displacement
f_n	natural frequency
T_r	rise time
d_{piston}	piston diameter
z’	unsteady component of z

1 Introduction

This last decade has seen a sudden increase of interest in the control of thermo-acoustic instabilities, in particular through the use of fuel modulation techniques. This increase can be attributed to the fact that thermo-acoustic instabilities have become more frequent and problematic as engines operate at higher temperatures and are met with more stringent pollution requirements. The gas turbine industry, faced with a strict new requirement regarding the emissions of nitrogen oxides of less than 25 ppm, have implemented the use of lean pre-mixed flames to reduce operating temperatures and thus the level of production of these nitrogen oxides. These lean pre-mixed combustors are especially prone to produce thermo-acoustic instabilities. The jet engine industry, in order to increase the performance and efficiency of its engines, is constantly trying to increase the temperature of the combustion process. The elevated temperatures created in high performance jet engines are also prone to promote thermo-acoustic instabilities. Thermo-acoustic instabilities present a concern for these industries for several reasons. The large pressure oscillations associated with thermo-acoustic instabilities, on the order of 10% of the mean combustor pressure, disrupts the combustion process limiting the power development, produces high-cycle fatigue and possibly failure of the combustor and turbine components, and can cause the combustion process to be extinguished. These consequences can be catastrophic for both the gas turbine and jet engine applications.

Efforts of the Virginia Active Combustion Control Group (VACCG), to date, have included the study of active combustion control on a laminar lean pre-mixed Rijke tube combustor. This is a very simple combustor specifically designed to induce a thermo-acoustic instability. Active combustion control experiments using a speaker [36,38] and fuel modulation [34] have been performed on this rig providing valuable information regarding the control of thermo-acoustic instabilities. Recently, a rig was built and characterized to begin the exploration of active combustion control for a more complex combustion process. This new combustor is liquid fueled and swirl stabilized, producing a flame structure more like those found in actual combustion applications. To explore the

effect of fuel modulation on the control of the instability required a fuel injection control system.

Because the results of research work involving the active control of combustion instabilities using fuel modulation has, to date, been limited by the effectiveness of the existing fuel injection systems [23] we were motivated to design and construct a specialized type of fuel injection system. We desired this fuel injection system to have a high bandwidth to accommodate the present needs as well as provide the performance that may be necessary in future exploration. It was also desired that the fuel injection system could modulate the flow in a proportional manner both to explore how this type of modulation interacts with the combustion process and to allow the comparison of proportional and pulsed fuel control. This fuel injection system would not only be used to try to eliminate the thermo-acoustic instability, but also to study the effect of different levels of modulation on the combustion process.

1.1 Thermo-acoustic instabilities

In order to appreciate this work, it is necessary to have at least a cursory understanding of what a thermo-acoustic instability is and how they occur.

1.1.1 Rayleigh Criteria

The conditions necessary to create a thermo-acoustic instability have been understood for over a century. Lord Rayleigh, in 1878, was the first to scientifically explain the nature of the interaction between heat release and acoustic waves. A convenient mathematical representation of this relationship can be seen in Equation 1.1.

$$R = \int_0^T P'(t)q'(t)dt \qquad (1.1)$$

where T is the period of oscillation, P' is the unsteady component of pressure, q' is the unsteady component of heat release rate and R is the Rayleigh index. The value of the Rayleigh index predicts the growth or decay of pressure oscillations. A positive Rayleigh index indicates that the pressure oscillations will be amplified while a negative index indicates that the pressure oscillations will be attenuated. This relationship holds as a general description at any point in space and applies to the each point in the volume of a

combustor where acoustics and heat release can effect each other in a self-excited loop, as can be seen in Figure 1.1.

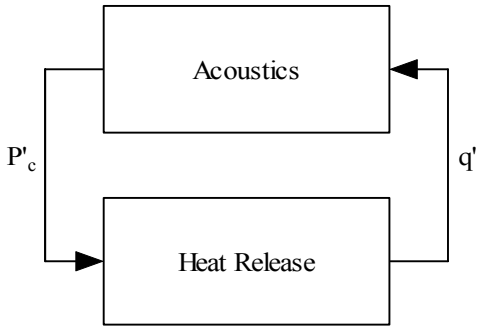

Figure 1.1 Self excited loop in combustor

If the flame present in the combustor is located at a point where the acoustics combine to produce a positive Rayleigh index, a thermo-acoustic instability will result. From a controls perspective, one could think of the acoustics and heat release simply as dynamic systems. If the closed loop poles of the system shown in Figure 1.1 are in the left half plane the system will be stable, and if the poles are in the right half plane the system will be unstable. Thus, a positive Rayleigh index corresponds to closed loop poles in the right half plane and a negative Rayleigh index corresponds to closed loop poles in the left half plane.

1.1.2 Limit Cycle Behavior

If this system were entirely linear in its nature and the Rayleigh index was positive, the magnitude of the pressure oscillations would increase infinitely. Because of the inherent nonlinearity of any physical system this result can never be physically realized. At some point in the growth of the pressure oscillations associated with a positive Rayleigh index, a limit cycle will be reached and the magnitude of the pressure oscillations will not grow any larger. The presence of this limit cycling behavior is the manifestation of a thermo-acoustic instability. The magnitude of the limit cycles associated with thermo-acoustic instabilities are typically on the order of 10% of the combustors mean operating pressure [4,18].

1.2 Methods of control

Methods of control for these combustion instabilities can be divided into two categories, passive and active. Both of these methods have received attention and have met with some success in reducing magnitudes of the pressure oscillations associated with thermo-acoustic instabilities. Passive control strategies can be effective but require a very accurate understanding of the performance of the system and the frequency of instability before implemention. One passive strategy involves installing a Hemholtz resonator that is tuned to the frequency of the instability, essentially taking the gain out of the combustor acoustics at the frequency of instability, which then results in a negative Rayleigh index. This method can be effective, however, small changes in the limit cycle frequency will dramatically lessen its effectiveness [8]. Simply changing the position of the fuel injector can eliminate an instability by introducing the heat release at a physical location where the Rayleigh index is negative. This technique has been limited in its effectiveness and to date has been a matter of trial and error [37].

Active control strategies have been explored to allow more flexibility in the control process. Active combustion control techniques involve interacting with the combustion process through the combustor pressure or unsteady heat release. Mechanical shakers and acoustic drivers placed in the combustor can be used to influence the combustor pressure, allowing the adjustment of the relative phase of the pressure and heat release, so as to reduce the magnitude of an instability. This technique has been limited by the ability of shakers and speakers to influence the large pressure oscillations present in full-scale combustors. Thus, the primary method for active control of combustion instabilities has involved the incorporation of a fuel modulation system. This method involves interaction with the combustion process through the heat release rate, which is the effect of modulating the flow rate. This technique has met with the most success in the control of thermo-acoustic instabilities on larger combustors and thus has been the focus of research in the active combustion control community.

1.3 Definitions

At this point, it is necessary to define several terms that will be important in accurately describing the specifications for, and performance of, our fuel injection system.

Percent modulation ($\%_{Qpeak}$): In order to speak quantitatively about the level of fuel modulation, it is necessary to define what exactly the term 'modulation' refers to. For the remainder of this work, the term percent modulation will refer to the relative magnitude of the peak-to-peak oscillating component of flow rate relative to the unmodulated, steady state, flow rate. The level of flow rate modulation shown in Figure 1.2 would then be described by the relationship in Equation 1.2.

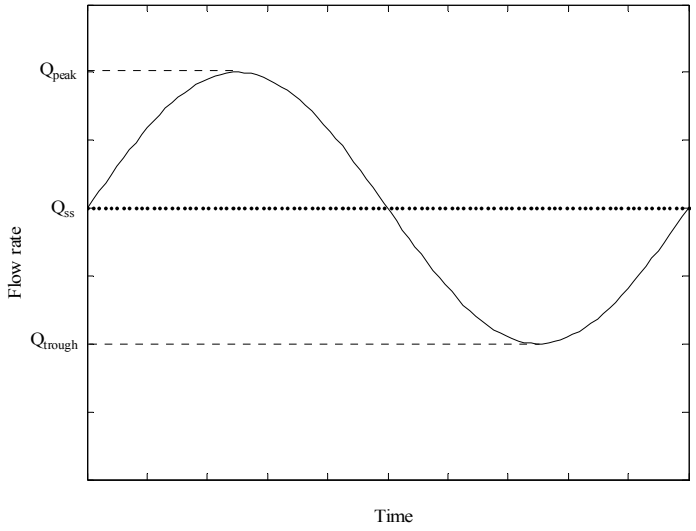

Figure 1.2 Generic flow modulation

$$\%_{Qpeak} = \frac{Q_{peak} - Q_{through}}{Q_{ss}} \tag{1.2}$$

Profile: The term profile will refer to the shape of a time signal, i.e. Figure 1.2 would thus be referred to as a flow profile.

Fuel injector: The physical device that is responsible for modulating the fuel flow.

Fuel injector controller: The physical device that provides the signals used to operate the fuel injector.

Fuel injection system: The system comprised of the fuel injector and fuel injector controller.

Combustion Control System: The control system, which includes the fuel injection system, used to control the combustion instability.

1.4 Project Goals

The main goal of this work was to design and construct a fuel injection system that could modulate the fuel flow rate for our combustor in a specific manner. It was desired that this fuel injection system be able to provide proportional modulation, not simply on/off, of the primary fuel supply and have a bandwidth and authority that is comparable to other fuel injection systems considered state-of-the-art.

We were also interested in studying the flow profile actually created by our fuel injection system, as this would allow closer study of the effect of fuel modulation on instability suppression. This knowledge could aide in the future sizing and design of fuel injection control systems.

After evaluating the ability of our fuel injection system to realize a specific flow profile, we wished to evaluate the authority the fuel injection system had over the combustion process. The quantities we were interested in measuring, as indicators of this authority, were the combustor pressure and the unsteady heat release associated with the fuel modulation.

Finally, we wished to utilize the fuel injection control system on a test combustor to determine the effectiveness of the system on attenuating the thermo-acoustic instability.

1.5 Project Overview

Chapter Two presents a summary of the work done to date involving the use of fuel modulation for the control of thermo-acoustic instabilities.

Chapter Three presents the design and construction of the fuel injection control system. First, a set of performance specifications was formed that could be used in designing the

fuel injection system. Several methods were discussed that could achieve the required performance of the fuel injector and one method was selected. The components necessary to create the fuel injector were examined and the performance specifications were then translated into physical requirements for these components. These components were designed, purchased or fabricated and assembled. The fuel injector controller was designed and created. Finally, the entire fuel injection control system was constructed. The design and construction of the fuel injector was performed along with a ME4015/4016 senior design class. This class aided in creating the performance specifications, designing and constructing the fuel injector and preliminary testing of the fuel injection system. The results of their work can be found in their final report for the class [42].

Chapter Four presents the testing involved in characterizing the performance of the fuel injection system. Testing was done on the individual components of the fuel injection system to ensure that they could provide their designed function. The fuel injector and fuel injector controller were incorporated into the fuel injection system, which was tested to evaluate the ability of the fuel injector to modulate the flow as desired.

Chapter Five presents the testing performed using the fuel injection control system. This testing examined the authority the fuel modulation had over the combustion process and the effectiveness of this system in eliminating the thermo-acoustic instability.

Chapter Six contains the conclusions found from this work and suggestions for future work.

2 Literature Review

Although much research has been performed on the study of thermo-acoustic instabilities in general, research involving the active control of thermo-acoustic instabilities is a relatively new field of study. Fuel modulation as a technique for active combustion control has only been explored in earnest over the last several decades. This chapter contains a review of the work performed to date on the control of thermo-acoustic instabilities using fuel modulation. Much of the work reviewed in this section can also be found in Richards [34].

2.1 [Hantschk et al. 1996]

Active combustion control testing was performed at the University of Munich, Germany involving a tuned fuel supply system and servo valve actuator. The combustor used in these experiments consisted of a pre-chamber and combustor section, where the fuel was injected and the flame was held on a flame holder. The experimental setup of the rig used in these experiments can be found in Figure 2.1.

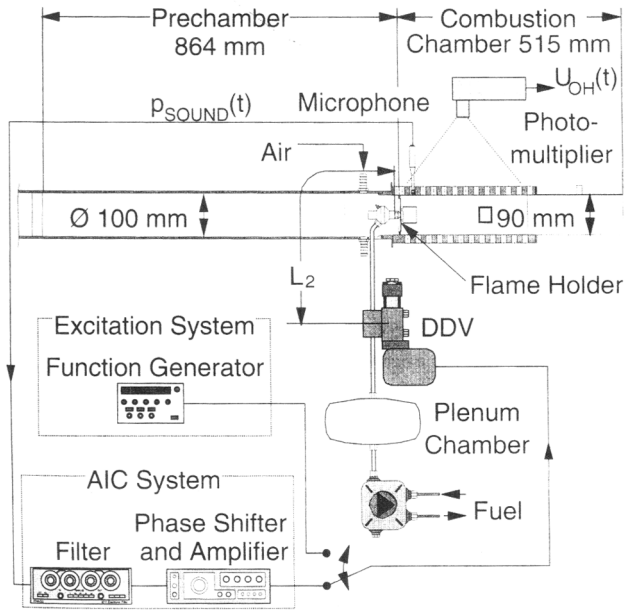

Figure 2.1 Experimental combustor rig[11]

This rig used diesel fuel at a flow rate of 11.75 kg/hr. A fuel to air ratio of 1.2 was used which provided 137 kW of thermal power. These conditions produced an instability at 275 Hz at a sound pressure level of 153 dB.

The control system implemented on this combustor consisted of a microphone located in the combustor, a phase shifting algorithm and an actuator to control the fuel flow. The actuator consisted of a high-speed servo valve made by MOOG, Germany. This direct drive valve (DDV) was equipped with a linear variable differential transformer (LVDT) that measured the position of the DDV spool. This signal was used to calculate the frequency response of the valve. The reported bandwidth of the DDV was 450 Hz. Special care was taken in the design of fuel line and fuel supply system to tune them to the instability frequency. Designing the resonant frequency of the fuel supply system to be at the instability frequency allowed the actuator to have maximum effect on the modulation of the fuel.

MOOG high-speed servo valves are becoming the industry standard for actuators in full scale active combustion control research. These DDVs can produce flow rates on the range of 1.5-26 gpm. Typical supply line pressures are on the order of 3000 psi. The reported full scale rise time of these valves are on the order of 2 ms. This corresponds to a bandwidth of 500 Hz for full scale operation. More information on MOOG servovalves is available at www.servovalve.com.

A chemiluminescence system was incorporated into the combustor to measure the unsteady heat release rate. Under control, an attenuation of 30 dB, at the 275 Hz instability frequency, and an RMS attenuation of 9 dB was obtained as can be seen in Figure 2.2.

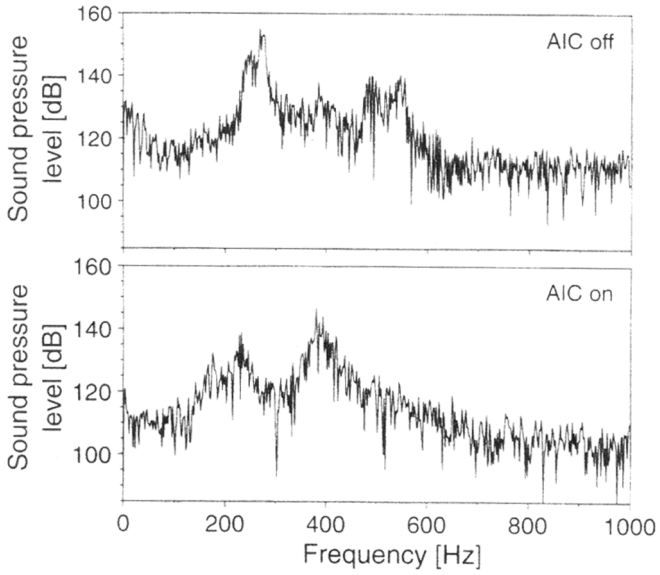

Figure 2.2 Results of instability suppression[11]

2.2 [McManus et al. 1998]

Active combustion control experiments were performed at Physical Sciences, Inc. using a solenoid valve actuator to modulate the primary fuel supply. These experiments were performed on an experimental combustor fueled by liquid heptane. These tests were performed at a nominal combustor pressure of 1.7-2 bar, air inlet temperature of 530 K, air flow rate of 150-250 gm/s and fuel flow rate of 3-4 gm/s. These operating conditions produced nominal thermal output power of 150-200 kW. A diagram of the combustor configuration can be found in Figure 2.3.

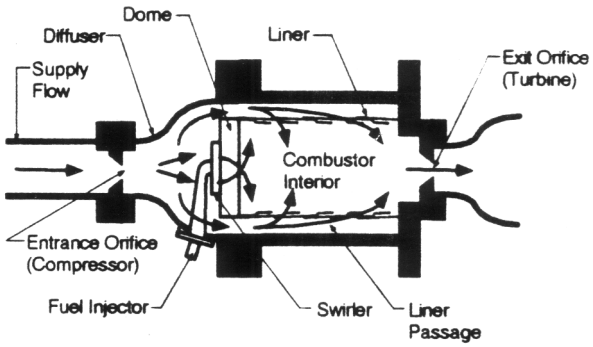

Figure 2.3 Combustor configuration for test rig[26]

An instability was encountered on this rig at about 140 Hz.

Open-loop experiments were conducted to determine the effectiveness of the fuel injection system on modulating the fuel. The actuator used in these tests was a General Valve, Series 9 valve attached to a General Valve, Iota One Solenoid Driver. This actuator modulated the primary fuel supply to the combustor. The frequency response of this fuel injection system was tested and the bandwidth of the system was reported to be 500 Hz. This was accomplished by measuring the spray density of the fuel pulses leaving the injector. The spray density of these fuel pulses was measured qualitatively by monitoring the amount of HeNe laser light that was allowed to pass through the spray field. The actuator was reported to modulate up to 10% of the total fuel flow at 200 Hz.

The unsteady heat release rate was measured using a chemiluminescence system. Open loop forcing of the system was performed during reacting flow experiments, at several frequencies, to determine the 'authority' of the actuator regarding its influence on the heat release rate. Frequency responses of the combustor pressure signal can be seen in Figure 2.4.

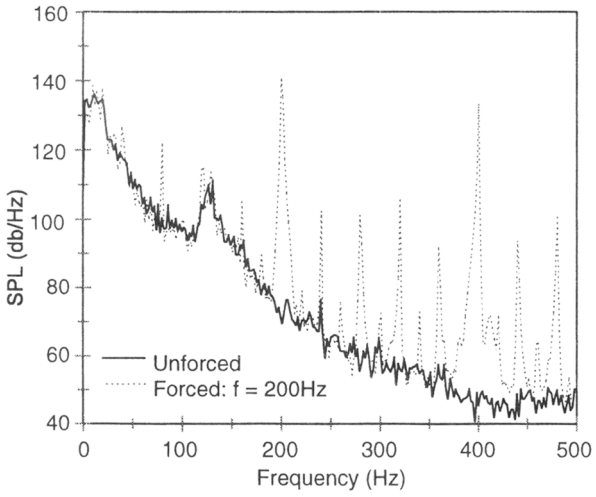

Figure 2.4 Results of forcing at 200Hz[26]

For the 200 Hz case, the fuel injection system demonstrated 20 dB of authority over the combustor pressure. This data was used to demonstrate the amount control authority that could be achieved through primary fuel modulation.

2.3 [Yu et al. 1998]

Active combustion control experiments were conducted at the Naval Air Warfare Center to investigate the effectiveness of secondary liquid fuel injection and vortex droplet interaction on the control of combustion instabilities in a dump combustor. Both gaseous and liquid fuels were used in this combustor. A premixed gaseous fuel supply of air and ethylene was fed continuously to the dump combustor. At the entrance to the dump, either ethanol or heptane was injected periodically. Different configurations of fuel type and fuel flow rates allowed the combustor to operate at two power settings, 70 and 270 kW. The combustor and control system used for this testing can be seen in Figure 2.5, along with a table summarizing the different sets of operation conditions.

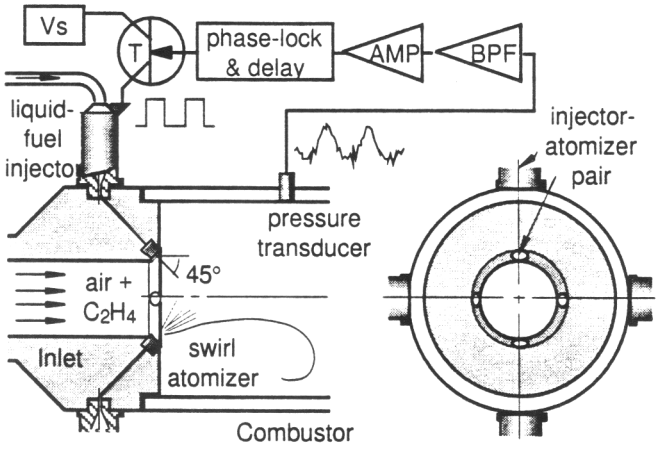

Figure 2.5 Combustor control system[38]

Table 1. Average flow conditions during unstable combustor operation.

Case	Flow Rate (g/sec)				Unstable Conditions			
	$\dot{m}_{air}$	$\dot{m}_{C_2H_4}$	$\dot{m}_{C_2H_6O}$	$\dot{m}_{C_7H_{16}}$	ϕ	$\overline{P}_{comb}/P_{exit}$	f (Hz)	$\sqrt{\overline{(p')^2}}/\overline{P}_{comb}$
1A	45	1.0	0.75	-	0.47	1.02	34	0.008
1B	45	1.3	0.75	-	0.58	N/A	35	0.005
2	146±2	5.1	-	0.73	0.59	1.59	98	0.092

* Uncertainties in the measured quantities are the same as the last digit except as noted.

Table 2.1 Summary of operating conditions[38]

It was found that for the lower power cases, 1a and 1b, there was a 35 Hz instability that was a result of both the quarter-wave mode of the inlet and the Hemholtz mode of the combustor-inlet system. When the combustor was operated at the high power configuration, an instability was produced at 100 Hz.

The control system implemented on this combustor consisted of a Kistler pressure transducer, located one inlet diameter downstream of the dump plane in the combustor, a phase shifting algorithm and four fuel injectors to control fuel supply to the combustor. These fuel injectors, Bosch Jettronics automotive fuel injectors, were mounted every 90˚ around the circumference of the dump plane. These Jettronics fuel injectors were essentially atomizers attached to solenoid valves. No information about the frequency response of these fuel injectors was given. The phase delay algorithm implemented on this combustor was unique because the delay timing was calculated such that the fuel pulses were injected with a specific phase to the shedding vortexes at the dump. This technique was used to more effectively control the local heat release rate rates within the vortices.

The best performance achieved in the controlled combustor, for the low power conditions, was a 15 dB attenuation at the instability frequency of 35 Hz. This can be seen in Figure 2.6.

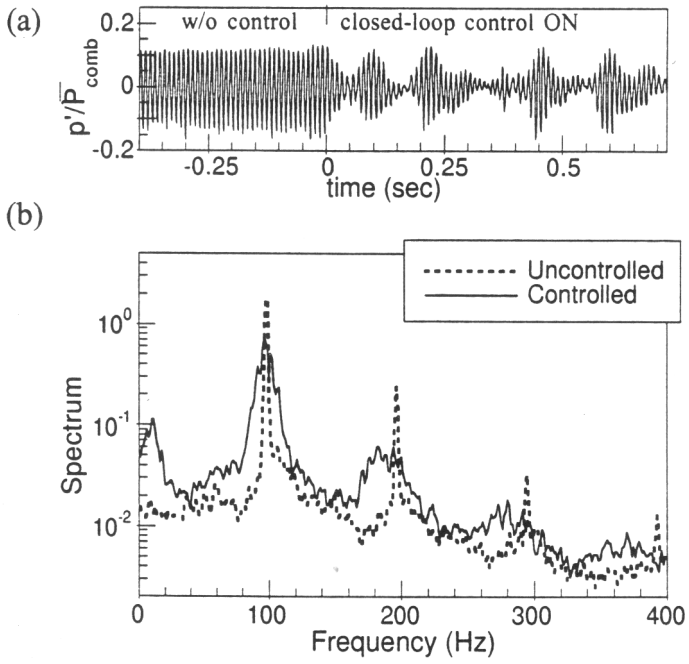

Figure 2.6 Results of combustion control at low power setting[38]

The instability encountered when the combustor was operated at the high power conditions could only temporarily be attenuated. When control began, there was an initial period of attenuation, which subsequently returned to the uncontrolled limit cycle amplitude.

2.4 [Cohen et al. 1998]

Work was done at the United Technologies Research Center to implement an active combustion control system on a 4 MW full-scale liquid fueled dump combustor. This combustor used No. 2 Diesel fuel. Testing of the combustor was performed at a mean combustor pressure of 1.56 MPa, air inlet temperature of 730 K and nominal output power of 4 MW. The setup of this rig can be found in Figure 2.7

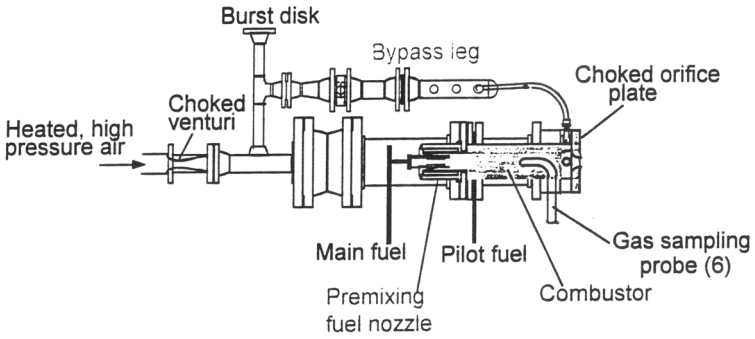

Figure 2.7 Setup of UTRC combustor rig[4]

It was found that a large amplitude instability was encountered in the range of 180–220 Hz, depending on the air-to-fuel operating ratio. This instability was attributed to the interaction of the flame dynamics with the first bulk acoustic mode of the combustor.

The control system implemented on this combustor consisted of a pressure sensor located in the combustor, a phase shifting algorithm, and a fuel injection system. The actuator on this rig modulated the fuel supply to one of six 'spokes' on the fuel nozzle head. The remaining five 'spokes' maintained a constant rate of fuel flow. A high-speed on/off solenoid valve was used for an actuator. Open loop testing showed that this actuator responded at frequencies up to 250 Hz.

An array of gas sampling probes was used to measure NO_x, and CO concentrations. A chemiluminescence measurement system was used to monitor the unsteady heat release rate. The pressure and heat release rate frequency responses for the open-loop system, using an air-to-fuel ratio of 0.51, can be found in Figure 2.8, along with the results from controlled combustion.

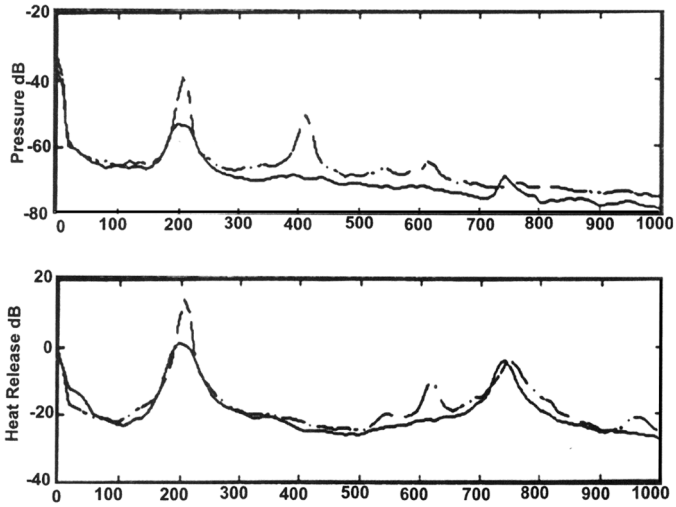

Figure 2.8 Combustor pressure and heat release rate frequency responses[4]

One can see the magnitude of the 200 Hz instability was attenuated 15 dB. Additionally, an overall RMS pressure reduction from 29.5 kPa to 11.5 kPa was reported.

2.5 [Hibshman et al. 1999]

A continuation of the work cited in Cohen et al. 1999 [4] at United Technologies Research Center, active combustion control experiments were performed on a 12MW liquid fueled sector combustor. This combustor also used No. 2 Diesel fuel. A 67.5˚ sector cut from an aeroderivative gas turbine used three fuel nozzles identical to the type that were used in experiments from Cohen et al 1999 [4]. Because of an inlet airflow limitation of the testing facility, testing was performed at a lower combustor operating pressure of 1.1 MPa. The air inlet temperature was 730 K and the fuel flow rate was nominally 460 kg/hr. This sector rig configuration can be seen in Figure 2.9.

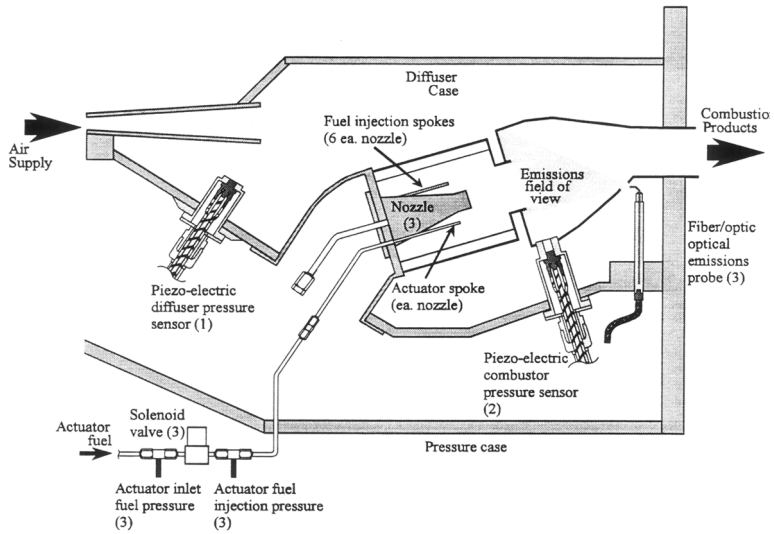

Figure 2.9 Configuration of the sector rig used at UTRC[14]

It was found that this set up produced an instability near 200 Hz. The instability exhibited a 'twin peak' behavior, with one peak at 200 Hz and the other at 230 Hz. These peaks were reported to be two bulk modes of the combustor.

The control system implemented on this sector combustor consisted of PCB pressure sensors located in the combustor, a phase shifting algorithm and a series of actuators to control fuel supply to the three fuel nozzles. For each of the three fuel nozzles, an actuator modulated the fuel supply to one of six 'spokes' on the fuel nozzle head. The remaining five 'spokes' of each fuel nozzle maintained a constant rate of fuel flow. The same fuel injectors used by Cohen et al 1999 were used in these tests. It was reported that open loop forcing of the actuator in one fuel nozzle could increase the combustor pressure spectra at the forcing frequency by 12.0 dB.

The heat release rate of the flame was measured with a chemiluminescence measurement system. An array of gas sampling probes was used to measure NO_x and CO concentrations. The best results achieved by the control system were obtained when using dual nozzle actuation as can be seen in Figure 2.10.

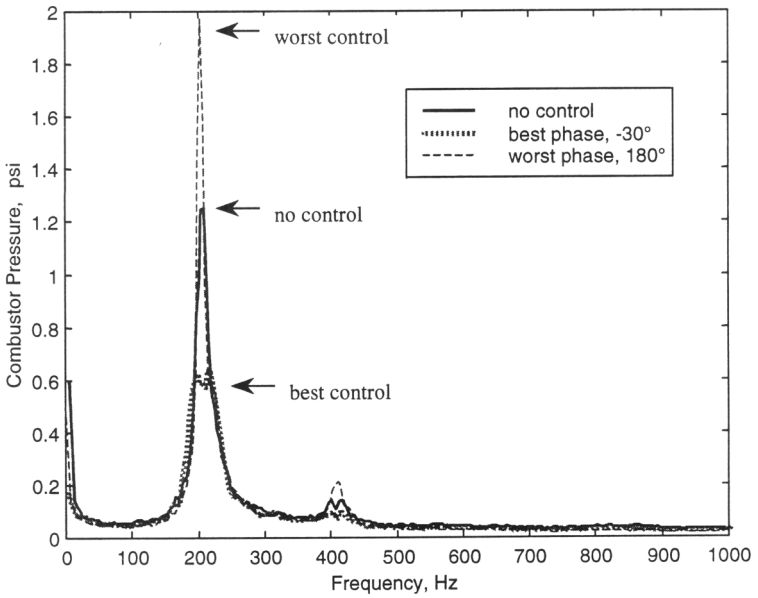

Figure 2.10 Results of controller combustion using dual nozzle actuation[14]

For this dual nozzle configuration, the magnitude of the bulk mode instabilities were attenuated 6.5 dB. Additionally, a 25% overall RMS pressure reduction was reported.

2.6 [Magill et al. 2000]

A continuation of the work cited in McManus et al 1998 [27] investigates the effectiveness of amplitude based pulse width modulation on the reduction of thermo-acoustic instabilities in a liquid fueled combustor. This experimental rig used liquid heptane for fuel. Tests were performed at a mean combustor pressure of 29 psia, air inlet temperature of 530 K, air flow rate of 350 gm/s and fuel flow rate of 30 kg/hr. These operating conditions produced a nominal thermal power output of 150-200 kW. A diagram of the combustor configuration can be found in Figure 2.11.

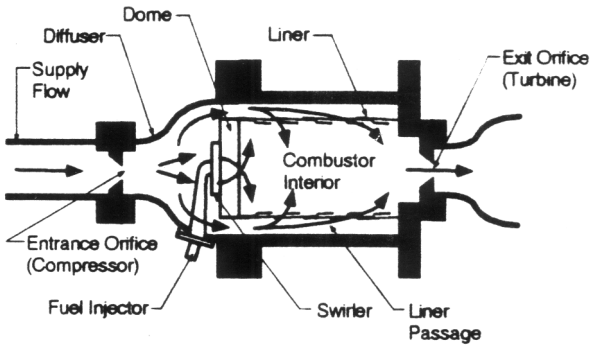

Figure 2.11 Experimental combustor configuration[23]

An instability was encountered on this rig at about 140 Hz.

The control system implemented on this combustor consisted of a PCB fast-response pressure transducer, an amplitude based pulse width modulation (PWM) controller and an actuator to control primary fuel supply through a dual stream nozzle. The (PWM) control scheme operated by detecting zero crossings of the unsteady pressure signal, adding a delay to ensure proper phasing with the heat release rate and then triggering a fuel pulse sent by the actuator. The width of the pulse was made proportional to the amplitude of the oscillating pressure component associated with the instability. This PWM technique is illustrated graphically in Figure 2.12.

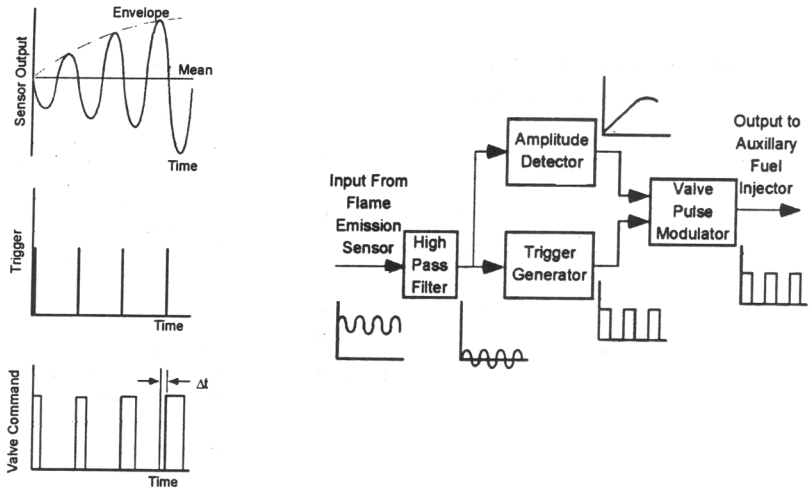

Figure 2.12 PWM technique[23]

The actuator used in these experiments was the same as the one used by McManus et al. 1998, a General Valve Series 9 valve attached to a General Valve Iota One Solenoid Driver. This actuator modulated the primary fuel supply to the combustor, which only

consisted of 28% of the total fuel flow. The remaining fuel flowed at a constant rate through a series of orifices around the periphery of the fuel injection nozzle. The frequency response of this open-loop injection system was tested and the bandwidth of the system was found to be approximately 500 Hz. The frequency response of the valve, along with its coherence, is shown in Figure 2.13 using water at 80 psig.

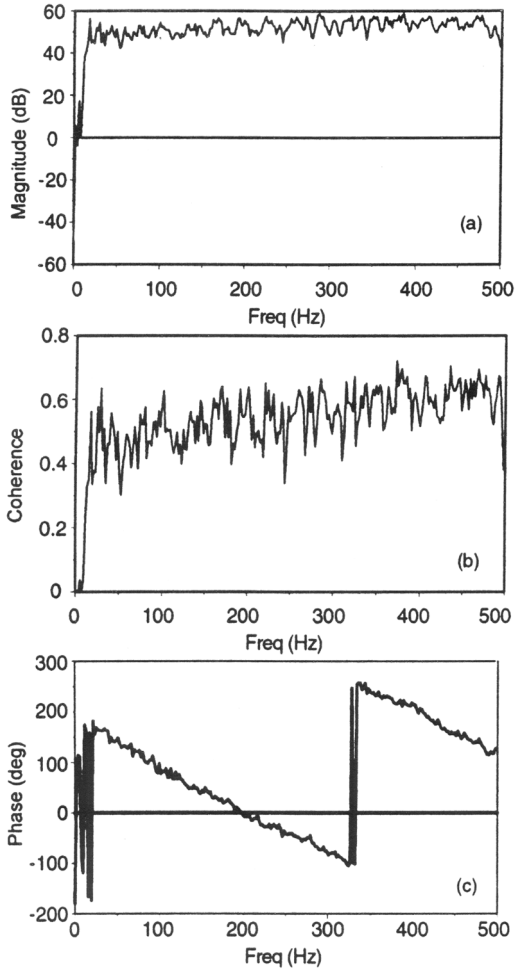

Figure 2.13 Frequency response of valve[23]

Closed loop performance of the PWM controller produced a 50% reduction in the 1psi peak-to-peak amplitude instability at 140 Hz. This limited reduction was attributed to limitation in actuator performance. It was suggested that a high-bandwidth proportional injector would be able to produce better performance than an on/off injector.

2.7 [Johnson et al. 2000]

Active combustion control experiments were conducted at Georgia Institute of Technology with the use of a fast adaptive control scheme and high bandwidth proportional fuel injector assembly (FIA). The rig used for these experiments consisted of the FIA, a conical flame holder and combustor tube. This combustor used liquid n-heptane for fuel. A diagram of the FIA and combustor can be found in Figure 2.14

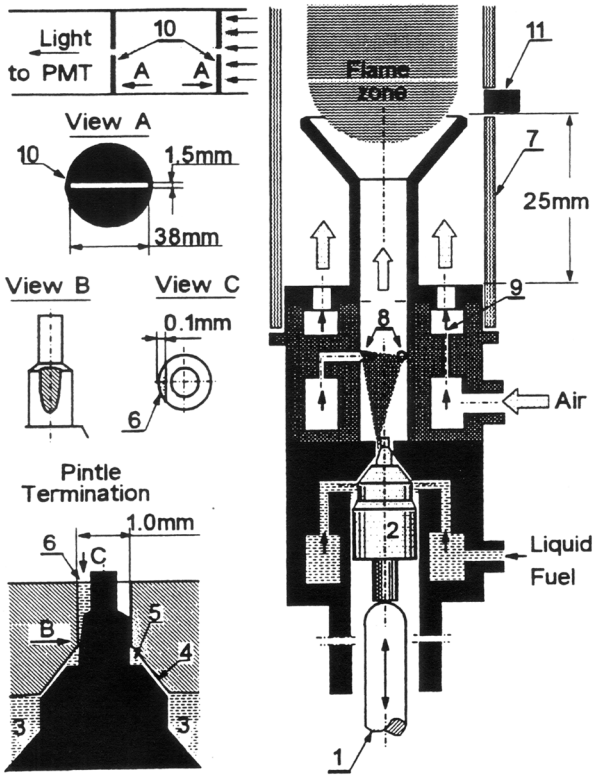

Figure 2.14 Fuel injector assembly and combustor setup[18]

This was an atmospheric combustor operating with an air flow rate of 15 g/sm, 33% swirl flow and 67% axial flow. The air inlet temperature was 200K and fuel flow rate was 1 g/s. When operated at equivalence ratio of 0.97 this combustor exhibited an instability with an amplitude of 1.4 psi at 400 Hz. This corresponded to the quarter wave mode of the combustor.

The control system implemented on this combustor consisted of a pressure sensor located in the combustor tube, a fast adaptive control algorithm and the FIA. The purpose of the

adaptive controller was to quickly converge to the optimal phase delay. Once this delay was found the controller would then continually adapt the control signal to maintain the maximum possible attenuation. The FIA assembly consisted of a terfenol-D actuator attached to a pintle valve. As the actuator displaced the pintle, the area closed off by the pintle increased allowing more fuel flow into the combustor. The reported bandwidth of this actuator was 1500 Hz. This actuator was reported to modulate 10-20% of the total fuel flow.

Time traces of the RMS pressure in the combustor, for two air-to-fuel ratios, can be found in Figure 2.15.

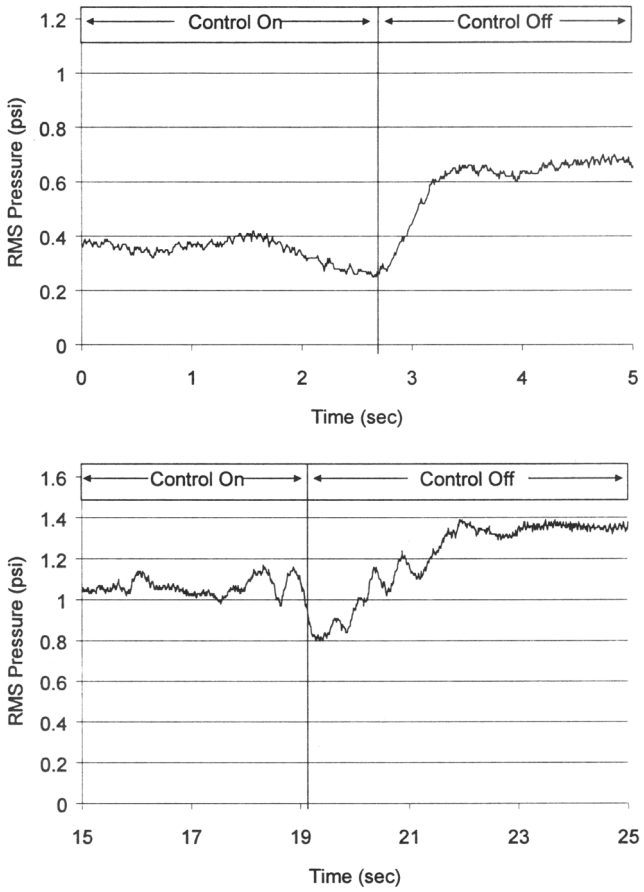

Figure 2.15 Pressure traces showing the results of control[18]

The result of the testing was a 40% RMS pressure reduction at the instability frequency, as well as a 20% reduction of the RMS pressure.

2.8 [Haile et al. 1998]

Work was done at l'Ecole Centrale Paris to characterize the quality of high frequency modulated flow through liquid fuel injectors. These were non-reacting experiments performed using diesel fuel. A fuel supply vessel was pressurized to 9 bar, which provided fuel flow through a rapid electro-valve to a Danfoss simplex hollow cone atomizer. The rise time of the electro-valve was reported to be roughly 1ms. This system provided a steady state flow of 1.85 kg/hr with the valve completely open.

Two methods were used to characterize the modulated fuel spray. Particle imaging velocimetry (PIV) and phase doppler anemometry (PDA) were used to gather information about droplet velocities and droplet diameter throughout the spray field. A Kistler pressure transducer and Dantec hotwire anemometer were mounted in fuel line to measure fuel flow into the injector system. This setup can be seen in Figure 2.16.

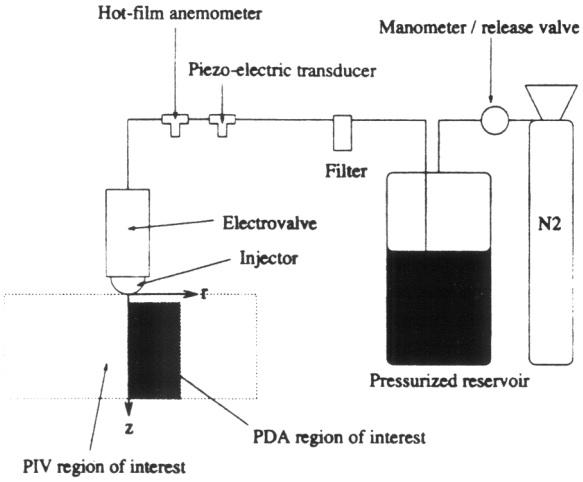

Figure 2.16 Experimental setup[10]

The modulation of the fuel flow rate was measured using the hot wire anemometer when the actuator was operating at 60 and 600 Hz. The results of this testing can be seen in Figure 2.17 and Figure 2.18 respectively.

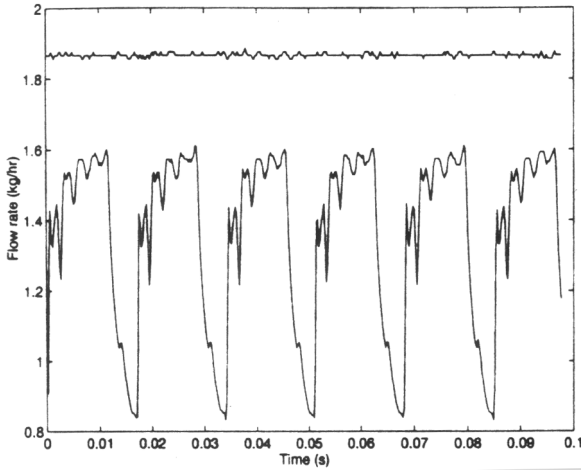

Figure 2.17 Actual flow modulation at 60Hz[10]

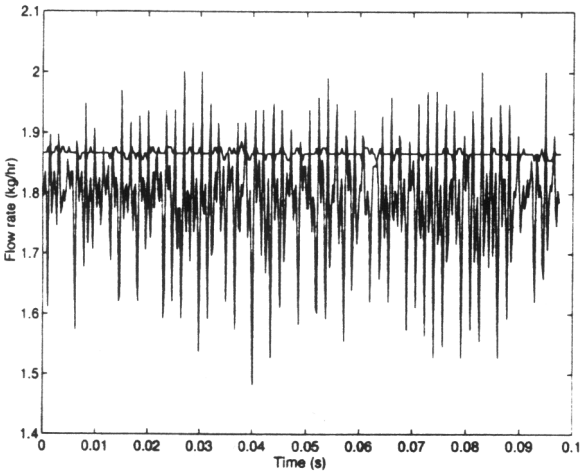

Figure 2.18 Actual flow modulation at 600Hz[10]

Spray characteristics were also examined at modulation frequencies of 60 and 600 Hz. Droplet diameters as a function of distance from the injector can be see for the 60 and 600 Hz case in Figure 2.19 and Figure 2.20 respectively.

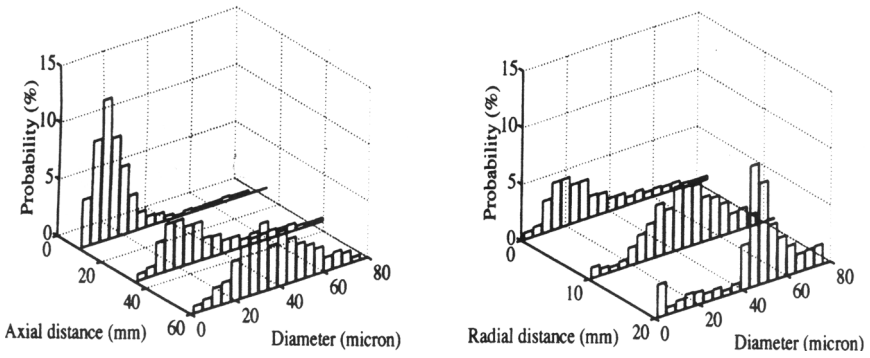

Figure 2.19 Spray characteristics at 60Hz[10]

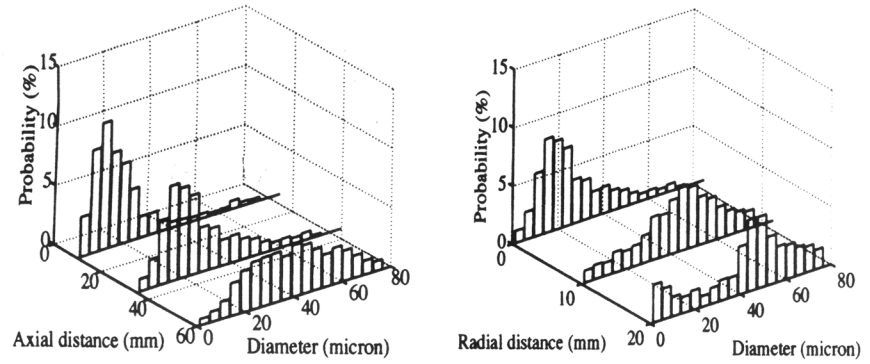

Figure 2.20 Spray characteristics at 600Hz[10]

It was found that the droplet diameter distributions were nearly unaffected by the frequency of modulation. This conclusion is a very promising result for active combustion control as it implies that high frequency modulation of the fuel flow will not change the characteristics of the atomization process and correspondingly the combustion dynamics.

2.9 Literature Review Summary

These papers are representative of the most recent work being performed on the control of thermo-acoustic instabilities using fuel modulation. Each of these papers describes tests performed on different rigs using different fuels at different power ratings with different actuators. A table providing a summary of the details of this research can be found in Table 2.2.

Researcher	Actuator type	Actuator Bandwidth (Hz)	Fuel Type	Combustor Power	Limit Cycle Frequency (Hz)	Claimed Fuel Modulation	System Performance
Hantschk	Servo	450	Diesel	4MW	275	NA	30dB reduction
McManus	Solenoid	300	Natural Gas	200kW	140	10%	NA
Yu	Solenoid	4x250	Ethanol/ Heptane	270kW	100	NA	15dB reduction
Cohen	Solenoid	250	Diesel	4MW	200	NA	15dB reduction
Hibshman	Solenoid	250	Diesel	NA	200	NA	6.5dB reduction
Magill	Solenoid	500	Liquid	NA	140	NA	6dB reduction
Johnson	Magneto-restrictive	1500	n-heptane	NA	400	10-20%	8dB reduction
Haile	Electro-valve	500	Diesel	NA	NA	10%	NA

Table 2.2 Summary of reviewed works

The results obtained for these tests are widely varied, 6-30 dB of reduction, and unexplained. This large variance seems to be strongly related to the fact that the fuel injection systems being used are not well characterized and may not provide the necessary modulation [23]. If the effect of the fuel injection system on the level and profile of the fuel modulation is unknown, then a true understanding of the effect of fuel modulation on the control of thermo-acoustic instabilities is not possible. Only one of these papers addresses in detail the fuel modulation produced by their fuel injection system. A proper investigation of the effect of fuel modulation on the reduction of thermo-acoustic instabilities will require the design and construction of actuators capable of modulating larger amounts of the flow with a specific profile.

3 Fuel Injector System Design and Construction

3.1 Target Specifications

The increased frequency of thermo-acoustic instabilities in real world combustors has created interest in designing fuel injection systems that can be used to interact with and control the combustion process. In an attempt to set reasonable target specifications for use in developing the fuel injection system to be used on our experimental combustor rig, several real world applications were researched. The performance requirements desired for these different applications were then used to develop a set of representative target specifications for our fuel injection system.

The jet engine and gas turbine industries comprise two major applications for which active combustion control is being explored. Based on the input of Ken Semega of the Air Force and Joe Saus of NASA Glenn Research Center, representatives of the jet engine industry, a set of desired performance requirements regarding bandwidth, mean flow rate and percent modulation were compiled for jet engine related fuel injection control systems. These performance requirements represent what the jet engine industry believe will be effective for use in controlling thermo-acoustic instabilities in jet engines. Lars Nord, an engineer at Alstrom Power and representative of the gas turbine industry, provided a set of desired performance requirements for a fuel injection control system to be used in the gas turbine industry. Some very basic combustor parameters are given in Table 3.1 that are representative of the jet engine and gas turbine industry along with the specific parameters for our experimental combustor rig.

	Jet Engine Application	Gas Turbine Application	Virginia Tech Experimental Rig
Fuel Type	JP-8 Jet Fuel	Natural Gas	Ethanol
Maximum mean mass flow rate (lb_m/hr)	50	200	2.6

Table 3.1 Summary of combustor parameters for the jet engine industry, gas turbine industry and VT rig.

Aside from the obvious differences in the types and sizes of the jet engine and gas turbine combustors, the ideal requirements regarding both bandwidth and percent modulation were quite consistent. This information was very useful in creating a set of target specifications for our fuel injection control system because they were so consistent. The target specifications representing the desires of the jet engine and gas turbine industry, along with the specifications decided upon for our fuel injection system, can be found in Table 3.2.

	Jet Engine Application	Gas Turbine Application	Virginia Tech Experimental Rig
Percent modulation ($\%_{Qpeak}$)	40	30	40
Bandwidth (Hz)	50-600	50-700	50-700

Table 3.2: Summary of fuel injection system target specifications for the jet engine industry, gas turbine industry and VT rig.

With these target specifications it was possible to begin the design of our fuel injection system. It was important, however, to first examine the existing fuel delivery system for our combustor rig to determine the range of performance that it was capable of providing.

3.2 Existing Fuel Delivery System

The original fuel supply system for our combustor consisted of a pressurized fuel storage tank and a fuel line leading up through the combustor to the atomizer. The fuel flow rate of the original fuel supply system was controlled by varying the tank pressure. The fuel flow rate, given a particular tank pressure, can be calculated using an empirical relationship that was found to be:

$$Q = 0.048P^{.44} + .053 \qquad (3.1)$$

where Q is the volumetric flow rate in units of cm^3/s and P is the line pressure in units of psi. The specific atomizer chosen, a Delevan 0.42 cm^3/s hollow cone simplex atomizer, could adequately atomize the fuel at line pressures above 70 psi. Because the maximum tank pressure available was 160 psi the existing fuel supply system could operate only along the curve shown in Figure 3.1.

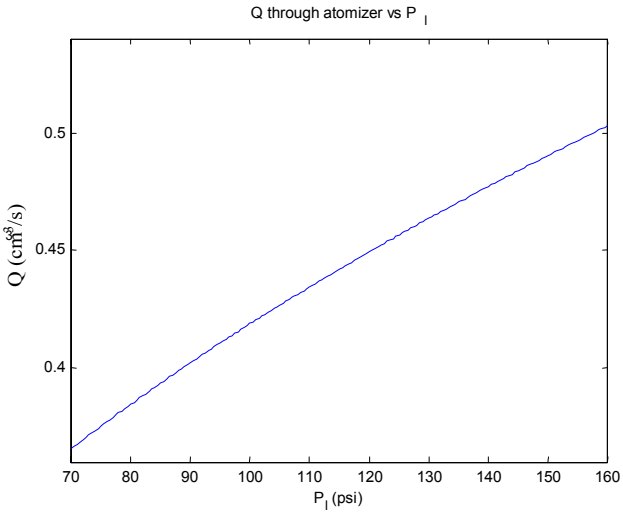

Figure 3.1 Volumetric flow rate through atomizer as a function of the tank supply pressure

3.3 System Level Design

It is clear from the Rayleigh criterion, as discussed in Section 1.1.1, that the stability of a combustion process is dependant on the phase relationship between unsteady pressure and heat release rate. By introducing a method to adjust the relative phase of these quantities, one can effectively control the stability of the combustion process. Thus the idea of a phase shifter controller has been widely used in the control of thermo-acoustic instabilities [36,38]. The concept of the phase shifter controller is to measure either the pressure or heat release rate as a reference signal to which a delay can be added. This delayed signal can then be used to control a device that can influence the pressure or heat release rate. The phase delay can be adjusted to ensure that the control device adds energy to the combustion process with a desired phase. A schematic showing the

interaction of phase delay controller with the combustion process, that uses the pressure as a reference signal and interacts with the combustion process through heat release, is illustrated in Figure 3.2.

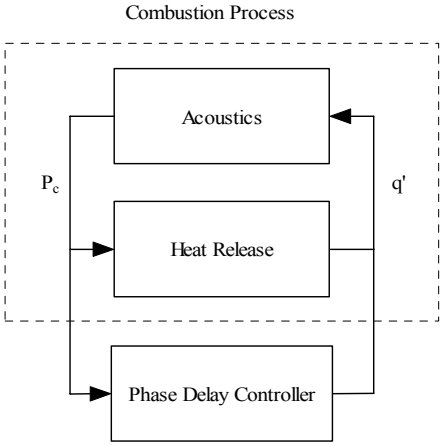

Figure 3.2 Schematic of the interaction of a phase delay controller with the combustion process

The pressure in the combustor could easily be measured with a pressure transducer and used as a reference but there is no direct way that the phase delay controller could interact with the heat release. Since the heat release of the flame is proportional to the fuel flow rate, it is clear that by modulating the fuel supply with a fuel injection system one could interact with the heat release in a secondary manner. The combustion control system created using this technique would have the form of the controller shown in Figure 3.3.

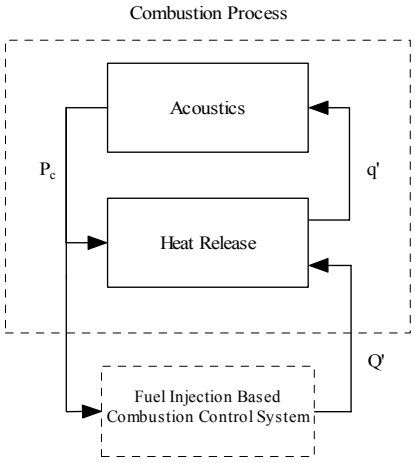

Figure 3.3: Schematic of the interaction of a fuel injection based combustion control system with the combustion process

The design of the fuel injection system began by examining the components necessary to realize the function controller. A schematic of these components can be seen in Figure 3.4. Obviously a pressure transducer would be necessary to sense the pressure within the combustor. A variable time delay would allow the user to adjust the relative phase of the signal given to the fuel injector. There would of course have to be a fuel injection system to modulate the fuel supply consisting of a fuel injector and fuel injector controller. The fuel injector controller would create and supply the appropriate signal(s) to operate the fuel injector.

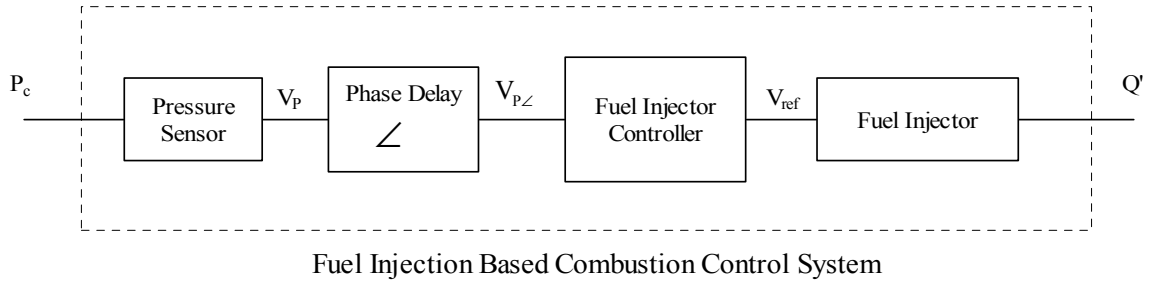

Figure 3.4 Schematic of combustion control system

The pressure sensor and phase shifter are relatively generic components of this control system. The fuel injector and related controller comprised the majority of the effort in the design of this combustion control system and thus will be the focus of this chapter.

3.4 Fuel Injector Component Concept Designs

Because it is the pressure drop across the atomizer that produces a given flow rate, it would follow that modulation of the line pressure would provide a corresponding modulation in the flow rate, according to the relationship given in Equation 3.1. Two concept designs, one making use of a throttling valve and the other a piston and check valve, were explored to create this pressure modulation.

3.4.1 Throttle Valve Design Concept

The pressure drop across the atomizer could be controlled by adding a throttling valve in the fuel line between the atomizer and the fuel tank. The pressure drop across the atomizer, and the corresponding flow rate, would then depend on the tank supply pressure as well as the position of the throttling valve. In the open position, with negligible pressure drop across the throttling valve, the atomizer would see the entire pressure drop of the system and the corresponding flow rate of the system as if the throttling valve was not present. In the closed position, with the entire pressure drop of the system across the throttling valve, the atomizer would see no pressure drop and correspondingly no flow. As the throttling valve varied its position between open and closed it would affect the pressure drop across the atomizer, producing a flow rate somewhere between the flow rates associated with the open and closed position. It is important to note that the throttling valve, at best, can only provide the tank pressure to the atomizer. Because the existing rig can only provide a tank pressure of 160 psi, the maximum flow rate available using a throttling valve would be 0.50 cm^3/s, based on Figure 3.1. If this was the peak flow rate achieved as the throttling valve was modulating the fuel supply, the maximum modulation achievable would then be $19\%_{Qpeak}$. This value of modulation is far below the goal of $40\%_{Qpeak}$. Because of the limitation of our rig, the need arose to find another means to achieve the goal of $40\%_{Qpeak}$ modulation. As a note, this method of modulation would be able to provide better performance if the maximum tank pressure could be increased. Thus, in future work this throttling valve concept could be implemented effectively if the existing fuel delivering system were modified to provide higher fuel supply pressures.

3.4.2 Piston and Check Valve Design Concept

In order to achieve the flow rates necessary for our goal of $40\%_{Qpeak}$ modulation it was necessary to find a way to produce a higher line pressure than was available from the existing fuel delivery system. A piston could be added in the fuel line between the fuel tank and the atomizer to increase the pressure in the system. However, unless there were

some means of closing off a volume of fluid for the piston to act against, the pressure added by the piston could back drive the flow upstream. If a check valve was placed upstream of the piston, the volume of fluid between the piston and the atomizer could be isolated and the pressure in that closed volume of fluid would only depend on the pressure provided by the piston. Thus the maximum amount of modulation would depend only on the force available to be applied to the piston, and of course the maximum piston displacement. This result makes this configuration very attractive as pistons and their actuators can provide very high pressures. There was, however, a drawback of using this configuration. At the end of a cycle the piston would have to be returned to its original position, in preparation to expel the volume of fluid for the next cycle. Thus, for at least part of the cycle the piston would be returning to its rest position. During this part of the cycle the check valve would be open, producing the unmodulated fuel flow rate. This assumes that the fuel supply system could produce the flow rate necessary to provide the unmodulated flow rate through the atomizer while replenishing the volume of the withdrawing piston. This would mean the fuel flow rate could not be modulated for at least part of a cycle.

Because obtaining a maximum modulation of $40\%_{Qpeak}$ was a primary goal of the fuel injector design, this method was chosen in spite of this handicap. The approach taken to address this shortcoming was to modulate the fuel supply only though the first half-period of a cycle. While this would not allow us to achieve true sinusoidal operation, it would still allow us to add energy in a sinusoidal fashion into the combustion process for half of the duration of operation.

3.5 Fuel Injector Design

Since it was a goal of this work to analyze the effects of various amounts of modulation on instability suppression it was important that the fuel injector could physically realize the desired flow profiles related to various levels of modulation. Namely, it was desired that the fuel injector system would be able to modulate between $0\%_{Qpeak}$ and $40\%_{Qpeak}$ of the fuel flow at frequencies up to 700 Hz for our combustor rig. Once again these target

specifications were developed based on the needs of the jet engine and gas turbine industry. The thermo-acoustic instability present on our rig it near 100 Hz and thus it is essential that the fuel injector be able to modulate the fuel effectively at this frequency.

3.5.1 Piston Component Design

In order to design the piston component of the fuel injector, the maximum piston displacement and maximum piston force required to modulate the flow as specified, had to be calculated. This process began by examining the type of flow profile that was desired from the piston and check valve design. This profile can be seen over one period in Figure 3.5.

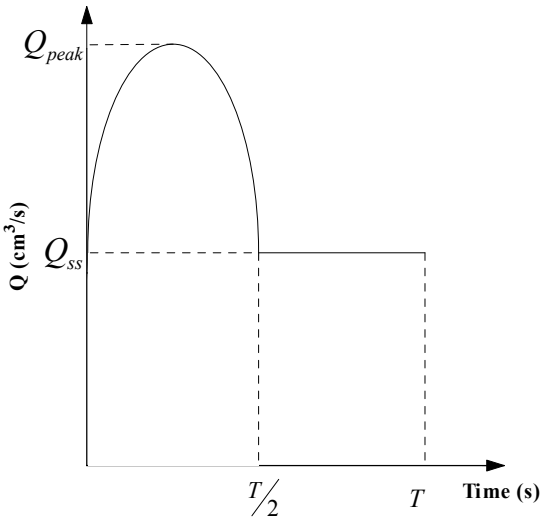

Figure 3.5 A generic flow profile

Q_{ss} indicates the unmodulated steady-state volumetric flow rate through the fuel injection system. Q_{peak} indicates the peak volumetric flow rate achieved in the modulating process. The height of Q_{peak} relative to the fixed Q_{ss} would change based on the desired modulation $\%_{Qpeak}$ through the relationship in Equation 3.2.

$$Q_{peak} = \%_{Qpeak} Q_{ss} + Q_{ss} \tag{3.2}$$

Required Peak Piston Displacement

The first half-period of this profile describes the portion of the cycle with the check valve closed and the piston providing the motivation for flow. During this first half-period, the

piston would not only have to produce the modulated component of the fuel flow but also the component related to the steady state flow, as described by regions A and B in Figure 3.6, respectively.

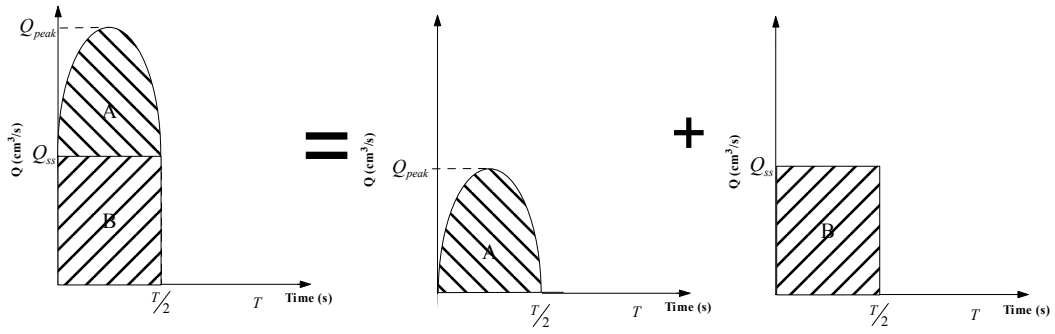

Figure 3.6 First half-period of flow profile shown as equivalent sum of steady state and modulated flow components

At the end of this first half of the cycle, the piston would have completed its stroke and begun to return to its original position. Thus, the displacement of the piston at the end of this first half of the cycle would be the maximum piston displacement necessary to create that particular flow profile.

An assumption was made at this point that the fuel behaves as an incompressible fluid. Thus, the volume of fluid expelled from the atomizer would necessarily equal the volume displaced by the piston within the closed volume of the fuel line created by the check valve. The relationship in Equation 3.3 would describe the total volume of fluid expelled from the atomizer over the first half-period of a cycle.

$$V_{T/2} = \int_0^{T/2} Q(t)dt \tag{3.3}$$

This expression can be evaluated in terms of the previously mentioned components A and B, to provide the relationship in Equation 3.4.

$$V_{T/2} = \underbrace{\int_0^{T/2} Q_{ss}(t)dt}_{\text{B}} + \underbrace{Q_{peak}\int_0^{T/2}\sin(\omega t)dt}_{\text{A}} \tag{3.4}$$

Separating these terms:

$$V_{T/2}^{B} = Q_{ss}\,T/2 \tag{3.5}$$

$$V_{T/2}^{A} = -\frac{Q_{peak}}{\omega}\cos(\omega T)\Big|_0^{T/2} = -\frac{Q_{peak}}{\omega}\left[\cos\left(\frac{\omega T}{2}\right)-\cos(0)\right] = -\frac{Q_{peak}}{\omega}[\cos(\pi)-\cos(0)]$$

$$V_{T/2}^{A} = \frac{(\%_{Qpeak}\,Q_{ss}+Q_{ss})}{\pi}T \tag{3.6}$$

Recombining:

$$V_{T/2} = Q_{ss}\,T/2 + \frac{(\%Q_{peak}Q_{ss}+Q_{ss})}{\pi}T = \frac{Q_{ss}}{f}\left(\frac{\pi+2\%Q_{peak}+2}{2\pi}\right) \tag{3.7}$$

Note that the volumetric displacement of the piston necessary to create a particular flow profile can be found explicitly in terms of Q_{ss}, $\%_{Qpeak}$ and the frequency.

The volume of the fluid displaced by the piston in the first half-period of the cycle can also be written in terms of the diameter of the piston and the displacement of the piston as in Equation 3.8.

$$V_{T/2} = \pi\frac{d_{piston}^{\,2}}{4}x_{\max} \tag{3.8}$$

Thus, one can find an expression for the piston's maximum displacement as a function of only d_{piston}, Q_{ss}, $\%_{Qpeak}$ and the frequency as shown in Equation 3.9.

$$x_{\max} = \frac{4Q_{ss}}{\pi d_{piston}^{\,2} f}\left(\frac{\pi+2\%Q_{peak}+2}{2\pi}\right) \tag{3.9}$$

This expression can now be evaluated over the desired range of operating frequencies, modulation levels and piston diameters to determine a reasonable piston diameter. Using

this piston diameter, one can obtain the absolute maximum piston displacement necessary to provide satisfactory performance over all operating conditions. The relationship between peak piston displacement, operating frequency and piston diameter can be seen graphically in Figure 3.7 for a fixed peak modulation level of $40\%_{Qpeak}$.

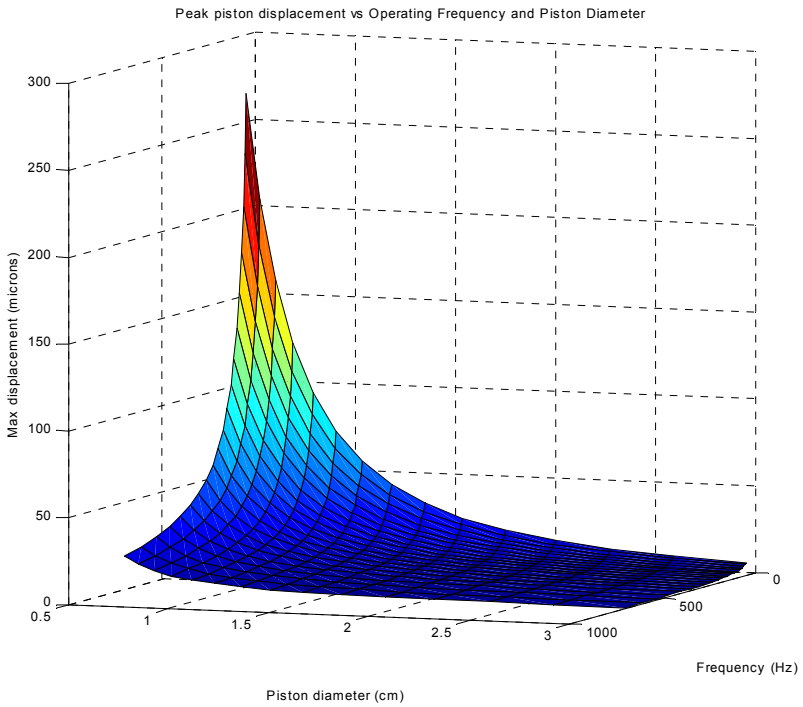

Figure 3.7 Plot of peak piston displacement in microns as a function of operating frequency and piston diameter, $40\%_{Qpeak}$

It was obvious that the peak displacement increased dramatically for smaller diameter pistons and lower frequencies. It was desired to minimize the necessary peak piston displacement, as smaller displacements would be easier to realize. For piston diameters greater 2.5 cm it was found that the gradient $\frac{\delta P_{peak}}{\delta d_{piston}}$ became small. Thus, it seems that a reasonable piston diameter to minimize the necessary peak piston displacement would be around 2.5 cm, or about 1 inch. Using this piston diameter, it was possible to examine in more detail the relationship between peak piston displacement, operating frequency and percent modulation. This relationship is presented graphically in Figure 3.8.

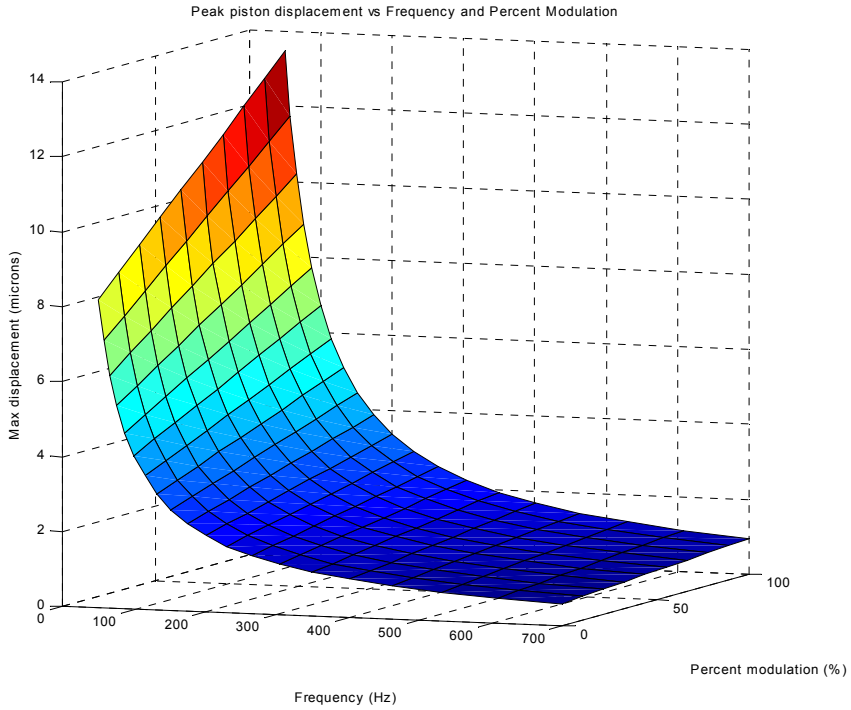

Figure 3.8 Plot of peak piston displacement in microns as a function of operating frequency and percent modulation, d_{piston}=1 inch

The peak piston displacement increases asymptotically as the modulation frequency approaches zero. This result was to be expected because as the frequency approaches zero, the period of the cycle increases. As the period of the cycle increases so does the time that the piston is solely providing the flow. Because the piston is minimally providing a steady state flow rate, the distance that the piston needs to displace to produce the desired flow will necessary increase as period increases. This result, however, was not a major concern as the fuel injection system was specified to operate only above 50 Hz. Examining the entire operating range of 50-700 Hz and 0-100%$_{Qpeak}$ modulation, with a 1 inch diameter piston, the maximum displacement required for operating was found to be 14 microns, as can be seen in Figure 3.8.

Pressure and Force Requirements

An assumption made at this point in the design process was that the flow rate versus pressure drop relationship found in Figure 3.1 was valid not only as a static relationship but also as a dynamic relationship. In other words, the relationship between flow rate and

pressure drop across the atomizer is frequency independent. If this is the case, then for any desired flow profile a corresponding pressure profile could be developed by simply passing the flow profile through the relationship between flow rate and pressure drop as seen in Figure 3.9

$$P = \left(\frac{Q - 0.053}{0.048} \right)^{1/0.44}$$

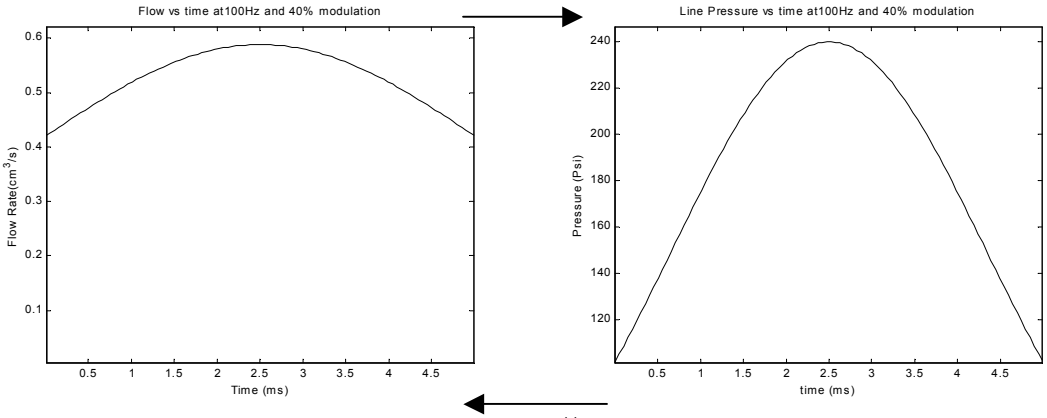

$$Q = 0.048P^{.44} + .053$$

Figure 3.9 Example of finding the pressure profile associated with a flow profile using the empirically found relationship.

Since this relationship was assumed to be frequency independent, it was possible to solve for the peak pressure required to produce the highest desired level of modulation. With $40\%_{Qpeak}$ modulation and Q_{ss}= 0.42 cm^3/s, Q_{peak}= 0.59 cm^3/s. Solving for the pressure that corresponds to this peak flow rate yields P_{max}= 241 psi. It is apparent that the pressure required to obtain higher levels of flow modulation increases dramatically as can be seen in Figure 3.10.

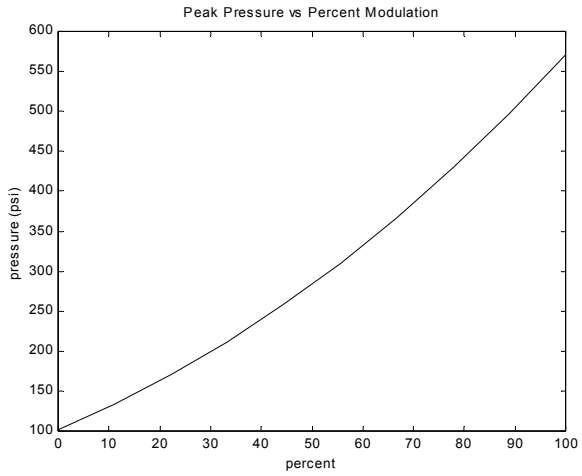

Figure 3.10 Peak pressure vs. percent modulation

For example, the pressure required to provide a modulation of $100\%_{Qpeak}$ is 574 psi, 5.7 times the pressure required for original steady state flow rate.

Since it was decided to use a 1 inch diameter piston in the calculation of peak piston displacement, it was also possible to calculate the force that would be required by an actuator to provide the necessary piston pressure. The relationship in Equation 3.10 can be used to solve for this peak actuator force.

$$F_{actuator} = P_{\max}\pi\frac{d_{piston}^{\ 2}}{4} \tag{3.10}$$

Recalling that for $40\%_{Qmean}$ the corresponding peak piston pressure was found to be 241 psi, the maximum actuator force was found to be 189 lbf.

A summary of the physical requirements for the piston derived in this and the previous section, which for a mean flow rate of 0.42 cm^3/s can provide any modulation level between 0-100 $\%_{Qpeak}$ at any frequency between 50-700 Hz, can be found in Table 3.3.

Piston Requirements			
Peak Piston Displacement (microns)	Peak Piston Pressure (psi)	Piston Diameter (inch)	Peak Piston Force (lbf)
14	241	1	189

Table 3.3 Summary of piston requirements allowing desired performance over the entire specified range of operation

Selection of piston assembly components

At this point, the components required to build the piston assembly needed to be selected. Before selecting an actuator for the piston assembly we performed extensive research on solenoid, magneto-restrictive and piezo-ceramic actuators. Based on the inherent high bandwidth and high force generating capabilities of piezo-ceramic materials, along with the fact that the typical displacements available from these actuators were well matched to our design specifications, it was clear that a piezo-ceramic actuator was best suited for our application. The piston assembly was created using a piezo-ceramic actuator attached to a piston cylinder. Once the physical requirements for the piston were calculated, it was possible to find an actuator that could provide the desired performance.

Piezo-Ceramic Stack Selection

Piezo-ceramic stacks are actuators that provide a displacement proportional to an applied voltage. Piezo-ceramic actuators are generally capable of providing large forces across small displacements over a large bandwidth [31,24,30]. The operation range of a typical piezo-ceramic stack revolves around the relationship shown in Figure 3.11, which illustrates the ability of a piezo-ceramic stack to provide a force at a given displacement.

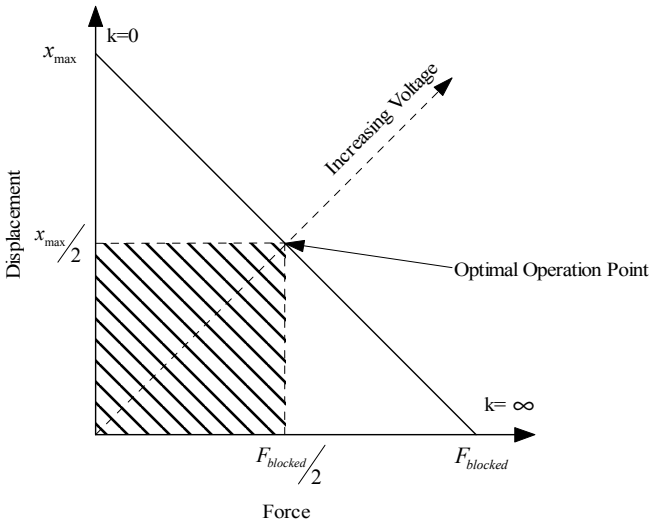

Figure 3.11 Typical force generation vs. displacement relationship for a piezo-ceramic stack

Piezo-ceramic stacks are capable of providing their largest force when they are constrained to produce zero displacement. The quantity describing the amount of force

that can be generated by a piezo-ceramic stack if it is not allowed to produce any displacement is called the blocked force. Conversely, the stack can produce no force at its maximum displacement. The optimal operating region, with regards to efficiency of operation over a cycle, of a piezo-ceramic actuator is around the shaded region shown in Figure 3.11 that is bounded by $x_{\max}/2$ and $F_{blocked}/2$ [30].

Thus, a piezo-ceramic stack whose blocked force was twice the calculated maximum required actuator force and whose maximum displacement was twice the maximum displacement required by the piston was required to ensure that our actuator would always be able to provide the necessary displacements and forces. Thus, a piezo-ceramic stack that could provide a blocked force of at least 380 lbf and a maximum displacement of at least 28 microns was required. After researching several companies, the PSt150/14/20 actuator manufactured by Piezomechanic was selected. The manufacturer's specifications for this actuator are provided in Table 3.4.

Model	Maximum Displacement (microns)	Blocked Force (lbf)	Resonant Frequency (kHz)	Voltage Range (V)	Capacitance (μF)
PSt 150/14/20	28	780	30	-10 to 150	7.2

Table 3.4 Manufacturers specifications for PSt 150/14/20 actuator

As a note, this actuator was purchased with strain gages mounted on the stack to allow measurement of the stack's displacement. The measured piston displacement during operation could be used in a displacement feedback control system, which would ensure that the piston was properly following the reference signal and thus producing the desired flow modulation. This will be discussed further in Section 4.3.

Piezo-Amplifier Selection

The selection of an amplifier for this piezo-ceramic actuator was also important in the design of the piston assembly. Because piezo-ceramics are capacitive in their electrical nature, it was important to purchase a special amplifier intended to drive capacitive loads. It was also important to select an amplifier that could provide the necessary bandwidth. Since, as was just stated, piezo-ceramic stacks are capacitive, the current required to drive

a stack is directly related to the driving frequency. For sinusoids the maximum current required is given through the relationship in Equation 3.11.

$$i_{\max} = \pi C_{stack} V_{\max} f \tag{3.11}$$

Thus, the bandwidth of a coupled amplifier and piezo-ceramic stack is entirely determined by the capacitance of the stack and the level and frequency of the driving signal. By simply substituting the relevant values from the PSt150/14/20 actuator using the 700Hz bandwidth specification, the maximum current can found to be roughly 2.4 amps for a full range driving signal. The amplifier used to power the piezo-ceramic stack should be able to provide a peak current of 2.4 amps and a supply voltage in the operating range of the stack. After some research, the LE150/200 manufactured by Piezomechanic was selected as the amplifier. The manufacturer's specifications for this amplifier are provided in Table 3.5 and Figure 3.12.

Model	Voltage Range (V)	Maximum Current (A)
LE150/200	-10 to 150	2.0

Table 3.5 Manufacturers specifications for LE150/200 amplifier

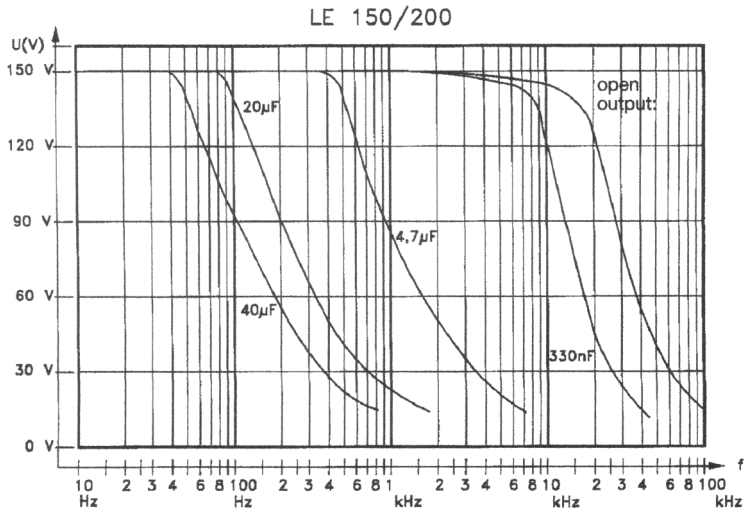

Figure 3.12 Frequency response for LE150/200 amplifier

The maximum current this amplifier is able to produce was a small amount less than required for full range operating of the piston assembly at 700 Hz. This restriction,

however, was acceptable as the required stack displacements at the higher frequencies are much less than the maximum available as can be seen in Figure 3.8, even when limited by this available peak current.

Piston Cylinder Selection and Assembly

A Bimba piston cylinder, model H-172-HUZ, was selected for use in the piston assembly. This piston cylinder had a 1 inch diameter piston per our specification. This cylinder was rated for 500 psi, which was well above the maximum pressure that it was predicted to encounter in operation. The piston cylinder was purchased with a threaded piston rod extending from the cylinder body. An adapter was purchased that would mount and facilitate the alignment of the PSt150/14/20 stack to the piston rod. An enclosure was fabricated to house these components. The completed piston assembly can be seen in Figure 3.13.

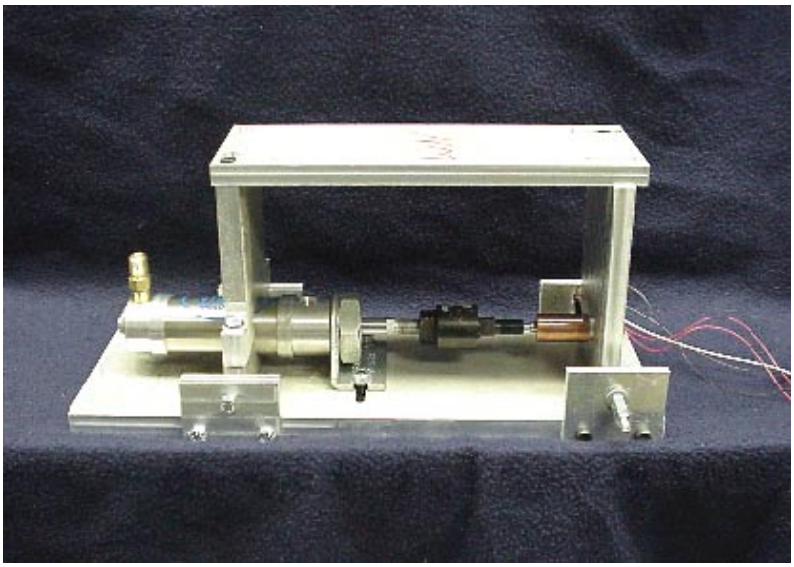

Figure 3.13 Completed piston assembly

3.5.2 Check Valve Component Design

As a review, the purpose of the check valve in the design of the fuel injection system was to prevent the reversal of the fuel flow into the upstream supply line when the piston was

operating. This would ensure that all the work produced by the piston be translated into volumetric flow rate through the atomizer. The physical requirements for the check valve were twofold. Most importantly, the bandwidth of the check valve must be high relative to the operating frequency. This is important because unless the check valve can reach its closed position very quickly after the piston begins its stroke, the check valve would not be able to impede flow reversal. Secondly, in the open position the pressure drop across the check valve must be small relative to the supply line pressure.

Analysis of Passive Check Valves

Passive check valves operate based on the pressure drop across the valve. There are several types of check valves [6], but the one most suited for our application was a simple ball-type check valve that can be seen in Figure 3.14. This spring-loaded design allows unidirectional flow control. When the supply pressure is great enough to overcome both the downstream pressure and the preloaded spring force, the ball and spring deflect allowing flow to pass through the valve. When the downstream pressure changes this force balance, the ball is returned to its seated position stopping any flow reversal. Ideally, the stiffness of the spring and ball size could be adjusted so that the valve would provide a large enough bandwidth.

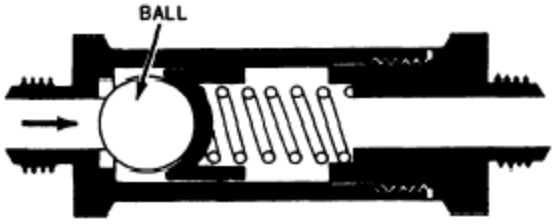

Figure 3.14 Ball-type check valve

A few considerations must be taken into account in order for the check valve to operate at the desired bandwidth and pressures required for use in the fuel injector. First, the rise time of the spring-ball system must be fast relative to the frequency of operation. If the check valve is not closed when the piston is operating, some of the flow will escape back into the upstream supply line. Because the check valve could not close instantaneously, it

would seem reasonable to desire the check valve be able to reach its closed position within 5% of the period of operation. This way, while there could possibly be some flow reversal in the early part of the cycle, the check valve would be closed by the time the substantial influence of the piston was occurring. At 700 Hz, 5% of the period is roughly 0.07 ms. For a simple spring-mass-damper system, the resonant frequency and rise time equations are as follows:

$$f_n = \frac{\sqrt{\frac{k}{m}}}{2\pi}, \qquad (5.5.1) \tag{3.12}$$

$$T_r \approx \frac{2.16\zeta + 0.6}{2\pi f_n} \tag{3.13}$$

These equations can be rearranged to find the stiffness as follows:

$$k \approx \left(\frac{2.16\zeta + 0.6}{T_r} \right)^2 m \tag{3.14}$$

Assuming the minimum effective mass of the ball and spring to be 10 g and a damping ratio of 50%, the spring stiffness required to produce a rise time of 0.07 ms is 5.7 MN/m.

The second consideration in the design of a passive check valve was the pressure force required to open the valve. Examining the force balance on the check valve ball in Figure 3.15 as a static relationship, it was possible to solve for the displacement of the ball given the pressure drop and preload force, applied by the spring, as can be seen in Equation 3.15.

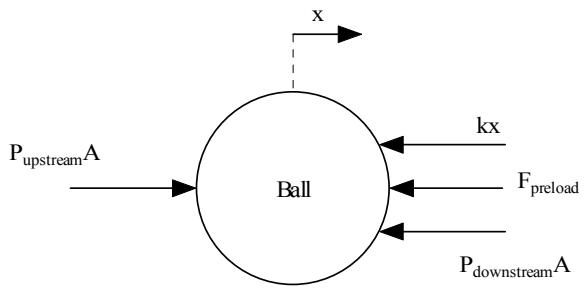

Figure 3.15 Force balance on check valve ball

$$x = \frac{\left(P_{upstream} - P_{downstream}\right)A - F_{preload}}{k} = \frac{\Delta PA - F_{preload}}{k} \tag{3.15}$$

One should note that the high spring stiffness required to provide the necessary rise time will tend to reduce the displacement of the check valve's open position. To continue, let us assume that there is no preload force and the stiffness of the spring is the value from in the previous discussion, 5.7 MN/m. Assuming also a ball diameter of 1/8 inch it was possible to solve for maximum displacement in the open position to be 0.2 microns. This would create an enormous pressure drop across the check valve in the open position, rendering the check valve useless.

The results of these calculations show that a passive check valve was not well suited for this particular application. This was also reflected in the fact that the maximum bandwidth of commercially available check valves, for the pressure ranges of interest, was less than 60 Hz. Thus it was necessary to consider another method to realize the check valve component of the fuel injection system.

Analysis of Active Check Valves

Because of the inadequacy of passive check valves, actively controlled valves were explored. These actively controlled valves could be operated on/off as a check valve. The most common commercially available active valves are solenoid actuated. Based on the generally low bandwidth and self-heating problems of associated with solenoids, it was decided not to pursue the use of a solenoid actuated valve. Once again, a piezo-ceramic actuator was used because of its intrinsically high bandwidth.

Active Check Valve Design

Because piezo-ceramic actuators are limited in their displacement, it was necessary to calculate the minimum displacement required to maintain a negligible pressure drop across the check valve in the open position. A Fluent model was created to examine what this necessary displacement should be. The open valve was modeled as a rectangular

orifice, as can be seen in Figure 3.16 that was 5 mm wide and 10 mm long. This orifice model was placed as an obstruction in a 5 mm diameter circular pipe, roughly the inner diameter of the ¼ inch fuel line pipe. The height of this orifice, h, was then adjusted until the pressure drop across the orifice was less than 1 psi for a flow rate of 0.42 cm^3/s.

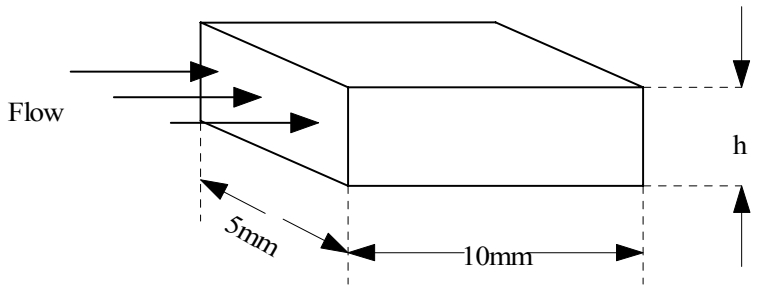

Figure 3.16 Orifice model

It was found that a 150 micron high orifice would only have a 0.4 psi pressure drop across it at 0.42 cm^3/s. At only 0.42% of the steady state operating pressure, this small pressure drop would minimally affect the steady state flow rate.

It was now necessary to find a piezo-ceramic actuator and amplifier that could achieve this 150 micron displacement with the shortest rise time possible. It was found that the best combination of actuator and amplifier was the PSt1000/10/150 actuator and the LE1000/100 amplifier, both manufactured by Piezomechanic. The specifications for this actuator and amplifier are provided in Table 3.6 and Table 3.7, respectively.

Model	Maximum Displacement (microns)	Blocked Force (lbf)	Resonant Frequency (kHz)	Voltage Range (V)	Capacitance (μF)
PSt 1000/10/150	150	900	5	0-1000	0.39

Table 3.6 Manufacturer's specifications for PSt 1000/10/150 actuator

Model	Voltage Range (V)	Maximum Current (A)
LE1000/100	0-1000	1.0

Table 3.7 Manufacturer's specifications for LE 1000/100 amplifier

The rise time for a 150 micron step using this actuator and this amplifier is approximately 2 ms. Although this rise time is substantially longer that the desired 0.07 ms, calculated as 5% of a cycle period at 700 Hz, there are some measures that could be taken to

improve the performance. Because this fuel injection system was going to be controlled by computer, the phasing of the piston and check valve signals can be modified. Anticipating the opening of the check valve, the control system could generate the check valve closing signal early, taking account of this rise time. This would ensure the check valve was closed when the piston begins its operation. This technique will work adequately at the lower frequencies in the range of interest. However, at higher frequencies, such as those above 500 Hz, where the rise time of the check valve becomes longer than the duration of the cycle, the maximum displacement achieved by the check valve would simply be limited to the position physically achievable in that time period. Even though this actuator arrangement would not produce ideal performance at the higher frequencies it still would provide some impedance to the reversal of flow, much more so than a passive check valve at these frequencies.

At this point it was necessary to find a valve that could be mounted to the actuator. Purchasing a valve that was specifically designed to be mounted to an actuator facilitated the attachment of our piezo-ceramic actuator. A Parker/Skinner poppet valve, Skinner 72218BN, was selected that was well-suited for use with the fuel we were using. This valve was sold with a solenoid actuator already mounted to it, but this actuator could easily be removed. The piezo-ceramic actuator was mated with the existing valve stem using an adapter that was fabricated to clamp on the part of the valve stem that protruded from the valve body. The finished check valve assembly can be seen in Figure 3.17.

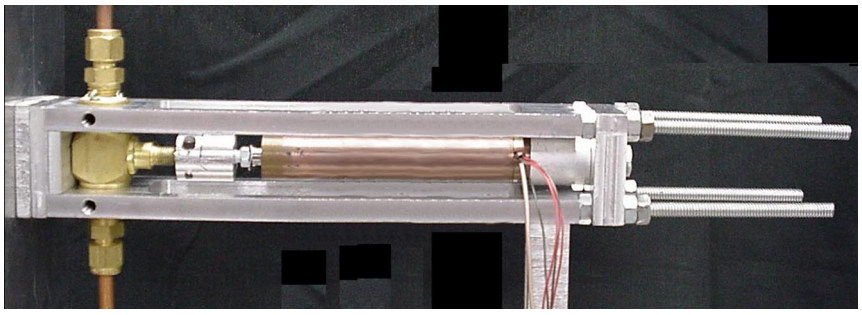

Figure 3.17 Completed check valve assembly

3.6 Fuel Injector Controller

The fuel injector controller that provides signals to operate the fuel injector components now needed to be designed and constructed. It was necessary at this point to examine the signals needed to operate the piston and check valve components of the fuel injector as well as address how to create and provide these signals. Because it was desired that the fuel injection system be able to produce a specific flow profile it was essential that the piston be able to realize a specific displacement profile, which corresponded to the desired flow profile. Thus, the development of a closed loop fuel injector controller, incorporating a displacement feedback controller for the piston assembly component of the fuel injector, was explored. The performance of the fuel injection system when using this closed loop fuel injector controller could then be compared to the performance when using the open loop controller to determine if it was able to modulate the flow better.

3.6.1 Piston and Check Valve Assembly Signals

There were two signals that needed to be created to operate this fuel injector, one signal for the piston and the other for the check valve. As was discussed in Section 3.5, the fuel injector operates by coordinating the motion of the piston and check valve. During the first half-period of the cycle, the check valve is closed while the piston produces a certain flow profile. During the second half of the cycle, the check valve opens, allowing the steady state flow rate, while the piston returns to its original position to begin the next cycle. Since the piston assembly would provide a piston displacement that is proportional to the voltage signal sent to the piston's amplifier, it was necessary to generate a displacement signal that corresponded to the proper flow profile. This displacement signal could be found using the generalized relationship found previously in Section 3.5.1 between flow rate and volume.

$$V(t) = \begin{cases} \int_0^t \left(Q_{ss}(t) + Q_{peak}\sin(2\pi ft)\right)dt & 0 \le t \le T/2 \\ \int_t^T Q_{ss}(t)dt & T/2 \le t \le T \end{cases} \tag{3.16}$$

$$V(t) = \pi \frac{d^2}{4} x(t) \tag{3.17}$$

Solving for x(t) over the first half-period of the cycle yields,

$$x(t) = \frac{4}{\pi d^2} \int_0^t \left(Q_{ss}(t) + Q_{peak} \sin(2\pi f t) \right) dt \tag{3.18}$$

This relationship says that the displacement signal for the piston that corresponds to the desired flow profile is simply the integral of the flow profile times a constant. The way that this signal could be realized in a computer is first by querying the user for Q_{ss}, $\%Q_{peak}$ and the operating frequency. The flow profile signal could then be constructed in the computer with the aid of a signal generator. This signal could be integrated in real time, multiplied by the correct constant and then sent through a digital-to-analog converter to the piston's amplifier. This relationship, however, would only be valid for the first half-period of the cycle. During the second half of the cycle, the piston must be returned to its original position. A convenient way to do this would be to simply mirror the displacement signal from the first half-period of the cycle to the second. Because the displacement signal is constructed by integrating the flow profile, an artificial flow profile signal for the second half-period of the cycle must be provided such that, when integrated, it would produce the mirrored displacement signal. One way to do this would be to add a sine wave to a pulse wave such that they create a signal that is oddly symmetric about the origin and whose mean per cycle is zero. The integral of this signal would then be a signal, symmetric about the half-period, whose value at the beginning and end of a cycle would be zero. This technique is easily illustrated graphically as can be seen in Figure 3.18.

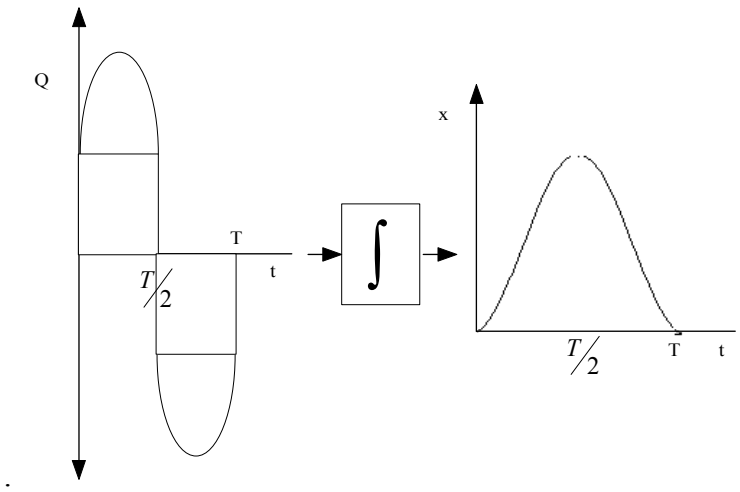

Figure 3.18 Flow profile that when integrated would produce displacement signal symmetric about the half-period

This signal could easily be created using a computer and a data acquisition system. A schematic of the signal processing necessary to create this signal can be seen in Figure 3.19. The comparator shown in this schematic outputs a value of 1 if the value of the input signal is larger than 0 and outputs a value of -1 if the value of the input signal is smaller than 0.

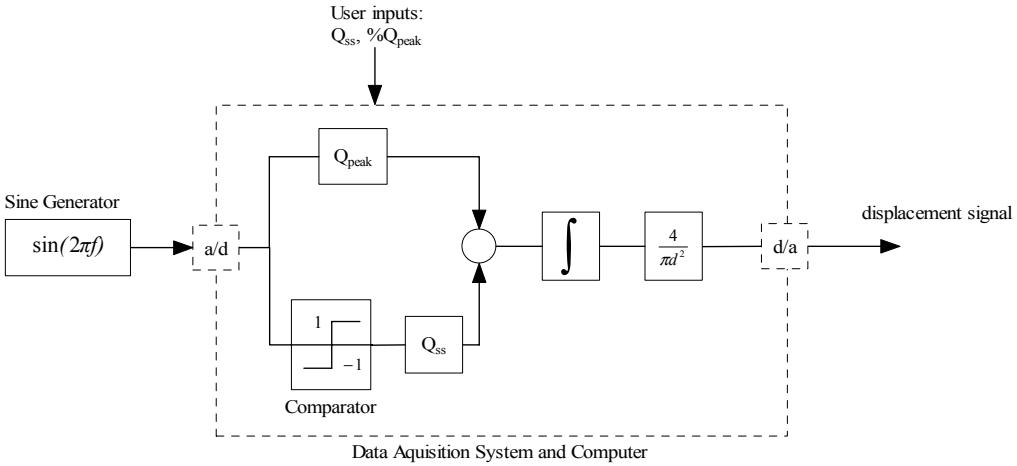

Figure 3.19 Piston signal generator

The signal required to operate the check valve is not as complicated as that for the piston. Because the check valve was designed to be closed for the first half-period of the cycle and open for the remainder of the period, a pulse wave could be created that is positive through the first half-period of the cycle and zero for the remainder. A schematic showing how this signal could be created can be seen in Figure 3.20. The comparator

shown in this schematic outputs a value of 1 if the value of the input signal is larger than 0, and outputs a value of 0 if the value of the input signal is smaller than 0.

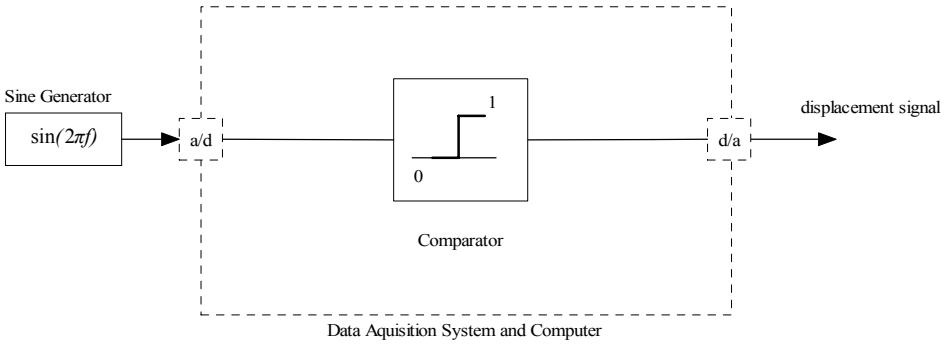

Figure 3.20 Check valve signal generator

All of the necessary signals required to operate the fuel injector could now be generated. As a note, all of the data acquisition and signal processing required for the operation of the fuel injection system was done using a Dspace, version 1103, data acquisition system in conjunction with Control Desk software. This data acquisition system had 8 simultaneous sample and hold a/d channels and 8 simultaneous sample and hold d/a channels. The Control Desk software allowed the implementation of C code and Simulink programs in real time to perform the signal processing.

3.6.2 Open Loop Fuel Injector Controller

Open loop operation of the fuel injector would entail first connecting the piston and check valve assemblies into the fuel line, then connecting the amplifiers for the piston and check valve assemblies to the corresponding assembly and signal generator. The user would then adjust the fuel supply tank pressure to provide a certain mean flow rate and then enter this mean fuel flow rate, desired modulation and operating frequency into the computer interface. A schematic of the open loop fuel injector system can be seen in Figure 3.21.

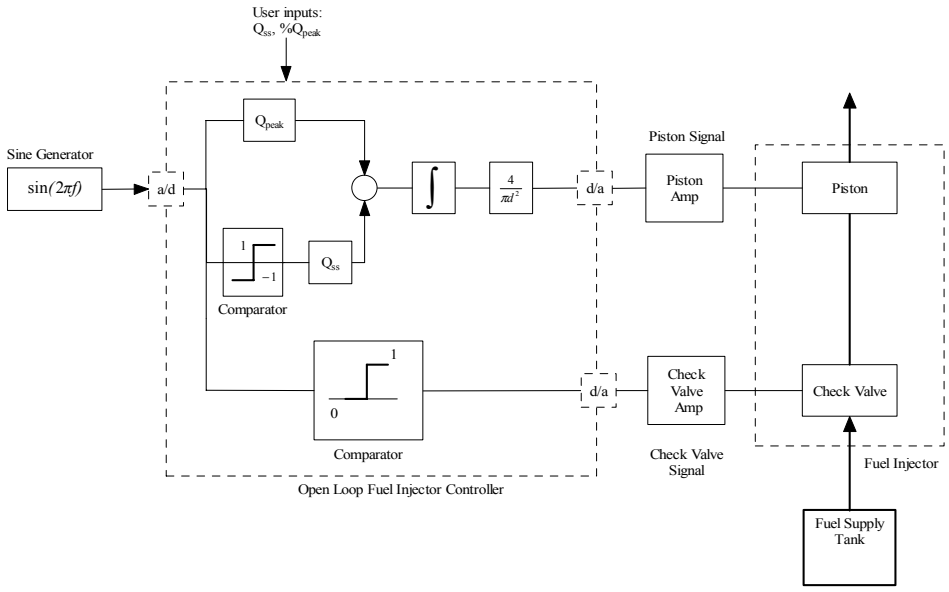

Figure 3.21 Open loop fuel injector system

3.6.3 Closed Loop Fuel injector Operation

Because it was desired that the fuel injection system be able to produce a specific flow profile it was essential that the piston be able to realize a specific displacement profile, which corresponded to the desired flow profile. Thus, the development of a closed loop fuel injector controller, incorporating a displacement feedback controller for the piston assembly component of the fuel injector, was explored. If the displacement of the piston could be measured, this signal could be used in a position feedback controller to track a reference input. A simple block diagram of this controller is shown in Figure 3.22.

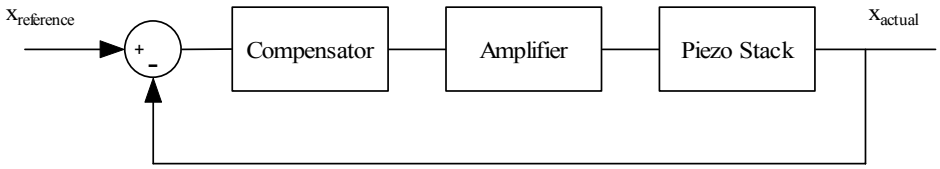

Figure 3.22 Simple displacement feedback control block diagram

The piezo-ceramic actuators were purchased with strain gages mounted to the stack. These strain gages allow the measurement of the displacement of the piston assembly during operation. In order to measure a signal using these strain gages they had to be connected in a half bridge configuration to a strain gage amplifier. After calibrating the

strain gage amplifier to provide specific voltage for a known displacement, the signal from the strain gage amplifier could be used to close the loop, as shown in Figure 3.22. This feedback controller could be incorporated into the fuel injector system as shown in Figure 3.23.

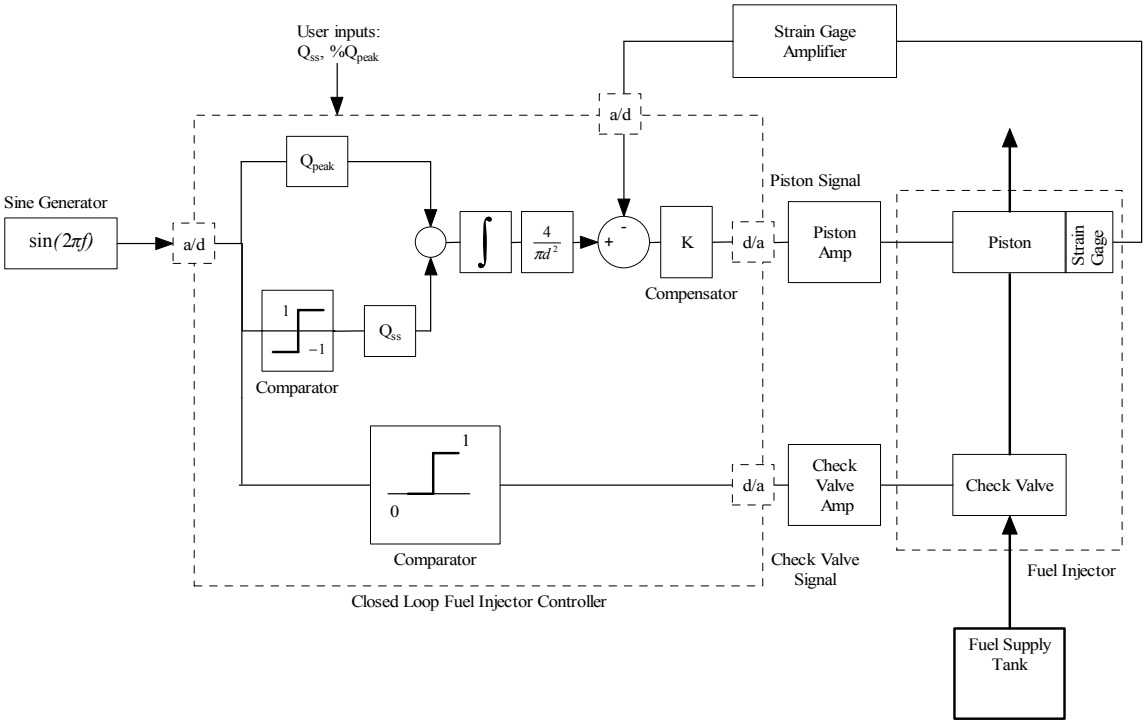

Figure 3.23 Schematic of closed loop fuel injector system

The design of the compensator, K, for the piston assembly feedback controller first requires some knowledge of the dynamics of the piston assembly. Thus, the design of the compensator will be discussed in Section 4.3 after the appropriate dynamic testing results have been presented.

3.7 Combustion Control System

Finally, all of the components required for the combustion control system have been completed. As a review the combustion control system consists of the pressure sensor, phase delay, fuel injector controller and the fuel injector, as seen in Figure 3.4. A schematic diagram showing how these components are connected with each other and the combustor can be seen in Figure 3.24.

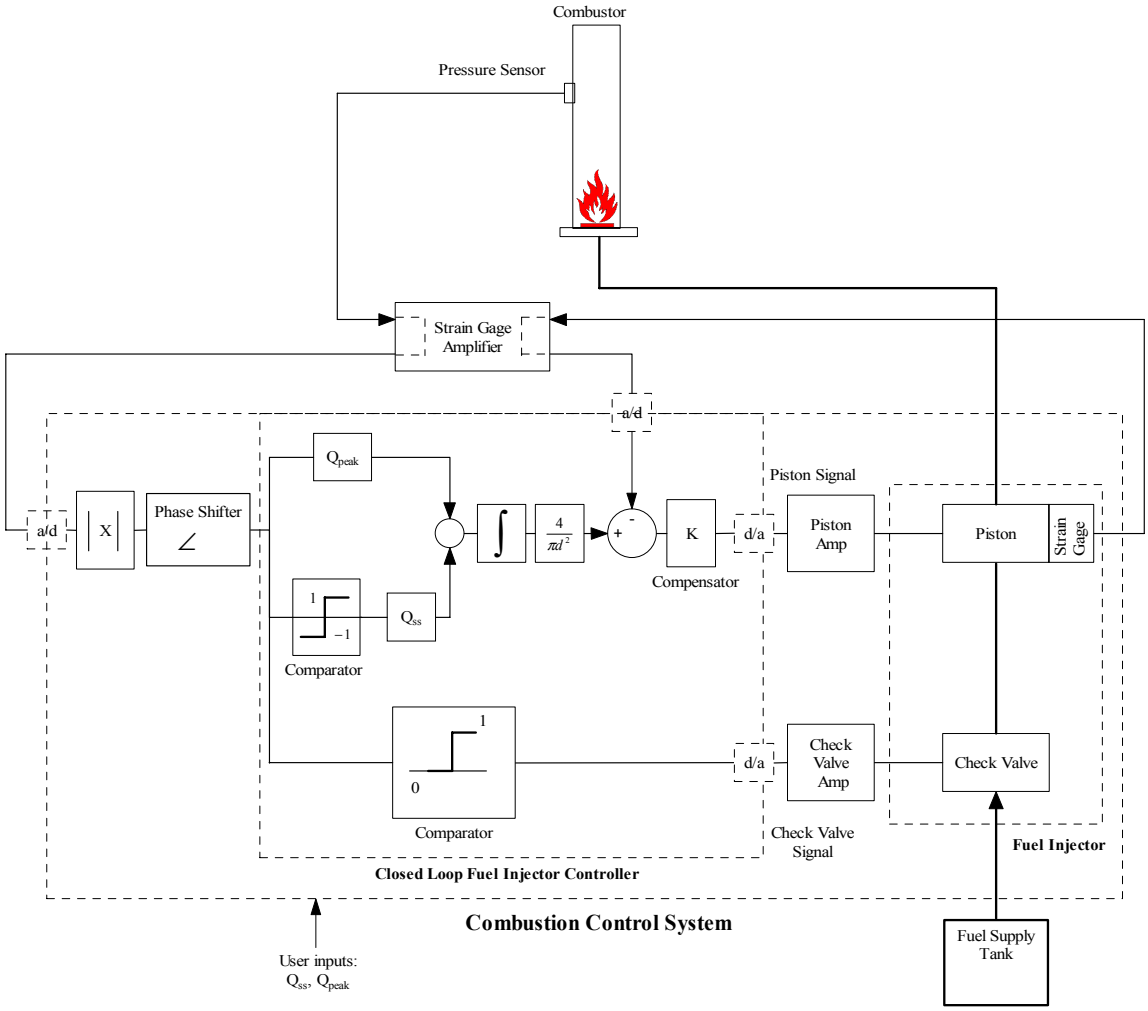

Figure 3.24 Combustion control system schematic

The Simulink program responsible for all of the signal processing performed to operate this combustion control system is included in Appendix A, along with a brief description of the program.

4 Fuel Injector Testing

4.1 Piezo-ceramic Stack Testing and Characterization

Several tests were performed to characterize the performance of the piezo-ceramic stack that was purchased as an actuator for the piston assembly. Free displacement tests were performed to determine if the actuator could achieve the manufacturer's claimed range of displacement. Tests were also performed to measure the frequency response function of the actuator and amplifier to be used in the piston assembly. This was necessary for the design of the closed loop control system for the piston assembly component of the fuel injector.

4.1.1 Free Displacement Testing

The first apparatus used to measure free displacement was a laser vibrometer. The laser vibrometer operates by shining a laser beam onto a reflective surface on an object being measured, which then reflects the beam back into the vibrometer. By measuring the interaction of the original beam and the reflected beam, the vibrometer can calculate the velocity of the object, as well as its displacement. Laser vibrometers can measure small displacements in the micron range very accurately over a large bandwidth. Measurements were first taken using this laser vibrometer not only to ensure proper operation of the stack, but also as a metric to compare against the displacement signal provided by the strain gages, which will be used to provide the displacement of the stack during the operation of the fuel injector.

After mounting the piezo-ceramic stack to a large cement support, the laser vibrometer was carefully aligned and the stack was connected to its amplifier. The laser vibrometer was zeroed when the amplifier was delivering 0 V. Then the full voltage signal was applied to the stack and the results of the laser vibrometer were recorded. The free displacement of the PSt150/14/20 actuator at 150 V was 20.2 microns. This was very close to the 20 micron at 150 V specification provided by the manufacturer.

The next free displacement test involved examining the stack's hysteresis. This test evaluated the linearity of the piezo-ceramic stack. A full range, low frequency sinusoidal input signal was given to the amplifier such that amplifier provided a 2 Hz sinusoid whose peak was at 150 V and trough at 0 V. This signal spanned the entire positive operating range of the amplifier and actuator. The displacement and applied voltage were recorded over one cycle and then plotted against each other as can be seen in Figure 4.1.

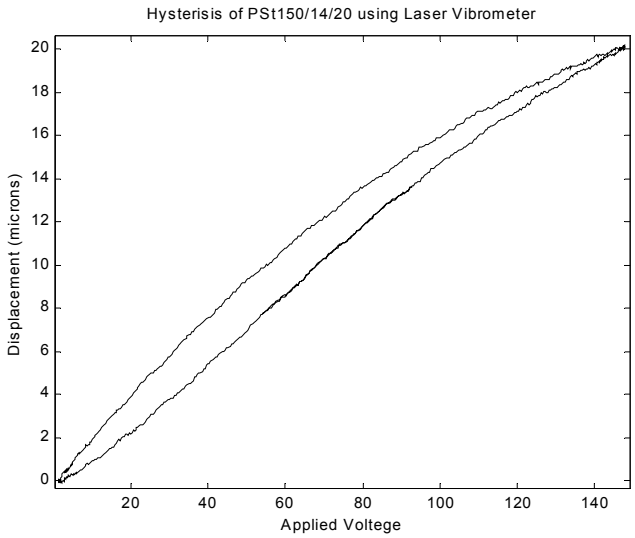

Figure 4.1 Hysteresis plot using laser vibrometer.

One can see that there was some amount of hysteresis in this actuator indicating that the actuator is slightly nonlinear. This small nonlinearity was not a detriment to our design aside from the fact that at high frequencies hysteresis created a significant amount of self-heating in the material.

4.1.2 Frequency Response

To experimentally find the frequency response of the desired components, the system was excited with a chirp signal and the HP Dynamic signal analyzer was used to take the FFT of input and output signals. Frequency responses were examined for the amplifier, actuator and the coupled amplifier and actuator system. It was the frequency response function of the coupled amplifier and actuator that was most important, as these components compose the plant for the closed loop piston assembly component of the fuel

injector discussed in Section 3.6.3. The frequency responses of the above components were examined at different operating levels to evaluate the performance of the actuator and amplifier over the full range of operation.

Amplifier Dynamics

The frequency response of the amplifier was measured between the source signal provided from the amplifier and the power signal generated by the amplifier. It was important to examine the frequency response of the amplifier while it was driving its actuator, because the amplifier was specifically designed to operate while driving a capacitive load. Operating the amplifier without a load could cause the amplifier to malfunction and even be destroyed. Because the amplifier did not have an operating range that was symmetric about 0 V it was not possible to simply send zero mean voltage signals to the amplifier without first adding a DC offset. The chirp signal generated by the HP dynamic signal analyzer has a maximum positive value equal in magnitude to its maximum negative value. A positive DC offset of the maximum magnitude of the chirp signal would provide an adjusted chirp signal whose magnitude would always be larger then 0 V. To examine different operating ranges of the amplifier would then require calculation of the input signal magnitude as well as the DC offset that would provide a signal spanning the range of interest. This concept is easily demonstrated graphically as can be seen in Figure 4.2 for operating ranges of 0-25 V, 0-50 V, 0-100 V and 0-150 V.

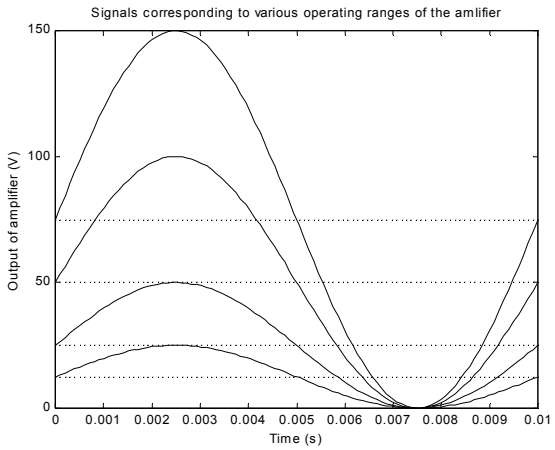

Figure 4.2 Signal corresponding to different operating levels of the amplifier

The signals corresponding to the operating ranges seen in Figure 4.2 represent the ranges for which the amplifier was tested. The input signal magnitude and DC offset required to create these signals are recorded in Table 4.1.

Operating Range	Input Signal Amplitude V_{peak}	Required DC offset V_{DC}
0-25V	0.42	12.5
0-50V	0.83	25
0-100V	1.66	50
0-150V	2.50	75

Table 4.1 Required signals for various operating ranges

Using chirp signals designed to evaluate the amplifiers performance over these operating ranges produced the frequency responses for the amplifier that can be seen in Figure 4.3.

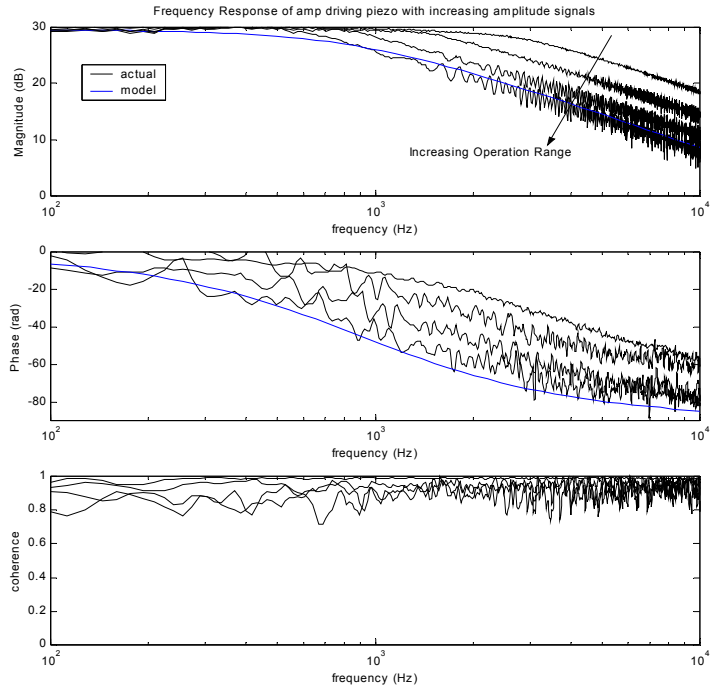

Figure 4.3 Frequency response of the amplifier

The frequency response labeled as the model in Figure 4.3 consists of a gain and one real pole at 800 Hz. One can see that the amplifier behaves as a simple low pass filter whose break frequency changes slightly based on the level of the range of operation. For smaller forcing amplitudes, the break frequency was higher than those associated with the larger forcing amplitudes. This was physically the result of the piezo-ceramic stack's

electrical capacitance changing based on forcing level, a known behavior of piezo-ceramic materials. For higher signal amplitudes, the piezo-ceramic stack's capacitance increases. Because the peak current of the amplifier was fixed, the increased capacitance had the effect of lowering the break frequency of the amplifier.

The result of this testing was that, although the break frequency changes slightly depending on the level of the range of operation, the amplifier could be modeled conservatively as a low pass filter with a break frequency of approximately 800 Hz.

Actuator Dynamics

The frequency response of the actuator, measured from the power signal generated by the amplifier to the laser vibrometer signal, was also evaluated over the same ranges of operation as those used in testing the amplifier. The results of this testing can be seen in Figure 4.4.

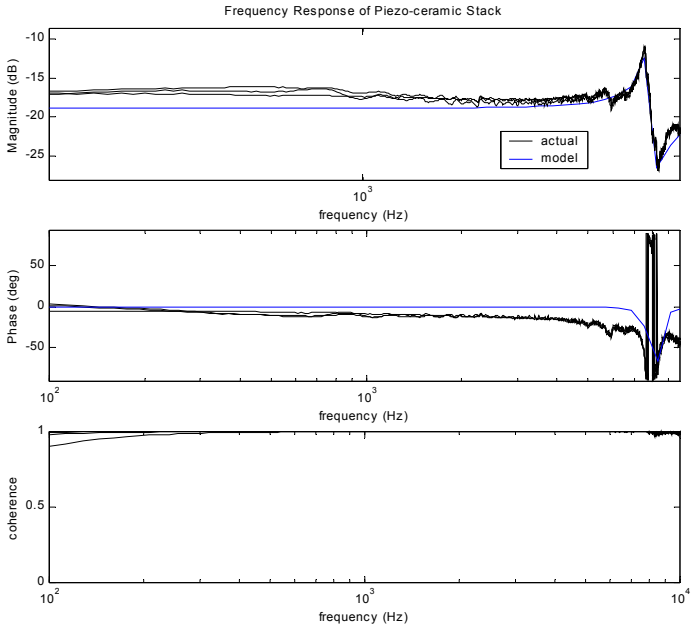

Figure 4.4 Frequency response of the actuator

The frequency response of the piezo-ceramic stack was nearly identical for each forcing level. This was an indication of the stacks relative linearity. It was clear that the only dynamics present in the actuator were above 7 kHz, well above the operating range of the fuel injection system. The model shown in Figure 4.4 consists of a pair of complex conjugate poles at 7.8 kHz with a damping ratio of 5% and a pair of complex conjugate zeros at 8.3 kHz also with a damping ratio of 5%. The reported natural frequency of the actuator was 30 kHz, a factor of almost 4 times larger than the one measured experimentally. This result could be attributed to the fact that the reported resonant frequency was that of the electrically uncoupled stack, i.e. the stack not connected to an amplifier. Because of the nature of piezo-ceramic materials, the physical properties of the stack, such as the stiffness, depend on the stacks electrical constraints. For instance, the mechanical stiffness of a piezo-ceramic stack whose electrical leads are short-circuited would be higher than the stiffness of the stack when the leads are open. This dictates that the natural frequency of a stack whose electrical leads are short-circuited would be lower than the natural frequency of the stack when the leads are open.

Coupled Actuator and Amplifier Dynamics

It was obvious that the frequency response of the coupled actuator and amplifier, measured from the source signal given to the amplifier to the laser vibrometer signal, should be the sum of the frequency responses of the individual components. The frequency response taken for the coupled actuator and amplifier indeed was found to be the sum of both of the individual components as can be seen in Figure 4.5 for a forcing level of 0-25 V.

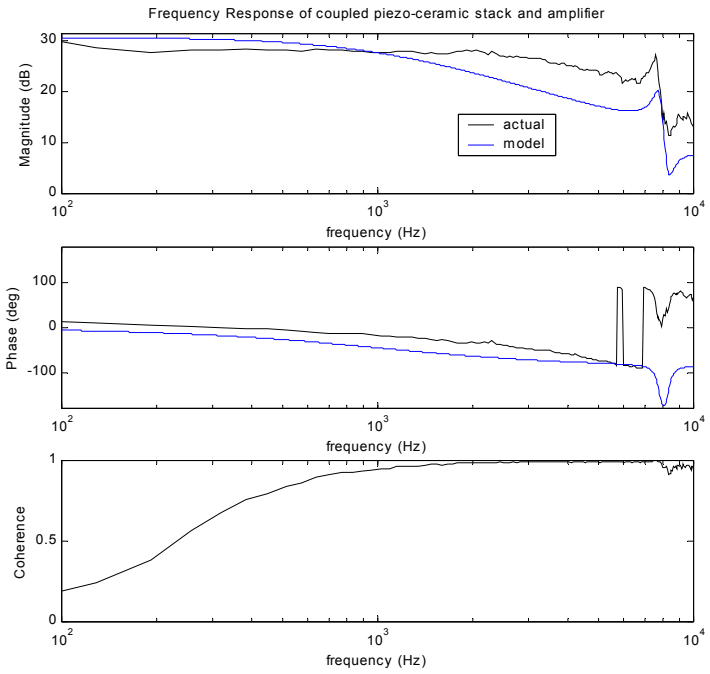

Figure 4.5 Frequency response of coupled actuator and amplifier

The frequency response of the model, formed using the conservative amplifier and stack models, slightly under predicts the magnitude of the actual system after 1kHz. This was a result of the conservative estimate of the amplifier break frequency. The model would better fit the data as the forcing amplitude is increased. This model provides a reasonably accurate tool for use in designing a control system.

4.2 Strain Gage Testing

Because the strain in a piezo-ceramic stack is relatively uniform it was possible to measure the strain in the stack to determine the displacement of its free end. Strain gages provided an easy and efficient way to measure the displacement of the stack while the fuel injector was operating. Because the stack was already characterized using the laser vibrometer, there was already a good basis for comparing the quality of the displacement signal found using the strain gages.

It was necessary at this point to connect the strain gages into a Wheatstone bridge configuration that could be used with a strain gage amplifier to produce a strain related voltage signal. The piezo-ceramic stack that was purchased had two strain gages bonded

to the actual stack. One strain gage was mounted along the axis of the stacks displacement and the other was mounted around the circumference of the stack. These strain gages could be connected in a half bridge configuration such that the circumferentially mounted strain gage could serve as a temperature compensation device. Temperature drift associated with strain gages can be considerably large and self-heating, due to the hysteretic nature of the piezo-ceramic stack, was expected to raise the temperature of the stack during operation. Thus, the ability to incorporate temperature compensation into the Wheatstone bridge circuit was required. In examining Figure 4.6, one can see that the resistance change due to the temperature increase of the two strain gages will cancel each other as a result of the voltage divider across the left half of the bridge. This will leave only the strain related resistance change and allow undisrupted measurement of the strain.

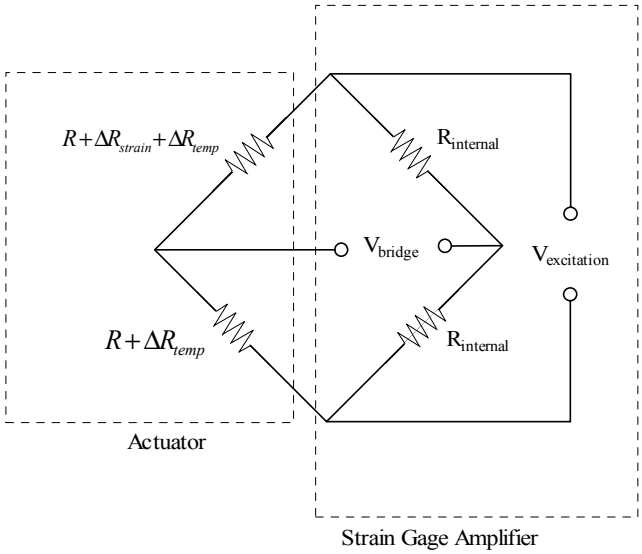

Figure 4.6 Wheatstone bridge schematic

Once the leads from the strain gages were connected appropriately to the strain gage amplifier, the amplifier was zeroed and the bridge was balanced. Then a 150 V signal was given to the stack, which corresponded to a displacement of 20.2 microns, and the gain on the strain gage amplifier was adjusted so as to provide a 10 V signal corresponding to this full range displacement signal. The output of the strain gage amp

was now set to provide a signal proportional to the displacement of the stack according to the relationship $\frac{1}{2}\left(\frac{V_{strain}}{\mu m}\right)$.

An identical hysteresis test was done using the strain gage signal as a measure of displacement that could then be compared to the results found using the laser vibrometer. The strain gage signal quite faithfully reproduced the results that were found using the laser vibrometer as can be seen in Figure 4.7.

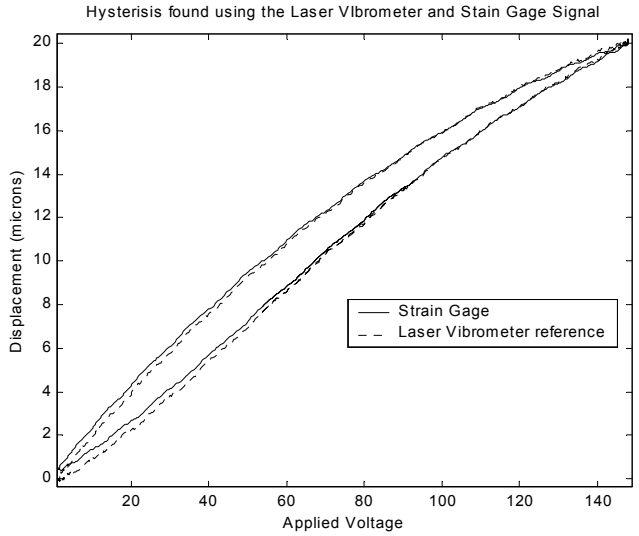

Figure 4.7 Hysteresis plot found using strain gage signal and laser vibrometer

Once again the frequency response testing was performed on the actuator, but this time using the strain gage signal as a measure of displacement. The results of these tests can be seen in Figure 4.8.

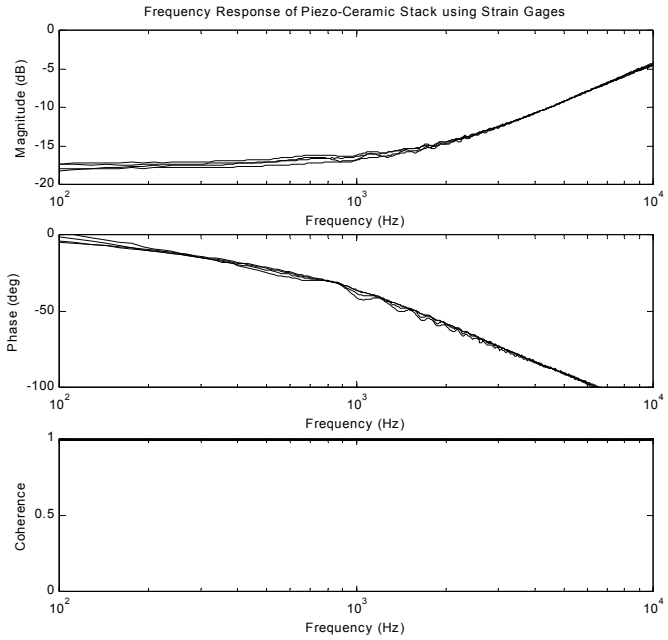

Figure 4.8 Frequency response using the strain gage signal

The frequency responses found using the strain gage signal obviously did not correspond to the frequency responses of the actuator found using the laser vibrometer. One of the first steps taken to examine the cause of this mismatch was to test the frequency response with the excitation voltage on the strain gage amplifier turned off. Because there would be no excitation voltage applied across the strain gage circuit, there should be no bridge voltage measured whatsoever. This however was not the result that was found and can be seen in Figure 4.9.

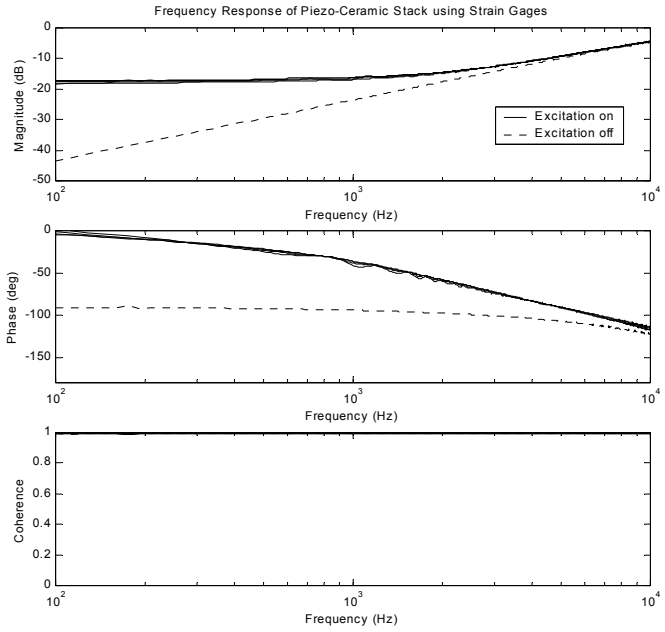

Figure 4.9 Frequency response of the actuator with and without bridge excitation voltage

Clearly the upward trend in the magnitude of the frequency response after 1 kHz, when the strain gage circuit excitation was on, was due to some 'noise' signal. This 'noise' signal was by definition the signal present when the strain gage circuit excitation was off. Because of the configuration of the bridge, the only way that a voltage could be measured at all with the excitation turned off was if a voltage was being induced across the strain gages. This induced voltage would then be the voltage measured across the bridge when there was no excitation voltage.

Two methods were explored to eliminate this noise signal, neither of which were implemented as a final solution. The first method was a simple compensation circuit that involved subtracting out the noise signal. The second method involved the use of an adaptive feed forward controller to eliminate any strain signal that was correlated with the noise. The difficulty in successfully implementing these methods was due to the fact that the noise term, the signal generated by the strain gage amplifier with excitation turned off, could not physically be measured when the strain gage circuit was operating with the excitation on. Thus a signal needed to be created that could represent the noise signal while the bridge excitation was on. It was noticed that the noise term behaved as a differentiator operating on the applied voltage, providing a 20 dB/decade slope in the

frequency response. The relationship between voltage and current in a capacitor, seen in Equation 4.1, shows that the current is the derivative of the voltage times the capacitance.

$$i = C\frac{dV}{dt} \tag{4.1}$$

Thus, if a signal proportional to the current in the piezo-stack could be measured, that signal would represent the noise. This signal could then be scaled to match the amplitude of the noise signal until they were effectively identical.

The current signal for the piezo-ceramic stack was measured by placing a resistor with a small impedance, 2 Ω, electrically in series with the stack. Because this impedance was small relative to the impedance of the stack, 10 MΩ and 7.2 μF, the resistor would only minutely change the behavior of the circuit. The voltage measured across this resistor, which would be proportional to the current, could then be scaled until it had the same magnitude as the noise signal. A frequency response showing the transfer function between the noise signal, V_{noise}, and the adjusted voltage related to the current signal, V_i, can be seen in Figure 4.10.

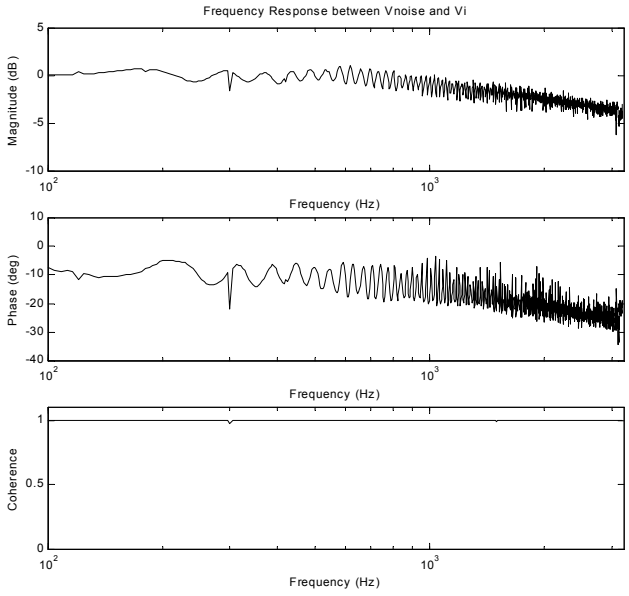

Figure 4.10 Frequency response between the noise signal and the adjusted current signal

One can see that these signals have nearly identical magnitudes and are almost in phase up to 1 kHz, after which the adjusted current signal no longer accurately represents noise

signal. Because this adjusted current signal was limited in how well it could represent the noise signal at these higher frequencies, it only allowed a minor reduction in the noise signal using either of the two previously mentioned methods. With the foresight that the reference tracking controller would take advantage of an integrator, whose slope in the frequency response would cancel that of the noise term, it was hoped that the controller could operate effectively without the need for any compensation of this noise. Fortunately this was the case and the piston assembly controller operated effectively.

4.3 Compensator Design

Now that the dynamics of the actuator and the amplifier have been described, it was possible to design the compensator for use in the piston assembly feedback controller. In the previous sections it was found that the amplifier could be modeled as a simple low pass filter with a break frequency of about 800 Hz and the actuator could be modeled as a set of damped complex conjugate poles near 7.5 kHz. Because the fuel injector was only being designed to operate between 0-700 Hz and because the resonance of the actuator would be attenuated by the roll off of the amplifier, it was decided to model the piezo-ceramic stack as a simple gain. The generic blocks in the controller block diagram discussed in Section 3.6.3 could now be replaced with the approximations found through our testing, being careful to account for the physical units around the loop. The piston assembly feedback controller could now be represented by the schematic found in Figure 4.11.

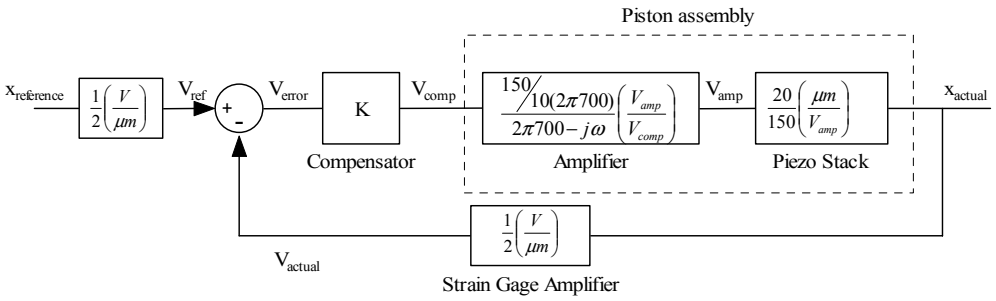

Figure 4.11 Piston assembly feedback controller

The controller was designed using classical techniques. As a first pass for the compensator design, a simple PI compensator was examined. The first step in designing the PI compensator was incorporating an integrator. This integrator would, in effect, try to eliminate the steady state error between the reference and actual signal. Gain could be added to the compensator that would increase the bandwidth of the system. The gain could be increased until the maximum control effort available was reached. Thus the compensator would be of the form found in Equation 4.2

$$K = \frac{K_p}{s} \tag{4.2}$$

This was a very simple compensator and required little effort to implement.

Before the controller was actually implemented on the piston assembly, a simulation was performed in Simulink to estimate the gain required for the actual controller and predict how well the system would track the designed reference input. Since the fuel injector, during combustion control would operate at near 100 Hz on our combustor rig, the performance using the reference displacement signal that corresponded to a 100%Q_{peak} modulation was examined at 100 Hz. The results of this simulation, using a gain of 5000, can be seen in Figure 4.12.

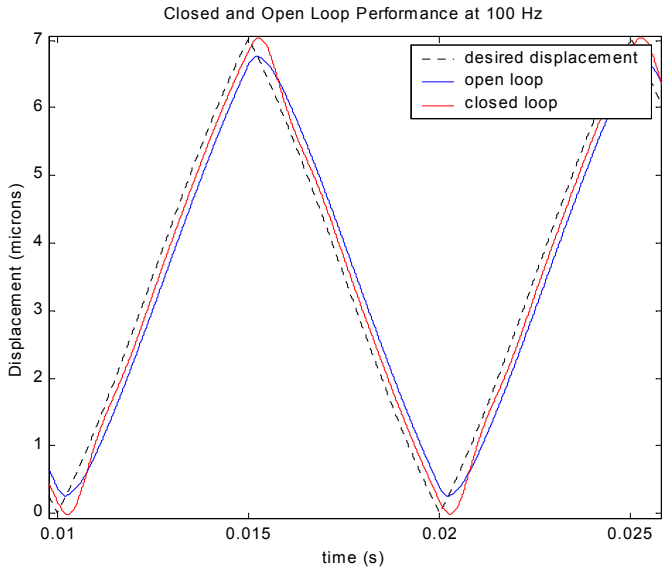

Figure 4.12 Closed loop performance simulation

It was apparent that the dynamics of the plant have not yet begun to affect the performance of the system drastically. This was expected since the dynamics of the plant do not manifest themselves until after several hundred hertz. One can see, however, that the open loop system does have a problem tracking the reference through its discontinuities. Because this reference signal was essentially composed of a sinusoid added to a saw tooth waveform, both at the same fundamental frequency, the harmonic content of the reference displacement signal was not only at this fundamental frequency. The saw tooth waveform has frequency content in the harmonics of the fundamental frequency. The magnitude of the harmonics in the reference displacement signal, relative to that of the fundamental frequency, was related to the relative magnitude of the sinusoidal and saw tooth waveforms. Thus it would be expected that the controller would actually provide better tracking at higher levels of modulation. This is because the frequency content in the reference displacement signal, corresponding to the higher modulation flow profile, would be dominated by the sinusoidal modulation component whereas the reference displacement signal corresponding to lower modulation flow profile would be dominated by the saw tooth waveform.

Satisfied that this controller simulation could produce adequate performance using the model, it was then implemented on the piston assembly. The resulting closed loop performance can be seen in Figure 4.13.

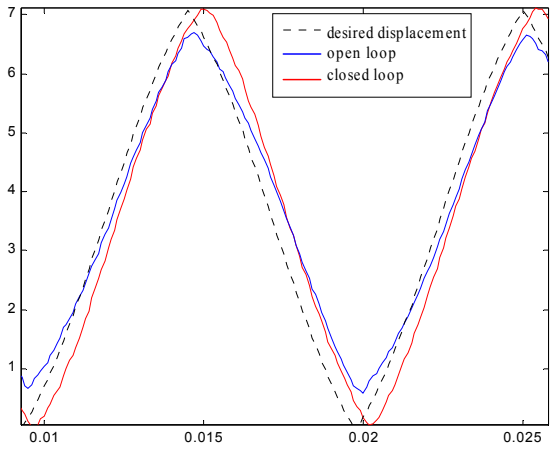

Figure 4.13 Actual closed loop performance using feedback controller

The results of the experimental closed loop testing showed performance similar to that of the performance predicted by the model. It was also apparent that closed loop piston assembly did a better job tracking the reference than the open loop piston assembly.

4.4 Check Valve Characterization

The first test performed with a fuel injector component physically placed in the fuel line was the check valve calibration. The performance of the check valve was examined to assure it could completely stop the flow in the closed position and produce a negligible pressure drop across it when in the open position.

This testing involved mounting the check valve in the fuel line in between the tank and the atomizer. To measure the volume of fuel being expressed from the atomizer, it was necessary to perform this testing on the lab table, as it would be inconvenient to perform these measurements while the atomizer was mounted in the combustor. This test setup can be seen in Figure 4.14.

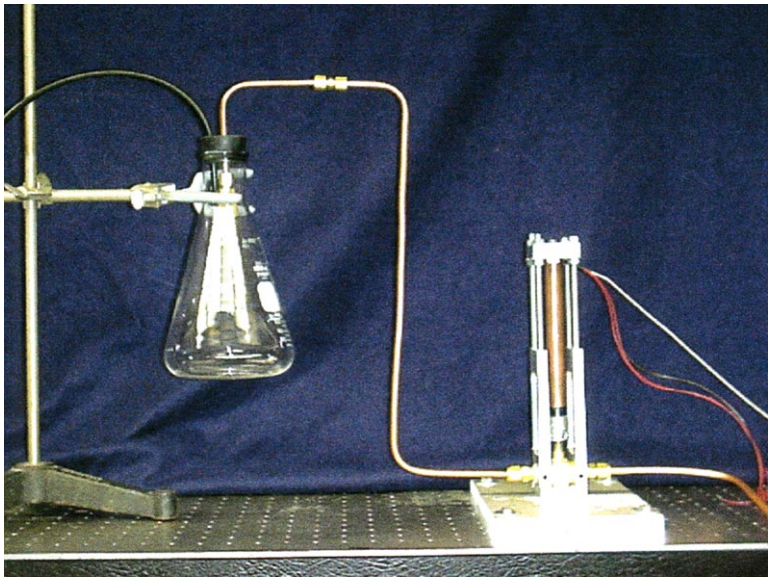

Figure 4.14 Test setup for check valve calibration

The calibration of the check valve involved first pressurizing the fuel line and letting the fuel run through the system, with the check valve wide open, for several minutes so as to flush out any air in the line. After several minutes of allowing the fuel to run through the system, the voltage corresponding to the maximum displacement signal, 1000V, was applied to the check valve assembly stack. The stack and its mount were then pushed

down by hand, seating the valve until the flow stopped. Nuts were used to secure the piezo-ceramic stack's mounting plate to the valve enclosure. The coupler that attached the stack to the valve stem, seen in Figure 4.15, was then used to fine-tune the displacement of the valve to provide only the minimum amount of closure necessary to entirely stop the flow.

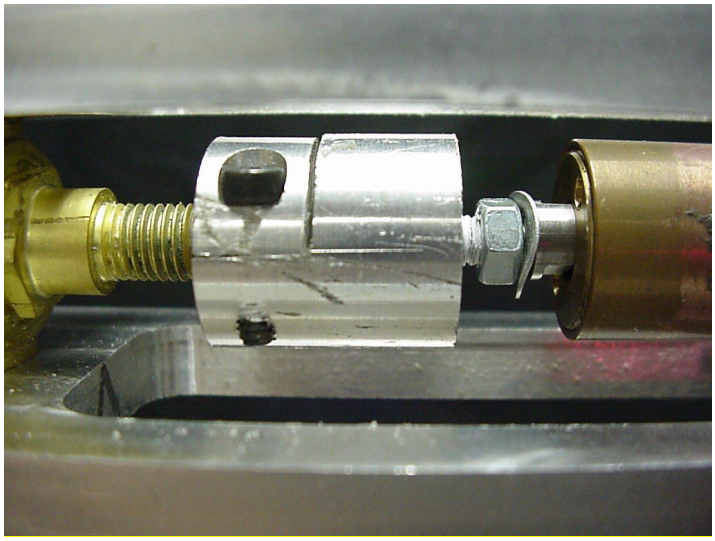

Figure 4.15 Coupling device for the valve stem to the piezo-ceramic stack

This was done by rotating the coupler, which was engaged to the treaded rod protruding from the stack, such that the coupler and valve stem would move up or down relative to the stack based on the direction the adaptor was turned. When this minimal closure position was reached, the voltage was then removed from the stack allowing the opening of the check valve. This open position will be referred to as the 'calibration point'. The flow rate with the valve in the open position was then measured over a fixed interval of time. Based on the volume of fuel expressed in this amount of time the pressure drop across the check valve in the open position could then be calculated.

It was found that the ability of the check valve to meet both requirements, completely stopping the flow when closed and providing negligible pressure drop when open, was very closely related to the calibration point of the check valve. It was relatively difficult to achieve the full function of the check valve using the 150 microns available. Once an optimal calibration point was found for the check valve, even a minor offset in the calibration point significantly diminished the valve's effectiveness. It was decided to

examine the sensitivity of the calibration point of the check valve on the valve's performance. In order to do this it was necessary to relate the relative distances of the check valve calibration points. Using the pitch of the threaded rod connecting the adapter to the stack, it was possible to calculate the displacement of the adapter corresponding to a degree of turn. This relationship was found to be 0.9 microns per degree. Thus the performance of the check valve could be evaluated for different calibration settings a known distance from each other. This test was performed for three calibration points, the results of which can be seen in Figure 4.16.

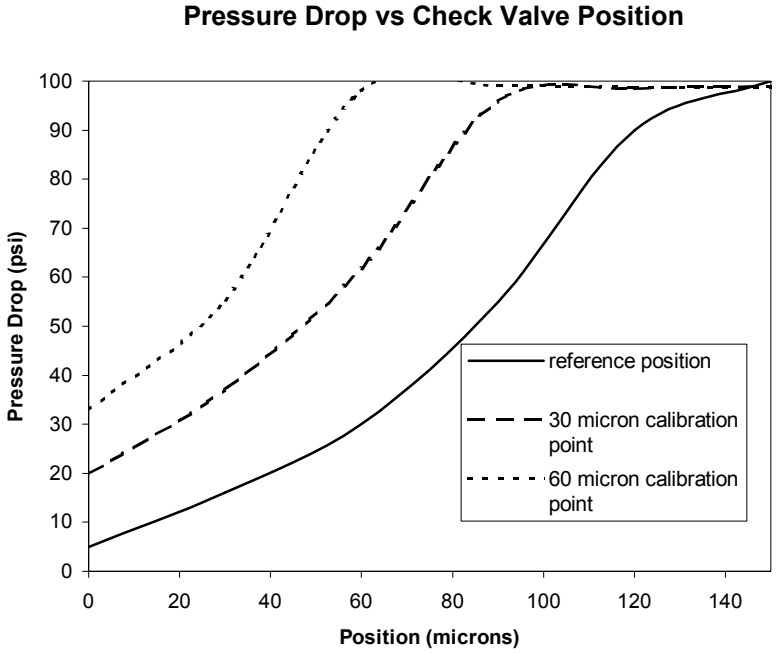

Figure 4.16 Pressure drop across check valve vs. displacement

One can see that the entire 150 microns of displacement was required to make the check valve as effective as possible. The result of this testing was that the check valve could perform the function needed for the proper operation of the fuel injector, but there was little room for error in the calibration process.

4.5 Inline Fuel Injector Testing

Now that the components of the fuel injector were tested and found to be working properly these components were incorporated into the fuel injection system and the performance of the fuel injector was tested. The first test to evaluate the performance of the fuel injector involved monitoring the line pressure during modulation. These pressures could then be compared the pressures predicted through our design process. The first step in this testing was to connect the piston and check valve into the fuel line between the supply tank and the atomizer, the check valve upstream of the piston. An Entran Pressure transducer, EPX-V0-500, was installed in the fuel line, downstream of the piston, to measure the effect of the piston on the line pressure. As with the check valve testing, a bleed valve was placed directly upstream of the atomizer to allow the air to be bled from the system. Once again, this testing was performed on the lab table to facilitate the measurement and collection of the fuel flow.

The pressure transducer was mounted into a machined piece of aluminum, which allowed the pressure transducer to be aligned properly in the flow. The inner diameter of the mount was designed to match that of the fuel line so as not to create any sudden expansions or contractions of the flow, allowing an accurate measurement of the line pressure. This transducer operated using a diaphragm, with a piezo-restrictive device embedded in it, to measure gage pressure, as can be seen in Figure 4.17. This sensor was capable of AC coupled dynamic measurements up to 30 kHz.

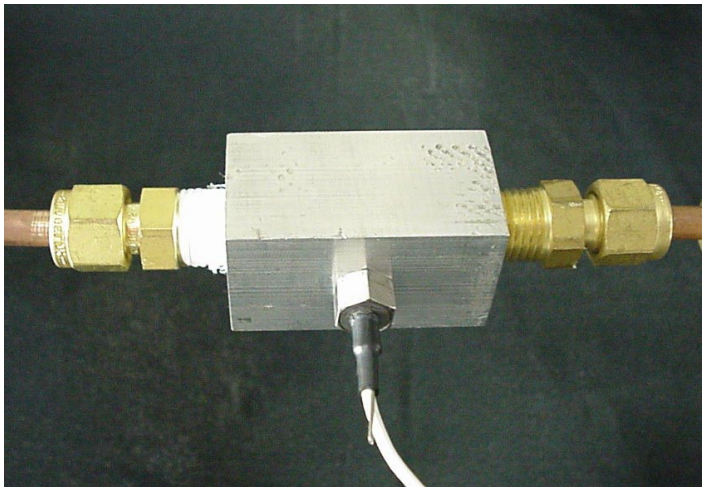

Figure 4.17 Pressure transducer and housing

With all of the proper fuel injector and measurement components installed in the fuel line, the fuel injector controller was connected to the fuel injector components through the appropriate amplifiers. The fuel injector was then ready to be operated. The fuel injection system was operated at a modulation level of $40\%_{Qpeak}$ where we expected to encounter a 240 psi peak pressure, but were surprised to find only a peak pressure of 105 psi. This would predict a modulation level of only about $1\%_{Qpeak}$. At this point, several tests were performed to help diagnose the problem and find a solution.

4.5.1 Diagnosis and Action

The first test that was performed to diagnose this problem involved leaving the fuel injector in the fuel supply line but only using the check valve to examine the impact of suddenly closing off the fuel supply on the flow rate through the atomizer. After bleeding the air and letting the fuel flow for several minutes it was found that suddenly closing the atomizer produced approximately a 0.5 s rise time, from atmospheric to full line pressure, and a 1 s fall time, from full line pressure to atmospheric pressure. The flow rate, monitored visibly, followed the rise and fall times seen using the line pressure sensor. The volume of fluid expressed from the atomizer after the check valve was closed was measured and found to consistently be $5cm^3$. The enclosed volume of fluid sealed off between the check valve and the atomizer was liberally approximated to be about 50 cm^3. This said that roughly 10% of the volume of fluid in this sealed region was being expelled from the atomizer after the check valve was closed. This in turn implied that there was some capacitive volumetric storage nature to the volume of fluid in the fuel

line. The cause of this observed compressibility was unknown. The results of this test explain why during operation, the fuel injector had such a small effect on the line pressure. After all, the volumetric displacement of the piston per cycle at a modulation level of $40\%_{Qpeak}$ at 100 Hz is only 0.004 cm^3, a factor 1400 times smaller than the volumetric capacitance measured in the fuel line at 100 psi.

It was essential at this point to eliminate the cause of this discrepancy between the modeled incompressible behavior and the highly compressible actual behavior of the fluid in the fuel line. The 10% value of compressibility was far greater than could be accounted for by the actual compression of the ethanol at 100 psi. More likely explanations would include air in pockets that could not be dislodged even after flushing the system or physical deformations of all or some components of the system including the piping, the piston cylinder, the piston face or the o-ring seal between the piston and piston cylinder.

Because there were obvious places in the system as it was presently arranged, where air could be trapped, a new mounting system was designed to ensure the minimization of these areas. This involved standing the piston assembly upright and mounting the rest of the components such that the flow could travel vertically, from bottom to top, through the system.

The fuel injector was then reinserted into the fuel line. The system was bled again and the response of closing the check valve on the line pressure and flow was remeasured. This reduced the rise and fall time of the line pressure to approximately 0.1 and 0.5 seconds respectively and the volume of fluid expelled from the atomizer was reduced from 5 cm^3 to 1 cm^3. This was an improvement but still only allowed for a minimum effect of the fuel injector on the line pressure. At this point it was decided to try another quick test to determine the pistons ability to raise the pressure of a totally closed volume of fluid. The atomizer was replaced with a cap and after bleeding the fuel line the check valve was closed, creating a totally closed volume of fluid. The piston was slowly pushed forward and a peak pressure of 107 psi, a rise of 7 psi, was measured at the maximum piston displacement. This pressure was maintained when the piston was held in its maximum position and the pressure returned to the original pressure when the

piston was returned to its rest position. As a note, the relationship between piston displacement and pressure increase appeared very linear. Assuming this relationship would remain linear for higher piston displacements and considering that at full stroke the piston now displaces 20 microns, it would require a piston displacement of over 400 microns to provide the additional 140 psi increase necessary for $40\%_{Qpeak}$ modulation!

It was decided at this point, since the actuator being used on the check valve could produce a displacement of 150 microns, to switch the actuators of the piston and check valve components to see if adding this extra piston displacement could help increase the line pressure. Minor adjustments had to be made to the piston and check valve housing to switch the actuators, but this could be accomplished without majorly affecting the design. This new and final fuel injector arrangement can be seen in Figure 4.18.

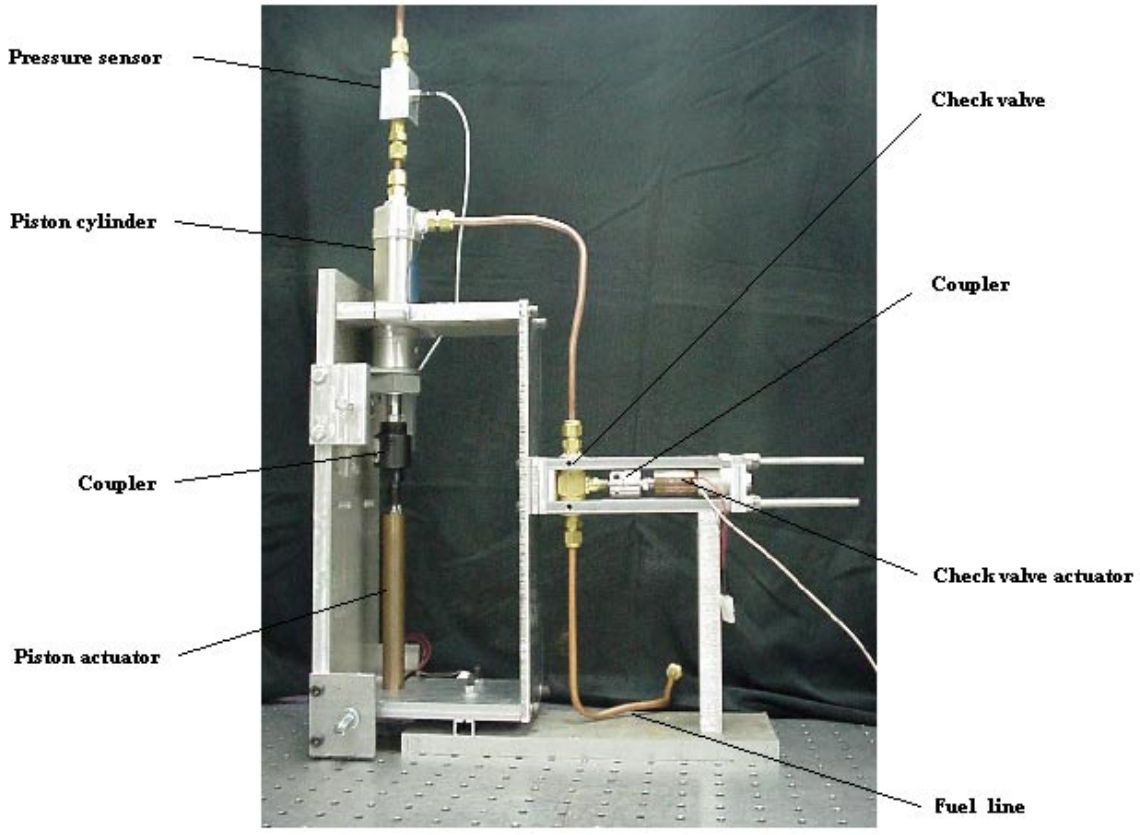

Figure 4.18 Final arrangement of fuel injector components

Performing the same test as before on the totally closed volume of fluid, it was found that the piston attached to the 150 micron displacement actuator could produce a peak

pressure of 158 psi. If this pressure could be created during operation it would correspond to approximately 19%$_{Qpeak}$ of modulation.

Unfortunately, the check valve now could only produce 20 microns of displacement. This was not enough to provide the complete function of the check valve. A solution for this limitation was to increase the tank pressure to its maximum level of 160 psi. The check valve could be calibrated to produce a 60 psi pressure drop across it in the open position, thus providing the necessary 100 psi pressure drop across the atomizer necessary for the steady state flow rate of 0.42 cm^3/s. In the closed position the check valve would not be able to completely stop flow reversal, but as a result of the increased tank supply pressure the pressure drop across the check valve that would result in the reversal of flow would be decreased. Thus, the reversal of flow could be minimized.

At this point, the reason for the compressibility effect seen within the volume of fluid closed off by the check valve was still not totally understood. Even though efforts were made to try to remove air from the line, 1 cm^3 of air is not a large volume for an air bubble and it could be entirely possible that the compressibility still observed had to do with some volume of air still present in the fuel line. A small deformation of the piston seal or the piston face could also account for the 1 cm^3 of compressibility. Future testing could involve finding a better way to bleed the fuel line to ensure absolutely no air be present and evaluation of the piston cylinder and piston face during operation to detect any unaccounted deformation. At this point, it was decided that everything had been done, within the time constraints of this project, to maximize the performance of the fuel injector. In summary, the steps taken to address this problem were to bleed the fuel line, arrange the fuel injector components to minimize places where air could be trapped and switch the piston and check valve actuators to provide more piston displacement.

4.5.2 K_u Factor

Because the fuel injector obviously was not operating as desired and because the reference signal generated for the piston assembly did not always make use of the entire range of displacement available from the piston assembly, a scaling factor, K_u, was implemented to take advantage of the entire operating range of the piston actuator at each frequency.

The cap used in the previous testing was removed and the atomizer was placed back in the line. The tank pressure was increased to 160 psi and the check valve was calibrated to provide a 60 psi pressure drop across itself in the open position. The fuel injector was operated at 100 Hz as before, except now the piston actuator was providing 7.5 times the displacement of the original actuator. With this new fuel injector configuration a peak pressure of 135 psi was produced, 28 psi more than when using the original fuel injector configuration. This pressure corresponded to $14\%_{Qpeak}$ modulation which was an improvement but which was still less than half of our goal of $40\%_{Qpeak}$.

Even though this actuator was providing 7.5 times the displacement of the original actuator configuration the fuel injector controller was still creating a reference signal whose magnitude varied with frequency according to the relationship in Equation 3.18. Since K_u was simply a scalar to be multiplied to the reference signal, the value of K_u necessary to take advantage of the maximum displacement would be different at each frequency. Thus, it was necessary to find the values of K_u that would generate a full-scale reference displacement signals at each frequency. This value of K_u would allow for the fuel injector to be operated at its maximum displacement at each frequency.

These maximum K_u values were experimentally found at representative frequencies and can be seen in Figure 4.19.

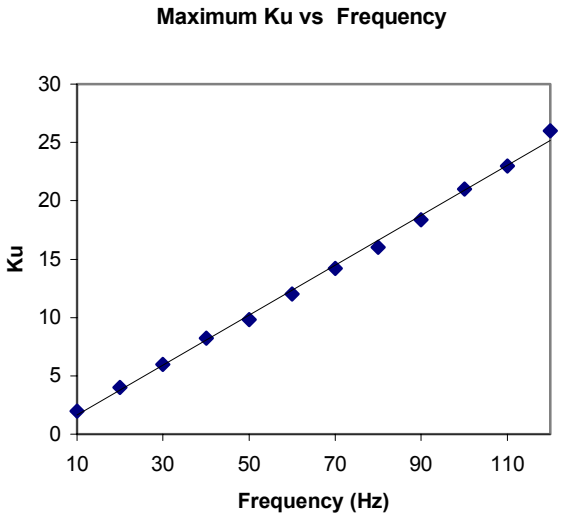

Figure 4.19 Maximum K_u vs. frequency

When, for a particular frequency, the maximum K_u was normalized and then varied over the K_u values corresponding to the range of 0-1$K_{u\ normalized}$, each frequency had the nearly the exact same trend in peak and trough line pressures as a function of the normalized K_u. A representative plot showing how varying K_u at a certain frequency influenced the peak and trough of the line pressure can be seen in Figure 4.20.

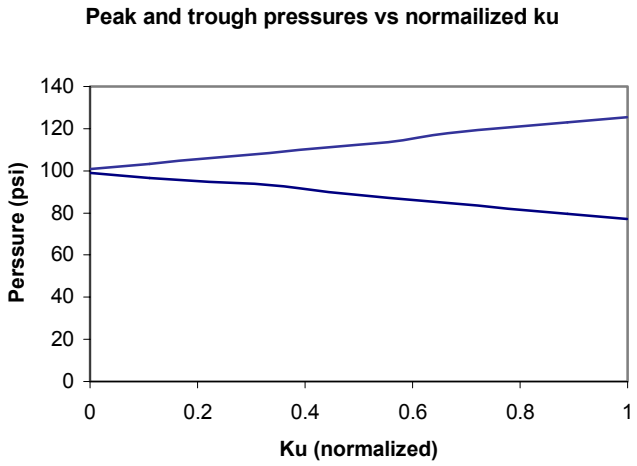

Figure 4.20 The effect of different values of K_u on the peak and trough values of line pressure

It was interesting to note that if one plotted the value of the difference between the peak and trough of the line pressure, ΔP, against the normalized value of K_u the relationship appeared linear. This relationship can be seen in Figure 4.21 along with a linear reference for comparison.

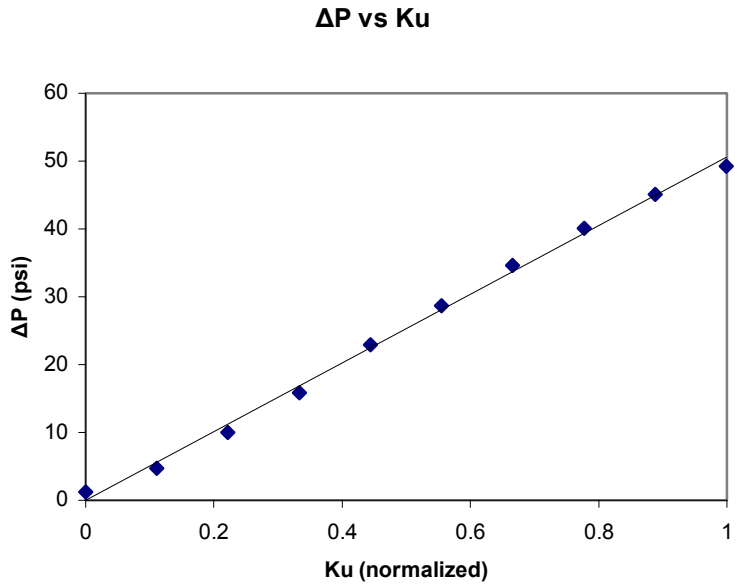

Figure 4.21 The ΔP provided by the piston versus normalized K_u over all frequencies

There were two conclusions that could be drawn from this K_u testing. The first was that the ΔP created when modulating the flow was related entirely to the maximum displacement achievable by the piston. The second was that the ΔP associated with a certain displacement was frequency independent.

It was also possible to say something about the displacements that would be necessary to produce the desired $40\%_{Qpeak}$ modulation. Since the normalized values of K_u from 0-1 could legitimately be replaced by the range of displacement produced by the piston 0-150 microns, the maximum displacement necessary to produce the desired $40\%_{Qpeak}$ modulation could be extrapolated to be 420 microns. If the compressibility present in this system could be reduced, the piston displacement required to provide the desired level of modulation would correspondingly be reduced.

4.5.3 Flow Testing

One of the goals of this project was to design and construct a fuel injection system that could modulate the fuel flow in a very controlled manner. Now that our fuel injector was constructed it was desired to test and verify that it could realize a desired profile. It was

also desired to test and verify that the relationship between pressure and flow rate used in the design process was valid as a static and dynamic relationship. In order to do this, a way to measure the instantaneous fuel flow rate being expressed from the atomizer was needed. Through the conservation of linear momentum it was possible to calculate the flow rate of a jet of liquid by measuring the force that the jet impinged on a fixed boundary. A schematic illustrating the concept as well as the solution of the conservation of linear momentum equation for the flow rate can be found in Figure 4.22 and Equation 4.3, respectively.

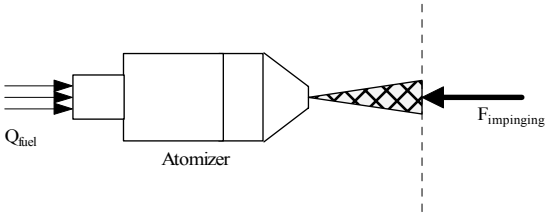

Figure 4.22 Flow measurement concept

$$Q_{fuel} = \sqrt{\frac{F_{impinging} A_{nozzle}}{\rho_{fuel}}} \tag{4.3}$$

In order to measure the force needed to stop the impinging jet, a cantilevered beam could be placed in the flow so as to obstruct and stop the entire jet. Strain gages mounted to the base of the cantilevered beam could provide information about the displacement of the end of the beam that could then be related to the force of the jet as it impinged on the beam. A schematic of this measurement system can be seen in Figure 4.23.

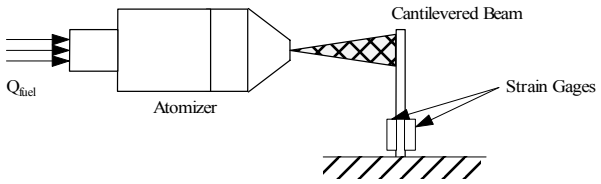

Figure 4.23 Schematic of flow measurement system

Because the flow rates being measured are relatively small the forces generated by the impinging jet are very small. The force that corresponded to a flow rate of 0.84 cm^3/s was only 0.004 lbf. Because the range of forces needing to be measured was so small and because the bandwidth of the force sensor had to be large enough to measure over the

entire range of operating frequencies, it was difficult to find a force sensor that could be used in this application.

Sensor One manufactured a force sensor, AE801, which was the most suited to measure forces in our range of interest and which had a bandwidth suitable for our measurements. This sensor consisted of a very small, and fragile, silicone cantilevered beam with piezo-resistive strain gages mounted to the base of the cantilevered beam. The sensors were very sensitive and thus needed to be coated in a protective layer of silicone sealant to avoid corrosion of the strain gages due to contact with the fuel. Dow Corning 3140RTV was used to coat the sensors and was allowed to dry for 2 days before handling. These force sensors came unmounted, and so it was necessary to create a mounting system that could securely hold the body of the sensor and position the tip of the cantilevered beam over the jet of fuel as it sprayed out of the atomizer. After the sensors were coated, longer wires were attached to the strain gage leads and the sensors were glued into a copper pipe, allowing only the beam of the force sensor to protrude. The strain gages were wired into a half bridge arrangement to be used with the strain gage amplifier. The copper pipe could then be mounted into a micro positioning device used to finely adjust the position of the force sensor. This positioning device was bolted to the table. The atomizer was supported in a clamp on a chemistry stand that was also bolted to the table. The rigid mounting of the atomizer and force sensor was a requirement because even light contact could break the force sensor. The positioning system for the force sensor can be seen in Figure 4.24

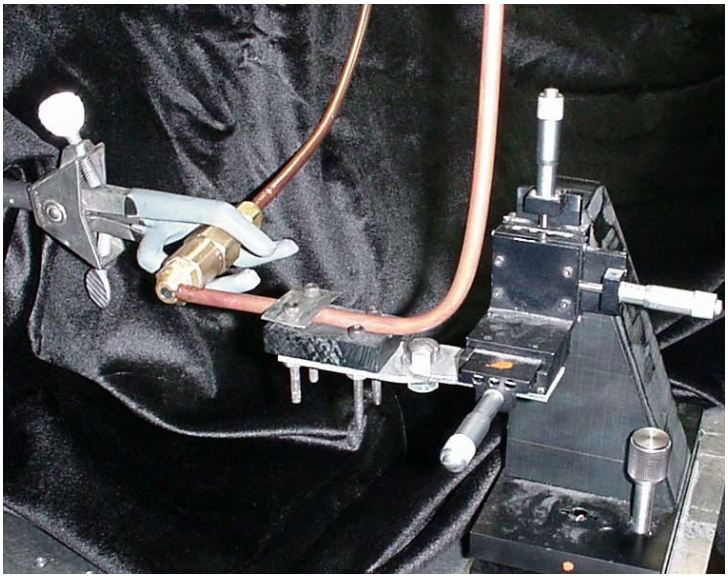

Figure 4.24 Positioning system for the force sensor

A close up of the force sensor positioned in front of the atomizer can be seen in Figure 4.25.

Figure 4.25 Close-up of force sensor in front of the atomizer

Note the size of the force sensor, mounted in the ¼ inch copper pipe, and the close proximity of the force sensor beam to the atomizer.

Unfortunately the force sensor was broken before substantial testing could be performed. Fortunately some data was taken showing the performance of the fuel injector at 10, 100

and 200 Hz using full-scale reference signals. The results of these tests can be seen in Figure 4.26.

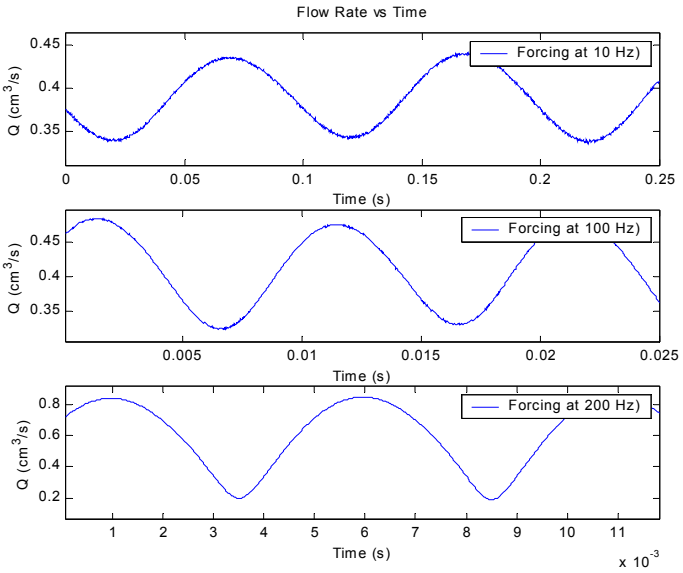

Figure 4.26 Flow testing results

These results show that apparently a higher amount of modulation occurred at the higher frequencies. The amount of modulation at 10, 100 and 200 Hz was found to be 21, 35 and 142%$_{Qpeak}$ respectively. The amount of modulation measured when forcing at 100 Hz and 200 Hz seems optimistic from what the line pressure data was indicating. One possible explanation for this behavior could be that the natural frequency of the force sensor, reported as 12 kHz in air, was reduced either because of its contact with the impinging fluid or more likely because of the silicon coating applied to the sensor. If the natural frequency was reduced below 1 kHz it could be possible that the dramatic increase in measured flow rate for increasing frequency might be a result of the force sensor nearing its resonance. A more likely explanation for the increase in measured flow modulation is the presence of an acoustic resonance in the fuel line. It was found that the quarter wave mode associated with a 6 ft open-closed pipe filled with ethanol, a crude approximation of the fuel line between the fuel injector and atomizer, would occur at 176 Hz. The effect of an acoustic resonance in the fuel line at this frequency would seem to explain the trend in the flow modulation data. Future work involving the

characterization of the force sensor could be used to identify this trend as the result of acoustic resonance in the fuel line or the spurious result of sensor dynamics. Naturally, much more extensive testing of the relationship between different pressure profiles and the corresponding flow profiles would be beneficial in understanding exactly how the fuel injector functions.

5 Combustion Testing

5.1 Testing with 18 Inch Combustor Chimney

With the fuel injection system constructed and tested, it was time to examine the authority of the fuel injector on the combustion process. The two quantities measured as indicators of authority were the internal pressure of the combustor, P_c, and the unsteady heat release rate of the flame, q'. The initial testing of the fuel injection system was performed using an 18 inch combustor chimney. This short length of chimney was used because the acoustics of the chimney did not allow the generation of a thermo-acoustic instability. Because there was no instability present using this short chimney, the pressure and heat release resulting from the fuel modulation could be more easily measured.

5.1.1 Pressure Authority

The combustor pressure was measured using a SenSym SLP004D pressure transducer that was easily mounted into a port in the combustor chimney wall. This sensor, like the Entran line pressure sensor, used a diaphragm with strain gages mounted to it to measure pressure relative to atmospheric. The sensor was capable of AC coupled dynamic pressure measurements in the range of 0-0.14 psi. With this pressure sensor installed and wired in a half bridge configuration, the fuel injection system was then incorporated into the fuel line that lead into the combustor.

The supply tank was pressurized and the combustor was lit and then brought to the operating condition corresponding to a geometric swirl number of 1.14. This was done by adjusting the axial and swirl flow rates using the valves on the combustor's control panel until they corresponded to the setting in Table 5.1.

Geometric Swirl Number	Total Air Flow (scfm)	Axial Air Flow (scfm)	Swirl Air Flow (scfm)
1.14	0.0115	0.0025	0.009

Table 5.1 Settings for producing geometric swirl number used in the operation of the combustor

This value of geometric swirl number was used as an operating condition because the flame dynamics at this setting had already been examined for this combustor and was found to produce a thermo-acoustic instability when using the 48inch chimney.

Once this swirl number was achieved, the check valve was adjusted to assure the line pressure seen at the atomizer was 100 psi. This pressure corresponded to the flow rate of 0.42 cm^3/s. At this point the combustor was allowed to warm up for approximately 30 minutes to reach equilibrium. The combustor was then ready to begin testing.

First, a power spectrum of the combustor pressure signal was taken with the fuel injector turned off. This would allow us to compare the results found when operating the fuel injector at different frequencies and amplitudes. Full displacement reference signals, created using the K_u factor, were then examined at 100 Hz increments to evaluate the authority of the fuel injector on the internal combustor pressure. The results of this testing, shown as a composite of the tests at each frequency, can be seen in Figure 5.1.

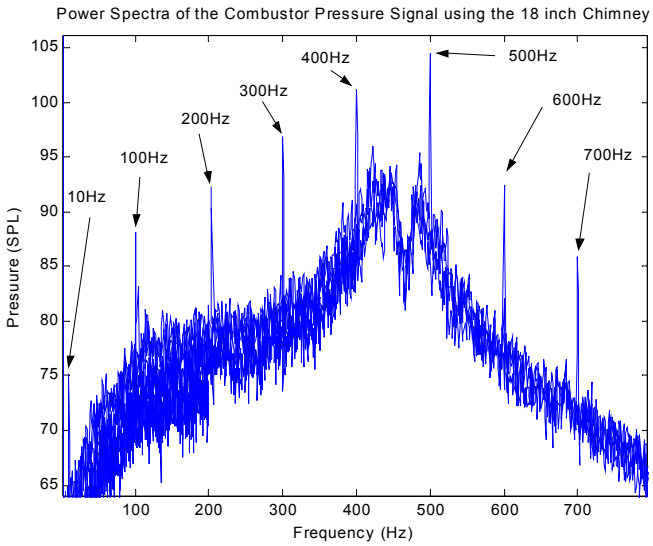

Figure 5.1 Effect of probe signals on the combustor pressure

It is obvious that the actual authority of the fuel injection system is only the pressure component added by the fuel injector, the difference between the peak pressure seen using a probe signal and the pressure due to the background pressure at each frequency. The results of the authority of the fuel injector at these frequencies can be seen in Table 5.2.

Frequency (Hz)	Combustor Pressure Authority (SPL)
10	9.4
100	10.0
200	13.7
300	14.2
400	10.1
500	14.6
600	14.2
700	13.18

Table 5.2 Authority of fuel injector on the combustor pressure

There did not seem to be a trend in this data and the average authority of the fuel injector on the combustor pressure for these specific frequencies was 12.4 dB SPL.

5.1.2 Heat Release Authority

The authority of the fuel injector over the heat release of the combustion process was measured using chemiluminescence. Chemiluminescence is a technique that involves measuring the concentration of a certain wavelength of light emitted from the combustion process that corresponds to the concentration of CH^*, a byproduct of the combustion process. The concentration of this wavelength of light can be correlated to the heat release of a flame [9].

The measurement of the chemiluminescence signal requires the use a photo multiplier tube (PMT), a power supply, signal conditioning amplifier and mirror system. Because the PMT could not conveniently be mounted directly above the flame, a mirror was placed several feet above the flame that could reflect the light emitted by the flame back down onto the lab table. Here the light could be gathered into the PMT. The PMT required a 900 V power signal, provided by a high voltage power supply, to operate. The signal produced by the PMT was a very small current signal that needed to be sent through a current amplifier to produce a voltage signal corresponding to the heat release. The mirror and the PMT tube had to be aligned with the use a laser beam to ensure the PMT was collecting as much of the light from the flame as possible. A schematic of the chemiluminescence setup can be seen in Figure 5.2.

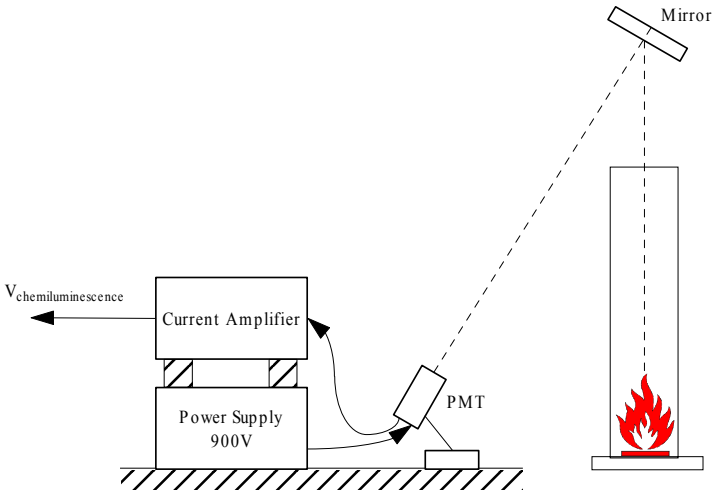

Figure 5.2 Chemiluminescence setup

Once the chemiluminescence measurement system was aligned properly the chemiluminescence signal of the combustor could be measured.

The rig was set up using the same procedure as for the combustor pressure measurements discussed in Section 5.1.1. The room lights had to be turned out during the actual measurement, as the PMT was very sensitive to exposure to bright light. The PMT, which is essentially a phototransistor, could become saturated if exposed to high intensity light and would need several weeks to return to operating condition. It was very important to keep the PMT covered when not in use and to keep the environment dark when the PMT was exposed. Identical probe signals to those used in the previous combustor pressure testing were then provided to the fuel injector. The results of this testing, shown as a composite of the tests at each frequency, can be seen in Figure 5.3.

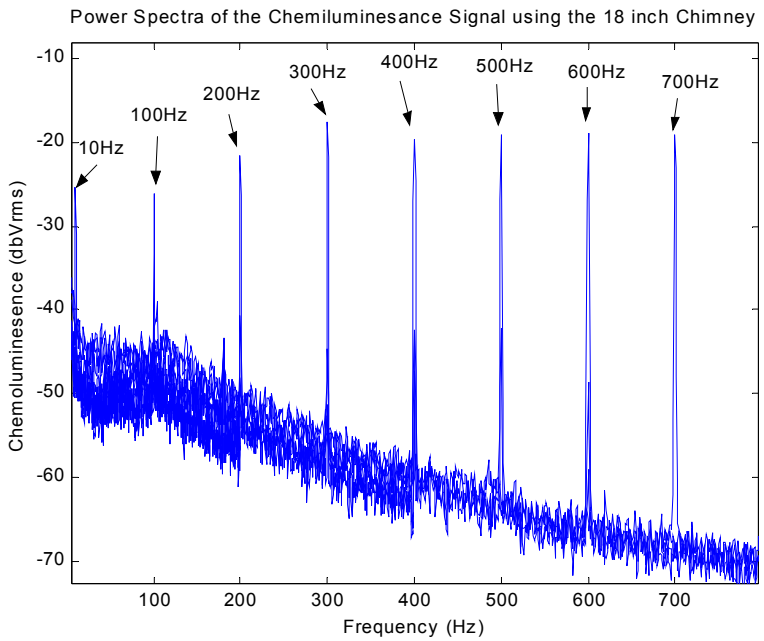

Figure 5.3 Effect of probe signals on the heat release

The actual authority of the fuel injector on the heat release of the flame is related to the amount of chemiluminescence signal added by the fuel injector, the difference between the peak chemiluminescence seen using a probe signal and the chemiluminescence signal due to the dynamics of the combustion process. The results of the authority of the fuel injector over heat release at these frequencies can be seen in Table 5.3.

Frequency (Hz)	Heat Release Authority (dBVrms)
10	15.6
100	17.3
200	28.1
300	35.1
400	37.1
500	40.9
600	44.5
700	46.6

Table 5.3 Authority of fuel injector on the heat release of the flame

These results show that the authority of the fuel injector over heat release actually increases with frequency.

5.1.3 Effect of K_u on Fuel Injector Authority

The previous two sections describe full scale testing of the fuel injection system to evaluate the maximum authority of the fuel injector. It was also desired to test the authority of the fuel injector when providing various amounts of modulation. The easiest way to examine the effect of different levels of modulation would be to examine the performance of the fuel injector over the range of 0-1 $K_{u\ normailized}$. This range of K_u values would correspond to the fuel injector's full range of modulation. The results of this testing can be seen in Figure 5.4.

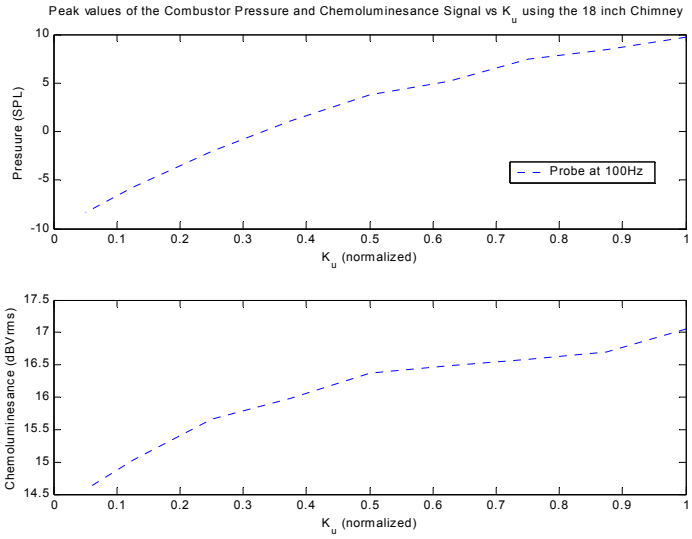

Figure 5.4 Effect of various levels of modulation on the fuel injector authority

One can see that various amounts of modulation correspondingly produce various amounts of authority over the combustion process. Because the amount of modulation produced given a particular pressure profile could not be quantified, it was not possible to directly relate the effect of different levels of fuel modulation on the authority of the combustion process. The trend was clear, however, that varying the amount of modulation correspondingly varied the authority over the combustion process. Future testing could involve documenting the exact relationship between the level of modulation and combustion authority.

5.2 Testing with 48 Inch Combustor Duct

The performance of the fuel injector, with regard to its authority over the combustor pressure and heat release, could also be evaluated when using the 48inch chimney. The fuel injector control system could then be implemented to evaluate its effectiveness on attenuating the thermo-acoustic instability present in this combustor.

5.2.1 Pressure Authority

The 48inch chimney created an instability near 100 Hz and thus the authority of the fuel injector was only evaluated in the range of 0-100 Hz. Full-scale reference displacement probe signals, employing the appropriate K_u factor, were sent to the fuel injector at 20 Hz intervals over the range of 10-90 Hz. The results of this testing, shown as a composite of the tests at each frequency, can be seen in Figure 5.5.

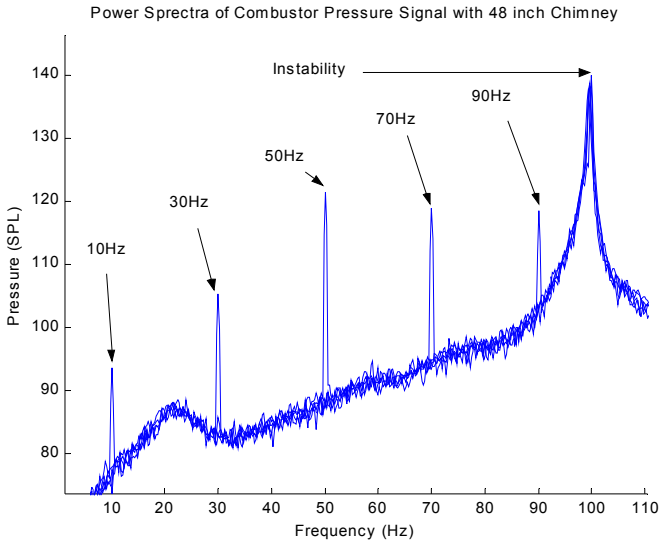

Figure 5.5 Authority over combustor pressure with 48 inch chimney

The first thing that was noticed was the large spike in the pressure signal near 100 Hz. This spike in the combustor pressure is the manifestation of the thermo-acoustic instability. One should also notice that the magnitudes of the peak pressures associated with the probe signals relative to the peak pressure associated with the instability seem to point towards the fact that the fuel injector does have significant influence on the combustor pressure in the presence of the instability.

Because the 48 inch chimney reached almost to the ceiling, it was not possible to mount the mirror system necessary to measure the chemiluminescence signal. As a result, the

authority of the fuel injector on the heat release would not be measured using the 48 inch chimney.

5.2.2 Thermo-acoustic Instability Suppression

Satisfied that the fuel injector had some degree of authority over the combustion process it was finally time to implement the fuel injection control system and evaluate the effectiveness of this system in suppressing the thermo-acoustic instability. The performance of the fuel injection control system, when the piston assembly was being operated both open loop and closed loop, was evaluated allowing a comparison of their performance.

Open Loop and Closed Loop Piston Assembly Results

The fuel injection control system as discussed in Section 3.6.3 was assembled. The test setup for the implementation of the combustion control system can be seen, with all of the components labeled, in Figure 5.6.

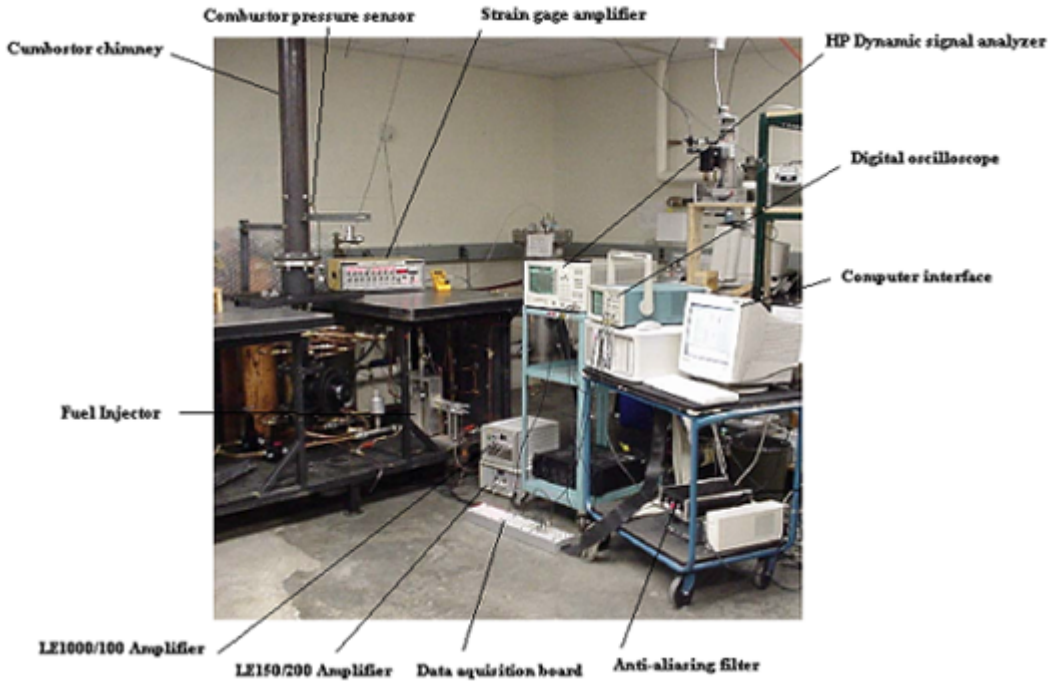

Figure 5.6 Test setup for the combustion control system

The procedure for starting the rig, including the lighting of the combustor, setting the swirl number, calibration of the check valve and the combustor warm up was performed as before. The combustor pressure signal was then switched to be used as the control reference signal for the fuel injection system controller. This control reference signal was previously provided by a separate signal generator. Because of the way the reference displacement signal was generated, see Section 3.6.1, it was necessary that the control reference signal have a maximum magnitude of exactly 1 V. This was easily accomplished when using a signal generator. However, when using the combustor pressure signal, which fluctuated sometimes by 30% from one cycle to the next, it was much more difficult. The simple solution was to present the combustor pressure signal to the user and prompt them to adjust the scaling of the signal to ensure the magnitude be less than 1 V. If the control reference signal was larger than 1 V, the reference displacement could exceed the maximum range of the amplifier. If the control reference signal was smaller than 1 V, the reference displacement signal generated would not be as large as it should be. Because our major concern was not to exceed the maximum available displacement, it was more important to ensure that the control reference signal never exceeded 1 V, essentially normalizing by the infinity norm of the signal. Setting the scaling factor for the control reference signal then became an artistic process of trying to adjust the control reference signal to have a magnitude as close to 1 V as possible without exceeding 1 V. As a note, for future testing this process could become much more automated and effective if a frequency estimator was used to estimate the frequency of the combustor pressure signal and then construct a sinusoid with a magnitude of 1 V_{peak} at the estimated frequency. This would always ensure that the magnitude of the reference displacement signal was accurate. Nevertheless, at this point the fuel injection control system was ready to operate.

The performance of the fuel injection system using the open loop piston assembly was evaluated first. The fuel injection control system was turned on and the phase delay was incremented in roughly three degree steps. At each step of phase delay the combustor pressure signal was monitored and the value of the peak was recorded. These peak pressures were then subtracted from the peak pressure of the uncontrolled combustor to find the amount of attenuation achieved. It was found that the best attenuation possible

with the open loop piston assembly was 5.75 dB. The exact same test was performed using the closed loop piston assembly and the maximum attenuation possible was found to be 8.15 dB. The values of attenuation versus relative phase delay can be seen in Figure 5.7 for both the open loop and closed loop piston assembly.

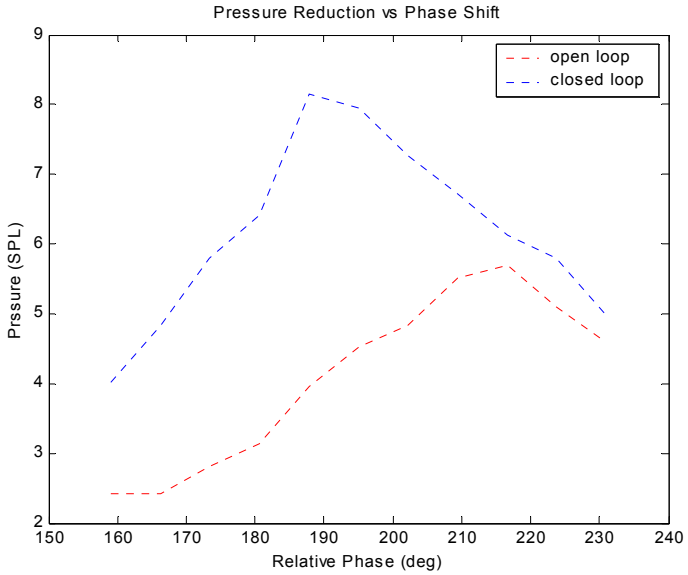

Figure 5.7 Instability suppression for different relative delay

The power spectra of the combustor pressure signal at the optimal phase delay for both the open loop and closed loop piston assembly controller can be seen in Figure 5.8.

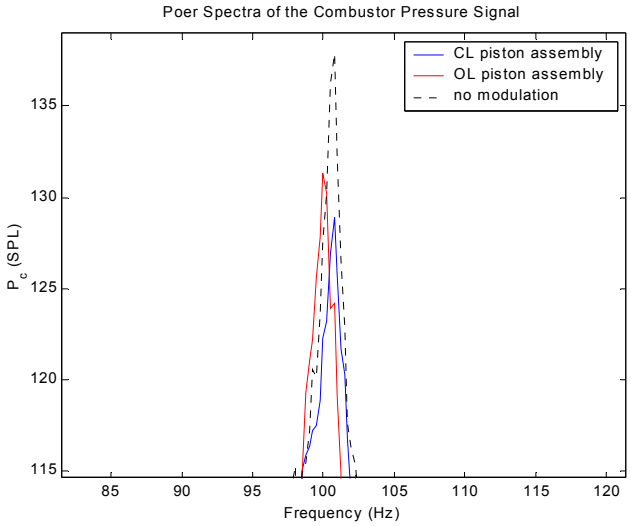

Figure 5.8 Power spectra of the combustor pressure signal using the open loop and closed loop piston assembly

The results of this testing show that the fuel injection system was not able to eliminate the instability, but it was able to reduce the magnitude of the pressure oscillations in the combustor by 8.15 dB, a reduction of 62%. It was interesting to note that the fuel injection system, when using the closed loop piston assembly, provided 14% more reduction than the fuel injection system when using the open loop piston assembly.

The reason that the closed loop piston assembly provided more attenuation was examined at this point. This exploration began by examining the actual displacement of the piston when the piston assembly was operating open and closed loop. The actual displacements, along with the reference signal, were recorded for both the open loop and closed loop piston assembly, when operating at the instability frequency near 100 Hz. The results of this test can be found in Figure 5.9.

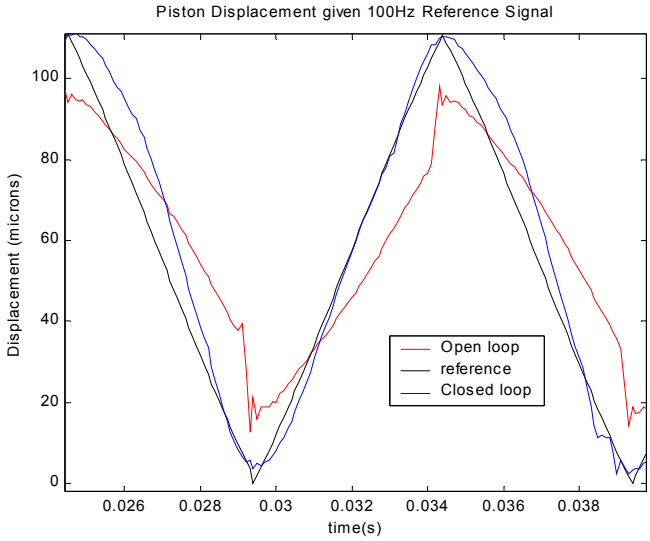

Figure 5.9 Actual displacement with open and closed loop piston assembly

It was clear that the closed loop piston assembly was tracking the reference displacement signal much better that the open loop piston assembly. Because the piston displacement was responsible for creating the line pressure, it would follow that the ability of the piston assembly to follow the reference signal would directly correspond to the effectiveness of the piston on controlling the line pressure. It was then decided to measure the power spectra of the line pressure created using the open and closed loop piston assembly. The power spectra of the line pressures created with the open loop and closed loop piston

assemblies that correspond to the displacement profiles shown in Figure 5.9 can be seen in Figure 5.10.

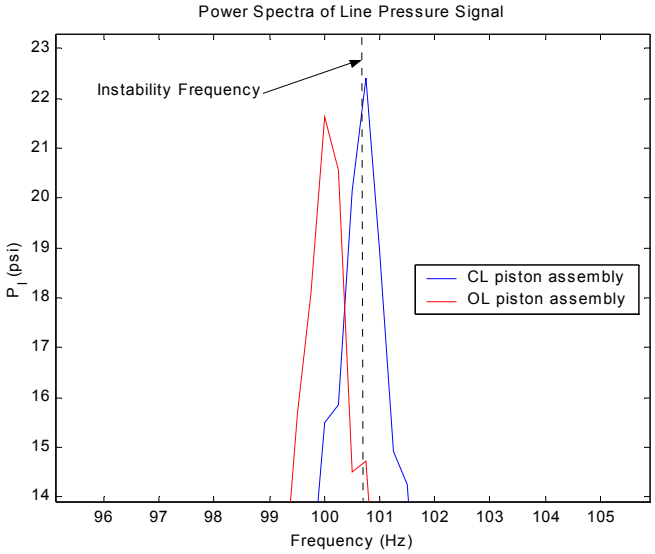

Figure 5.10 Power spectra of the line pressure signals corresponding to open loop and closed loop operation of the piston assembly

One can see that the peak spectral component of the line pressure corresponding to the closed loop piston assembly contains more energy than the open loop case and that the energy was more concentrated at the frequency of the instability. Thus it appears that the effectiveness of the closed loop piston assembly in reducing the magnitude of the thermo-acoustic instability could be attributed to the fact that the closed loop piston controller could add energy more effectively into the line pressure signal at the desired frequency and thus could modulate the flow more effectively at that frequency.

5.2.3 Existence of a Thermo-acoustic Instability

The oscillating pressure measured when the 48 inch chimney was installed had a magnitude of about 0.05 psi. The magnitude of this oscillating component of pressure, relative to the mean combustor pressure of 14.7 psi, is only 0.3%. This relative magnitude is quite small when compared to those found in the active combustion control literature, which report values in the range of 10%. This implies that the oscillating

pressure component measured on our rig might not be a true thermo-acoustic instability. It is possible that the behavior seen in our rig might be the result of a system containing lightly damped stable poles. The identification of this system as stable or unstable, based on its physical behavior, is not necessarily a simple matter.

One could imagine the following two scenarios. First, the dynamics of the system are a set of lightly damped complex conjugate stable poles, just on the left hand side of the imaginary axis. Second, the dynamics of the system are a set of complex conjugate unstable poles, just on the right hand side imaginary axis. Assuming the non-linearity present in the second system behaves like the one present in the combustor, the unstable system would produce a limit cycling behavior, possibly looking very much like the behavior of the stable system. At this point in the characterization of our combustor, it was not exactly clear what the behavior of the combustor should be attributed to.

It is easy to imagine that, for the second system, it might not take much gain to move the poles back across the imaginary axis, if the poles are initially not far in the right half plane. It is also easy to imagine that the gain necessary to move the unstable poles into the left half plane could result in a major reduction in the oscillating pressure amplitude, while the same amount of gain might only be able to produce a marginal reduction in the oscillating pressure amplitude of the initially stable system.

Thus, the small attenuation of the oscillating pressure amplitude achieved using our fuel injection system might only be a result of our combustor not being truly unstable. If in actuality the combustor was stable and produced 8.15 dB of attenuation, it is possible to imagine that the fuel injector might have been able to produce a much higher level of attenuation if it was operating on an unstable system like the second system discussed above. Future testing involving the evaluation of the true dynamics of the combustor could help credit or discredit this explanation. If the combustor was not truly unstable, some method would need to be devised to encourage the system to go unstable. At this point, testing could be performed to evaluate the attenuation available from the fuel injection control system on a combustor with a true thermo-acoustic instability.

6 Conclusions and Future Work

6.1 Conclusions

The main goal of this work was to design, construct and characterize a fuel injection system that could provide proportional modulation of our primary fuel supply. We desired that this fuel injection system have a bandwidth and authority comparable to other fuel injection systems being used in the active combustion control community. A fuel injection system was designed to modulate up to 40%Q_{peak} of the primary fuel flow, for a mean flow rate of 0.42 cm^3/s, over a bandwidth of 50-700 Hz. This fuel injection system was designed to produce a specific sinusoidal flow profile whose modulation level could be adjusted by the user. This fuel injection system made use of a piston and check valve to influence the line pressure and correspondingly the flow rate. These components were constructed and were individually able to provide their designed function. The piston assembly, when incorporated into a feedback controller, was found to have a bandwidth of approximately 1 kHz and could track the reference signal corresponding to a desired 100 Hz flow profile very well. The check valve could also meet its design goal, being able to completely stop the flow in the closed position and produce negligible pressure drop, 4 psi, in the open position. The check valve, because of the limited current available from the amplifier, would only able to provide its full range of operation for frequencies under 500 Hz. At frequencies higher then 500 Hz the check valve would not be able to reach its full closed position in the time required, which implies that the check valve would not be as effective at these higher frequencies. Aside from this limitation the piezo-ceramic actuators chosen to operate these components were particularly well suited for this application, providing the necessary displacements and forces over the required bandwidth. When these components were used in the fuel injection system, however, the system was only able to produce line pressures corresponding to a modulation of 1%$_{Qpeak}$. This failure to meet the design goal was the result of a large level of compressibility present in the fuel line, which was found to be approximately 10%. The consequence of this compressibility was that the system could simply not create the line pressures necessary to achieve the desired flow modulation. This compressibility was not accounted for in the design process where the fluid was

assumed incompressible. The source of this compressibility could likely be attributed to either air trapped in the fuel line or physical deformation of some component of the fuel injection system. Much effort was put forth to eliminate this observed compressibility including bleeding the fuel line of air and remounting the fuel injector components to minimize places where air could be trapped. These efforts reduced the observed compressibility to approximately 2%. Even this smaller amount of compressibility did not change the ability of the fuel injection system to produce a higher peak pressure. For the volume of fluid present in the fuel injection system, the volume change associated with the 2% of compressibility was a factor of 1400 times greater than the volume displaced by the piston per cycle for $40\%_{Qpeak}$ modulation at 100 Hz. This implies that the desired pressures could not be achieved because the bulk of the piston work was being used to compress the volume of fluid in the fuel injection system, not add pressure to the fluid. By switching the actuators used in the piston and check valve assemblies, to increase the maximum piston displacement from 20 to 150 microns, we were able to produce a line pressure corresponding to a modulation level of $18\%_{Qpeak}$. During testing, it became apparent that the relationship between the displacement of the piston and the corresponding pressure created in the fuel line was linear over the range of displacements that we could provide. If this linear relationship is used to estimate the displacement necessary to produce the desired $40\%_{Qpeak}$ of modulation, the required piston displacement would be 420 microns!

A test fixture was developed to measure the flow profile produced by the fuel injection system. The measurement system was used to provide data for three frequencies of modulation but was broken before a substantial amount of data could be taken. It was apparent from the available data that the flow was being modulated in a sinusoidal fashion, i.e. proportionally. This data showed higher flow modulation than predicted, between 21 and $142\%_{Qpeak}$. These quantitative results are, however, held in question because the experiment was never fully characterized before the sensors were broken. When the dynamics of the sensor are fully understood then these results can be verified or discredited.

The fuel injection system was operated at specific frequencies to evaluate the effect of the fuel injection system on the combustion process. The fuel injector was found to have

significant authority over the combustion process at the frequency of instability, near 100 Hz, with a 10.0 dB influence on the combustor pressure and 17.3 dB influence on the unsteady heat release. The fuel injection system also exhibited a significant influence on both the pressure and heat release over the entire range of 10-700 Hz. The combustor pressure authority over this range was found to be 12.4 dB on average. The authority over the heat release was very significant over this range and actually increased with frequency providing 46.6 dB of influence at 700 Hz.

Combustion control experiments were conducted when the fuel injector was using both the open loop and closed loop piston assembly. These open and closed loop fuel injection systems were used in the combustion control system to determine the effectiveness of both modes of operation. The combustion control system was able to produce a 5.75 dB, 48 %, reduction in the oscillating combustor pressure when the fuel injector was run open loop and an 8.15 dB, 62%, reduction when running closed loop. The closed loop fuel injector performance was significantly better than the open loop, resulting in an additional 14% reduction in the amplitude of the oscillating combustor pressure. It was found that the closed loop fuel injector was able to track the displacement reference signal significantly better during operation than when operating open loop. This resulted in more energy being provided to the line pressure at the exact frequency of instability. In other words, the closed loop fuel injection system had more gain at the frequency of instability. This result was very important as it pointed towards the effectiveness of a closed loop fuel injection system as well as the advantage of proportional control.

In summary, a fuel injection system was designed and constructed that was able to modulate approximately $35\%_{Qpeak}$ of the primary fuel flow at 100 Hz, based on the flow measurement data. The data also showed that the ability of the fuel injection system to modulate the fuel flow actually increased with frequency. This fuel injection system was shown to have sizable influence over the combustion process across this bandwidth and could attenuate the magnitude of the oscillating combustor pressure by 8.15 dB. Although there were some major challenges encountered in this work, i.e. the observed compressibility and broken force sensor, this was a very productive first attempt for the

design, construction and characterization of this fuel injection system. This work will provide a solid basis for the next generation of fuel injector.

6.2 Future Work

There is a great deal of work that could be done to expand and improve on the work presented in this project. One of the major challenges to be dealt with is characterizing the compressibility of the volume of fuel in the fuel line. A thorough study of the nature of this compressibility would provide valuable information on how to either remove the effect of the compressibility or redesign the fuel injection system to take account of any compressibility that cannot be removed. Even if this compressibility could not be reduced further it is evident that increasing the displacement available from the piston would allow the generation of higher line pressures and corresponding higher flow rates. A simple solution, at this point, would be to purchase an actuator capable of producing more displacement so that, even if the compressibility could not be reduced, the fuel injection system could provide a higher level of modulation.

The characterization of the fuel injector, with regard to its ability to modulate the flow, is a second area in which this work could be expanded. The construction of a more rigid test stand and mounting apparatus for the force sensor and atomizer would be necessary to ensure that future force sensors not be broken during testing. The dynamics of the force sensor, before and after being coated, could be studied to ensure that the sensor provides usable information over the frequency range of interest. With a fully characterized force sensor, the trend in the modulation data could be identified as either the actual result of an acoustic resonance in the fuel line or the spurious result of undesired sensor dynamics. The validity of the empirical relationship between pressure and flow through the atomizer could be then be examined during dynamic operation and used to refine the design of future fuel injection systems. With the results of this testing, it would be possible to characterize the exact effect of certain levels of fuel flow modulation on the combustion process.

It would also be beneficial to further evaluate the dynamics of the combustor to determine if this combustor is actually unstable. If the combustor is found to be stable, then a method could be implemented to force the combustor to be unstable. One way of

doing this would be by adding a new chimney that will not radiate as much heat from the combustion process as the iron chimney. This would in effect increase the gain of the heat release component of the combustion process.

Once the fuel injection system has been characterized and the ability of the fuel injection system to attenuate the thermo-acoustic instability has been determined using the phase shifting controller, new control schemes could be implemented. A subharmonic controller or any other type of control algorithm could be implemented to further study the effect of fuel modulation on the reduction of thermo-acoustic instabilities.

A method could be implemented to reduce the high level of acoustic noise associated with the operation of the fuel injector. For instance, the fuel injector could be enclosed in a case made of material that would dampen the acoustic vibrations emitted into the surrounding environment.

Finally, if the supply pressure of the system could be increased, the effect of back flow through the check valve could be reduced allowing the system, at present, to be operated more effectively. This could be done by purchasing a supply tank with a higher pressure rating or by implementing the use of a fuel pump system. A higher upstream pressure would also allow the use of the check valve as a throttling valve. The performance and effectiveness of a throttling valve based fuel injection system could then be explored with minimal construction of new parts.

Bibliography

[1] A.M. Annaswamy, and A. F. Ghoniem, "Active control in combustion systems," *IEEE Controls Systems,* Vol. 15, pp 49-63, Dec 1995.

[2] S. M. Candel, "Combustion instabilities coupled by pressure waves and their active control," *Proceedings of the Twenty-Fourth Symposium (International) on Combustion*, pages 1277-1296, 1992

[3] Y. C. Chu, A. P Dowling, K. Glover, and S. M. Evesque, "Algorithms for feedback control of combustion oscillations," *Proceeding of the IEEE Conference on Decision and Control*, Vol. 3, pp. 28863-2868, 1999.

[4] J. M. Cohen, N. M. Rey, C. A. Jacobson, and T. J. Anderson, "Active control of combustion instability in a liquid-fueled low-NO_x combustor," *43rd ASME/IGTI Gas Turbine Expo and Congress*, Stockholm, Sweden, June 2-5, 1998.

[5] R. H. Dorf, and R. C. Bishop, *Modern Control Systems*, Addison Wesley Publishing Company, Menlo Park, 1998.

[6] J. L. Foszcz, "Check Valve Basics," *Plant Engineering, Vol. 50, number 9*, pp. 76-80, 1996.

[7] Y. T. Fung, and V. Yang, "Active Control of Nonlinear pressure oscillations in combustion chambers," *Journal of Propulsion and Power, Vol. 8*, pp 1282-1289.

[8] D. L. Gysling, "Combustion system damping augmentation with Hemholtz resonators," *ASME 98-GT-268*, Stockholm, Sweden, 1998.

[9] L. C. Haber, "An investigation into the origin, measurement and application of chemiluminescent light emissions from premixed flames," *Master's thesis, Virginia Polytechnic Institute and State University*, October 2000.

[10] E. Haile, F. Lacas, C. Desrayaud, D. Veynante, and D. Durox, "Characterization of a liquid fuel injector under continuous modulated flow conditions," submitted to CNRS et de l'Ecole Centrale Paris, Grande Voie des Vignes, 1998.

[11] C. Hantschk, J. Hermann, and D. Vortimeyer, "Active instability control with direct-drive servo valves in liquid-fueled combustion systems," *26th International Symposium on Combustion,* pp. 2835-2481, 1996.

[12] R. Heising, E. Lubarsky, M. Nuemeier, Y. Neumeier, and B. T. Zinn," Periodic liquid fuel spray combustion processes and their damping of combustion instabilities," *AIAA 00-1024*.

[13] J. Hermann, S. Gleis and D. Vortmeyer, "Active instability control of spray combustors by modulation of the liquid fuel flow rate," *Combustion and Science, Vol. 118, pp. 1-25*.

[14] J. R Hibsman, J. M. Cohen, A. Banazuk, T. J. Anderson, and H. A. Alholm, "Active control of combustion instability in a liquid-fueled sector combustor," submitted to *IGTI,* June 1999.

[15] B. S. Hong, V. Yang, and A. Ray, "Robust control of combustion instability with model uncertainty," AIAA 98-0354.

[16] G. Huelsz and E. Ramos, "A physical interpretation of the thermoacoustic effect," *Journal of Non-Equilibrium Thermodynamics, Vol. 21*, pp278-284, 1996.

[17] M. D. Jackson, and A. K. Agrawal, "Active control of combustion for optimal performance," *Journal of Engineering for Gas Turbines and Power – Transactions of the ASME, Vol. 121, number 3*, pp. 437-443, 1999.

[18] C. E. Johnson. Y. Nuemeier, E. Lubarsky, Y. J. Lee, M. Nuemeier, and B. T. Zinn, "Suppression of combustion instabilities in a liquid fuel combustor using a fast adaptive control algorithm," *AIAA 00-0476*.

[19] B. V. Kiel, "Review of advances in combustion control, actuation, sensing, modeling and related technologies for air breathing gas turbines," *39th Aerospace Sciences Meeting and Exhibit, AIAA 01-0481*.

[20] P. J. Langhorne, A. P. Dowling, and N. Hooper, "Practical active combustion control system for combustion oscillations," *Journal of Propulsion and Power, Vol. 6, p. 324*, 1990.

[21] A. H. Lefebvre, *Gas Turbine Combustion*, Hemisphere Publishing Corporation, 1983.

[22] C. P. Liou, "Dynamics of spring-loaded swing check valves," *Proceeding of the 1998 ASME Energy Sources Technology Conference, Houston, TX.*

[23] J. Magill, and M. Bachmeann, "Combustion dynamics and control in liquid-fueled direct injection systems," *AIAA 00-1022*.

[24] L. Mauck, and C. S. Lynch, "Piezoelectric hydraulic pump," *Proceedings of SPIE- the International Society for Optical Engineering, Vol. 3668, number 2*, pp. 844-852, 1999.

[25] K. L. McElhaney, "Analysis of check valve performance characteristics based on valve design," *Nuclear Engineering and Design, Vol. 197, number 1*, pp. 169-182, 2000.

[26] K. R. McManus, J.C. Magill, and M. F. Miller. "Control of unstable combustion oscillations in liquid-fueled gas turbines," *International Conference on Control Applications, 1998*

[27] K. R. McManus, J.C. Magill, and M. F. Miller, "Combustion instability suppression in liquid-fueled combustors," *AIAA 98-0642*.

[28] B. D. Mugrudge, "Combustion driven oscillations," *Journal of Sound and Vibration*, Vol. 70, pp. 437-452, 1980.

[29] M. R. Murray, C. A. Jacobson, R. Dasas, A. I. Khibnik, C. R. Johnson Jr., R. Bitmead, A. A. Peracchio, and W. M. Proscia, "System identification for limit cycling systems: A case study of combustion instabilities," *Proceedings of the American Control Conference, 2004-2008*, Philadelphia, PA, June 1998.

[30] K. Nasser, and D. J. Leo, "Efficiency of frequency-rectified piezohydraulic and piezopneumatic actuation," *Proceedings of the Adaptive Structures and Materials Symposium, ASME, Vol. AD-60*, pp. 485-498.

[31] C. D. Near, "Piezoelectric actuator technology," *Proceeding of the Smart Structures and Materials Conference., Vol. 2717*, pp. 246-258, 1996.

[32] L. Nord, "The thermoacoustic characterization of a rikje-type tube combustor," *Master's thesis, Virginia Polytechnic Institute and State University*, February 2001.

[33] C. L. Phillips, and R. D. Harbor, *Feedback Control Systems*, Prentice Hall, Upper Saddle River, 1996.

[34] J. S. Richards, "An exploration of secondary fuel injection as actuation for control of combustion instabilities in a laminar premixed tube combustor," *Master's thesis, Virginia Polytechnic Institute and State University*, May 2000.

[35] G. D. Roy, "Performance enhancement and thermoacoustic suppression by combustion control," *39th Aerospace Sciences Meeting and Exhibit, AIAA 01-0221*.

[36] W. R. Saunders, M. A. Vaudrey, B. A. Eisenhower, U. Vandsburger, and C. A. Fannin, "Perspectives on linear compensator design for active combustion control," *37th AIAA Aerospace Sciences Meeting, Reno, NV*, Jan11-14, 1999.

[37] R. C. Steele et al., "Passive control of combustion instability in lean premixed combustors," *ASME 99-GT-052*, Indianapolis, IN 1999.

[38] M. A. Vaudrey, W. R. Saunders, and W. T. Baumann, "Control of combustor instabilities using an artificial neural network," *ASME/IGTI Turbo Expo,* Munich, Germany, 2000.

[39] K. Yu, K. J. Wilson, and K.C. Schadow, "Liquid-fueled instability suppression," *27th International Symposium on Combustion*, pp 2039-2046, 1998.

[40] K. Yu, K. J. Wilson, and K.C. Schadow, "Active combustion control in a liquid-fueled dump combustor," *AIAA 97-0462.*

[41] B.T. Zinn. Y. Neumeier, "An overview of active control of combustion instabilities," *AAIA 970461*, 1997.

[42] J. Allem, M. Al-Nakhi, R. Brown, J. DeCastro, J. Desrosiers, D. Henke, M. Herbaugh, H. Jones, S. Knight, M. Lollis, S. Mauck, D. McLaughlin, O. Miller, C. Maloney, M. Wills, "Acive Combustion Control Device – Final Report," ME4016 Senior Design Class, 2001

Appendix A – Control Code

This appendix includes a description of the code used to operate both the fuel injector system and the combustion control system. This code was written as a Simulink model and implements the system discussed in Section 3.7.

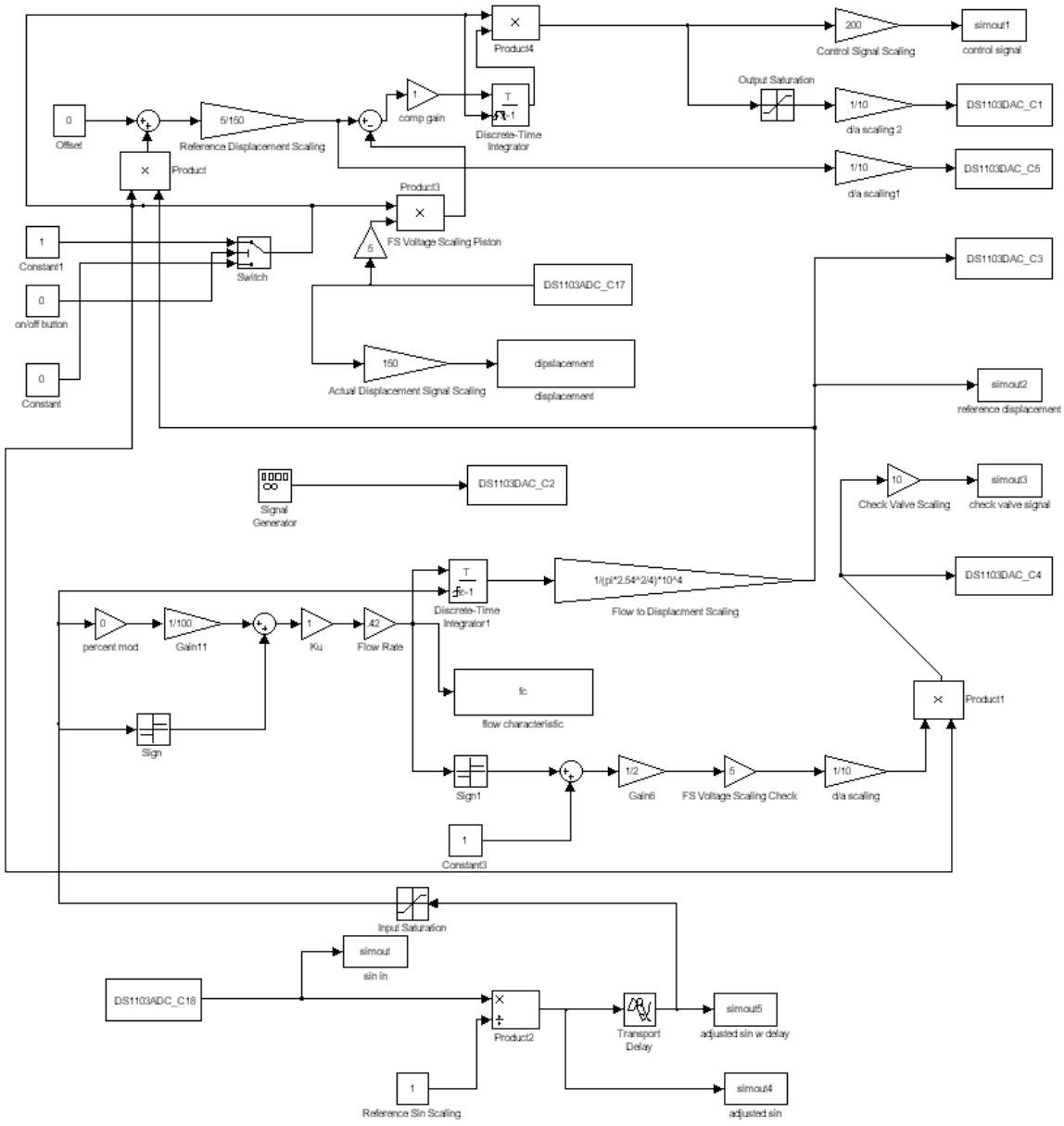

This program essentially implements the systems discussed in Section 3.6 and 3.7. The blocks marked as ADC and DAC are points where either a signal is read into or sent out

of the data acquisition system. This physically occurs through the pin board of the data acquisition system shown below.

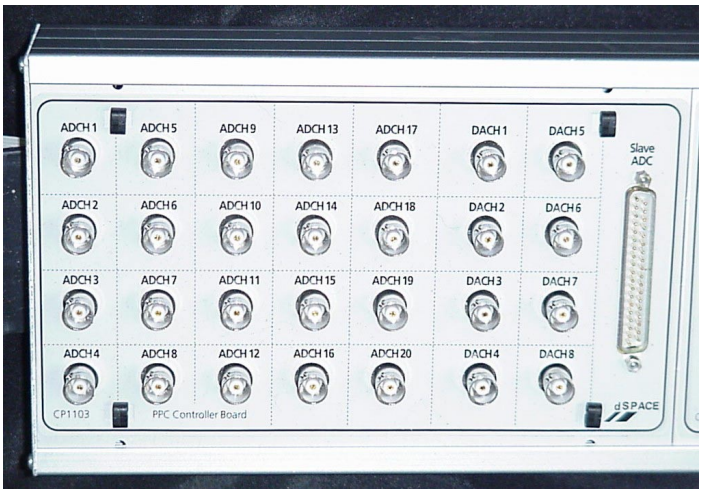

The value of many of the block diagram components shown in the Simulink code are associated with numeric inputs in the Control Desk control panel. This allows the value of the blocks to be changed in real time when the control code is running on the Dspace DSP processor. The Control Desk control panel facilitates all of the data presentation to the user and allows the user to input and adjust desired parameters such as the percent modulation and K_u factor during operation.

Operation

There are several modes in which this control code can operate the fuel injection system. This code allows the user to operate the fuel injection system either as part the combustion control system or as an independent system. It can, for both of these modes, operate the piston assembly of the fuel injector open or closed loop.

Operating the fuel injection system at particular frequency requires the connection of d/a channel 2 to a/d channel 18 on the data acquisition pin board. This supplies a sine reference whose frequency the user can change in the Control Desk control panel. The user can also select whether to operate the fuel injector with an open loop or closed loop piston assembly by selecting which pins to connect to the piston assembly amplifier. Running the fuel injector open loop requires the piston assembly amplifier to be connected to d/a channel 5. Running the fuel injector closed loop requires the piston

actuator's strain signal from the strain gage amplifier to be connected to a/d channel 17 and the piston assembly amplifier to be connected to d/a channel 1. The check valve amplifier would be connected to d/a channel 4 for operation using both the open and closed loop piston assembly. At this point the operating frequency, steady state flow rate, percent modulation, K_u factor and proportional gain, if operating the piston assembly closed loop, could be entered in the Control Desk control panel. Once these connections are made and these settings are entered into the Control Desk control panel, the on/off button on the control panel can be clicked to turn the fuel injection system on and off.

Channel	Signal
d/a 1	CL Piston Assembly Signal
d/a 2	Sin Generator
d/a 4	Check Valve Signal
d/a 5	OL Piston Assembly Signal

d/a Channel Summary

Channel	Signal
a/d 17	Actual Piston Assembly Displacement
a/d 18	Reference Sine

a/d Channel Summary

Running this code to implement the combustion control system requires that combustor pressure signal be fed from the strain gage amplifier into a/d channel 18. This signal can then be viewed on the Control Desk control panel. The magnitude of this signal would need to be adjusted, using the scaling factor on the control panel, such that the magnitude of the signal shown on the control panel has a peak of 1. This will ensure that the displacement reference signal generated for the piston assembly has the correct magnitude. The user can select whether to operate the fuel injector with an open loop or closed loop piston assembly by selecting which pins are used to drive the piston assembly and check valve assembly amplifiers, as discussed in the previous paragraph. Once the desired steady state flow rate, percent modulation, K_u factor and proportional gain, if using the closed loop piston assembly, are input in the control panel, the on/off button on the control panel can be used to turn the system on and off. When this system is

operating, the phase delay slide bar on the control panel can be used to explore the effect of phase delay on the attenuation of the combustor pressure signal.

Subtleties

There are some subtleties that are worth noting with regard to the operating and changing of this code for future users. The first important note is that the a/d and d/a converters have a range of –10 to 10 V. A 10 V signal fed into an a/d channel will create a signal whose magnitude is 1 inside Control Desk. Likewise a signal whose magnitude is 1 in Control Desk will send a 10 V signal out through a d/a channel. It was an important consideration in the design of this code to ensure that the magnitudes of the signals read in and created through the Dspace system were the correct order. A second note is that it was important to zero the relevant signals when turning off the fuel injector, in particular it was important to zero the values entering and leaving the integrators. This ensured that when the system was turned off, the integrators were reset and the output from all the d/a channels would be zeroed until the fuel injector was turned on again. Finally, there were several saturators included in the control code to ensure the signals created did not become large enough to damage any of the system components.

Appendix B – Component and Operation Settings

This appendix prvides information about components and operation settings used during testing. The configuration and relavant information for the sensors used during testing can be found in the table below:

Component	Strain Gage Bridge Configuration	Bridge Excitation Voltage (V)	Strain Gage Amplifier Gain	Sensitivity (no gain)	Sensitivity (with associated gain)
Combustor Pressure Sensor	half	6	8.8x20	56μV/Pa	10.0 mV/Pa
Fuel Line Pressure Sensor	full	10	3.6x20	0.3mV/psi	23.5 mV/psi
PSt1000 Actuator	half	10	5.8x200	NA	66 mV/μm
PSt150 Actuator	half	10	1.3x200	NA	0.5 V/ μm
Force Sensor	half	6	NA	1.5V/N	NA

Component Settings

The settings required to operate the combustor at the desired swirl number can be found in the table below:

Geometric Swirl Number	Total Air Flow (scfm)	Axial Air Flow (scfm)	Swirl Air Flow (scfm)
1.14	0.0115	0.0025	0.0090

Combustor Settings

The settings used during operation of the combustion control system, when using both the open and closed loop piston assembly, can be found in the table below:

Operating Mode	K_u	Q_{ss} (cm^3/s)	$\%_{Qpeak}$	Compensator Gain	Smoothing Filter Break Frequency (kHz)
OL Piston Assembly	21	0.42	40	NA	5
CL Piston Assembly	21	0.42	40	490	5

Combustion Control Experiment Settings

Appendix C – Vendor List

This appendix provides the manufacturer name and contact information for all of the components used in the testing of the combustion control system.

Component	Vendor	Address	Telephone	Website
Piezo-ceramic Actuators and Amplifiers	Piezomechanik	Berg-am-Laim-Str. 64 D-81673 Munchin Germany	+49/89 / 4 31 55 83	www.piezomechanic.com
Piston Cylinder	Bimba	Laneir Engineering Services 4703 Ritchie Highway Baltimore, MD 21225	(410)789-6800	www.bimba.com
Check Valve Body	Parker/Skinner		(800) C Parker	www.parker.com/skinner/
Atomizer	Delevan Spray Technologies	4115 Corperate Research Center Monroe, NC 28110	(704) 291-3100	
Line Pressure Sensor	Entran	10 Washsington Ave Fairfield, NJ 07004	(973) 227-1002	www.entran.com
Combustor Pressure Sensor	SenSym			www.inensyssensors.com
Force Sensor	SensorOne	315 Bridgeway Blvd. Sausalito, CA 94965	(415) 398-6109	www.sensorone.com
Force Sensor Coating	Dow Corning	Dow Corning Corp 1225 Northmeadow, Suite 104 Roswell, GA 30076	(517) 496-6000	www.dowcorning.com
Strain Gage Amplifier	Measurements Group, Inc.	P.O. Box 27777 Raleigh, NC 27611	(919) 365-3800	www.measurementsgroup.com
Data Acquisition System	DSpace	Technologiepark 25 33100 Penderborn, Germany	+49 5251 1638 0	www.dspace.de

Appendix D – Technical Drawings

B-0001

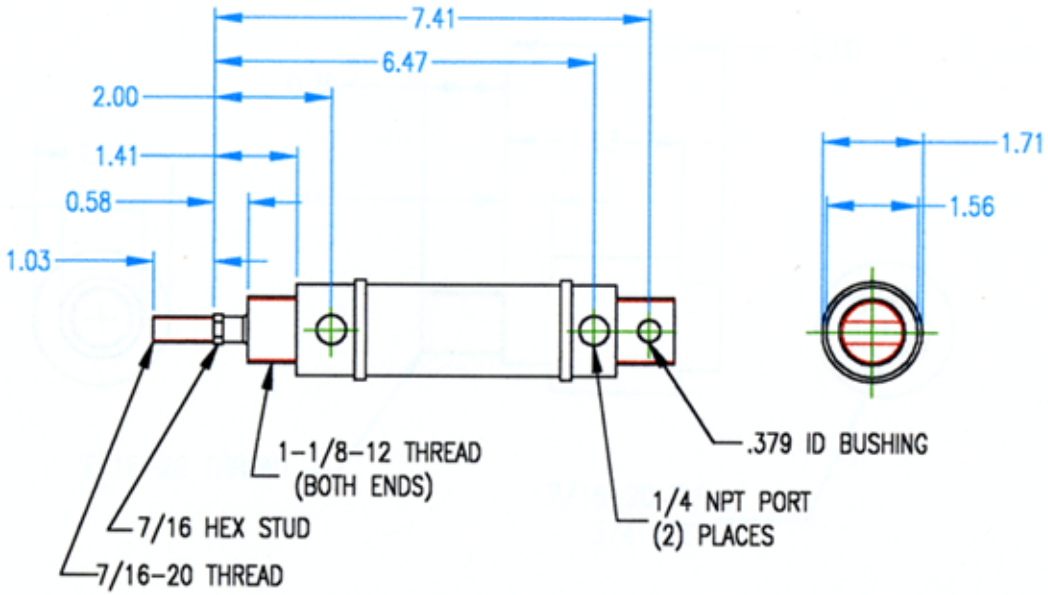

VENDOR:

BIMBA
P/N H-172-HUZ
1.5" BORE HYDRAULIC CYLINDER
2" STROKE
ALUMINUM PISTON AND ENDCAPS
PUSH FORCE = 1.77 X PSI
PULL FORCE = 1.57 X PSI

M	LTR	CHANGE	BY	DATE	CHK'D

ENGLISH DWG.
UNLESS OTHERWISE SPECIFIED, DIM ARE IN INCHES.
TOL. .XX ± .015
.XXX ± .005
ANGLES ± 1°
CHAMFERS & C'SINKS 45°
SURFACE ROUGHNESS IS IN MICROINCHES. √
REMOVE ALL BURRS
BREAK SHARP EDGES

PROPORTIONAL FUEL INJECTOR — 2/06/01
RELEASED FOR — DATE

VIRGINIA POLYTECHNIC INSTITUTE & SU
BLACKSBURG VA 24060

TITLE
HYDRAULIC CYLINDER 1.5" BORE.

REPRO MADE FROM

SCALE NONE — SIMILAR TO

FIRST MADE FOR — SUP.

DRAWN	CHECKED	APPROVED	SUP. BY	SHEET 1 OF 1
BY RRB	BY RRB	BY RRB		B-0001
DATE 2/06/01	DATE 2/06/01	DATE 2/06/01		

B-0004

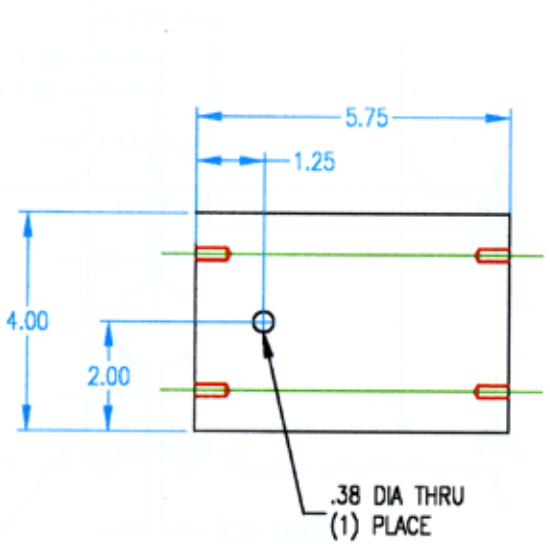

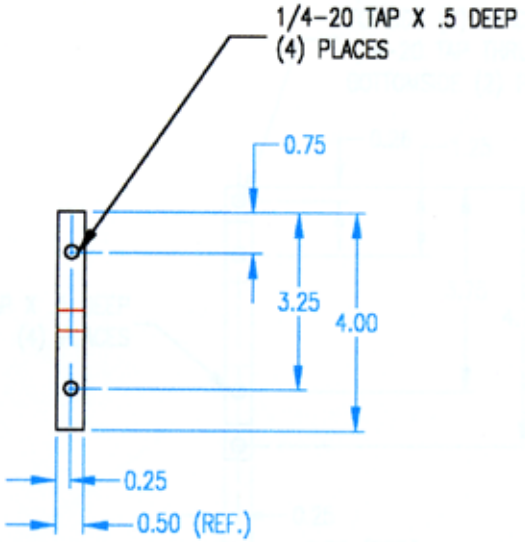

MATERIAL:

1/2" 2024 ALUMINUM PLATE

M	LTR	CHANGE	BY	DATE	CHK'D

ENGLISH DWG.
UNLESS OTHERWISE SPECIFIED, DIM ARE IN INCHES.
TOL .XX ± .015
.XXX ± .005
ANGLES ± 1°
CHAMFERS & C' SINKS 45°
SURFACE ROUGHNESS IS IN MICROINCHES. ✓
REMOVE ALL BURRS BREAK SHARP EDGES

PROPORTIONAL FUEL INJECTOR — 4/01/01
RELEASED FOR — DATE

VIRGINIA POLYTECHNIC INSTITUTE & SU
BLACKSBURG VA 24060

TITLE
PLATE PIEZO SUPPORT

REPRO MADE FROM

SCALE NONE — SIMILAR TO

FIRST MADE FOR — SUP.

DRAWN	CHECKED	APPROVED	SUP. BY	SHEET 1 OF 1
BY RRB	BY RRB	BY RRB		
DATE 4/01/01	DATE 4/01/01	DATE 4/01/01		B-0004

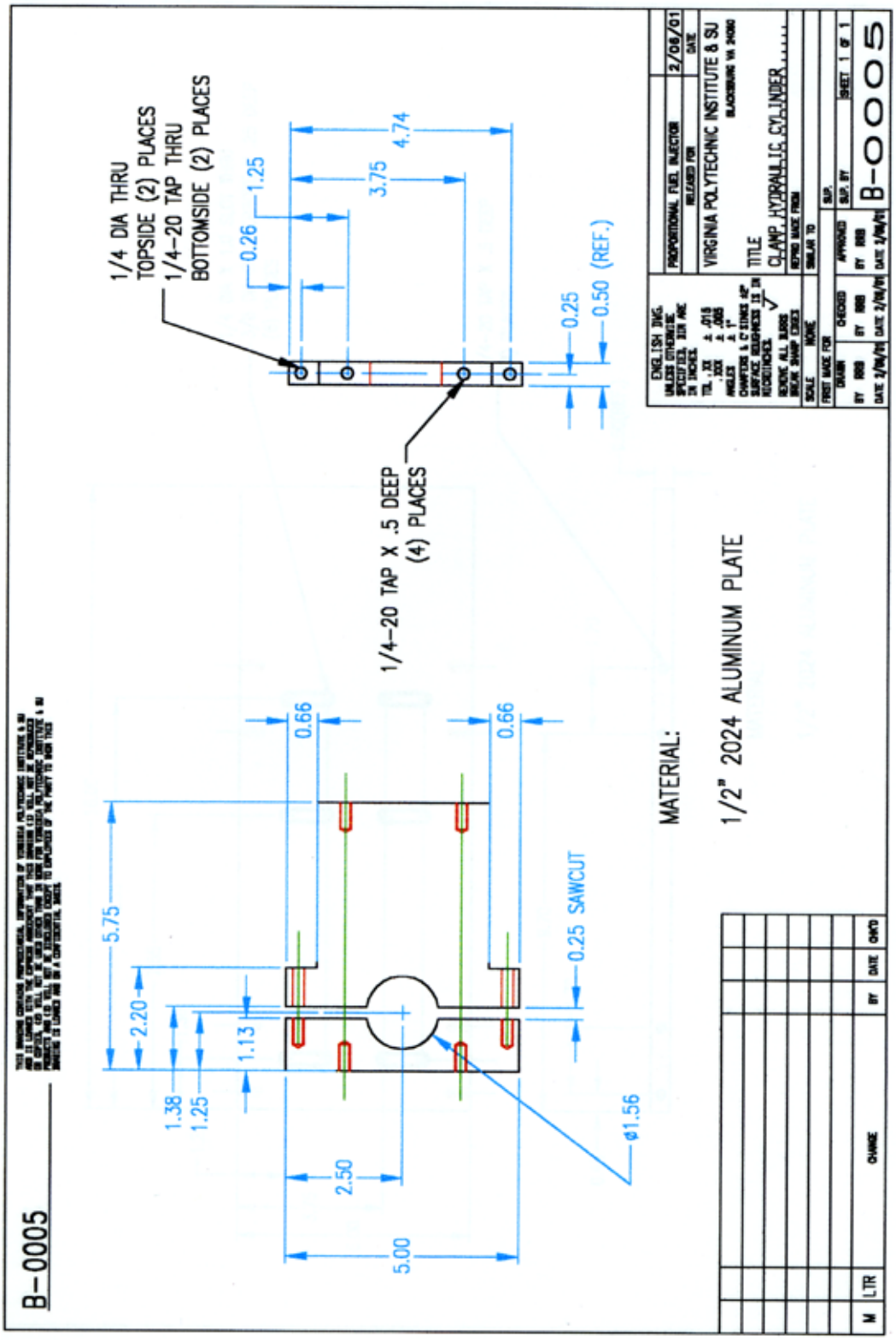
B-0005
1/4 DIA THRU
TOPSIDE (2) PLACES
1/4-20 TAP THRU
BOTTOMSIDE (2) PLACES
1/4-20 TAP X .5 DEEP
(4) PLACES
MATERIAL:
1/2" 2024 ALUMINUM PLATE
0.25 SAWCUT
ø1.56
5.75
2.20
1.38
1.25
1.13
0.66
0.66
2.50
5.00
0.26
1.25
3.75
4.74
0.25
0.50 (REF.)
PROPORTIONAL FUEL INJECTOR
2/06/01
VIRGINIA POLYTECHNIC INSTITUTE & SU
TITLE
CLAMP, HYDRAULIC CYLINDER
B-0005
SHEET 1 OF 1

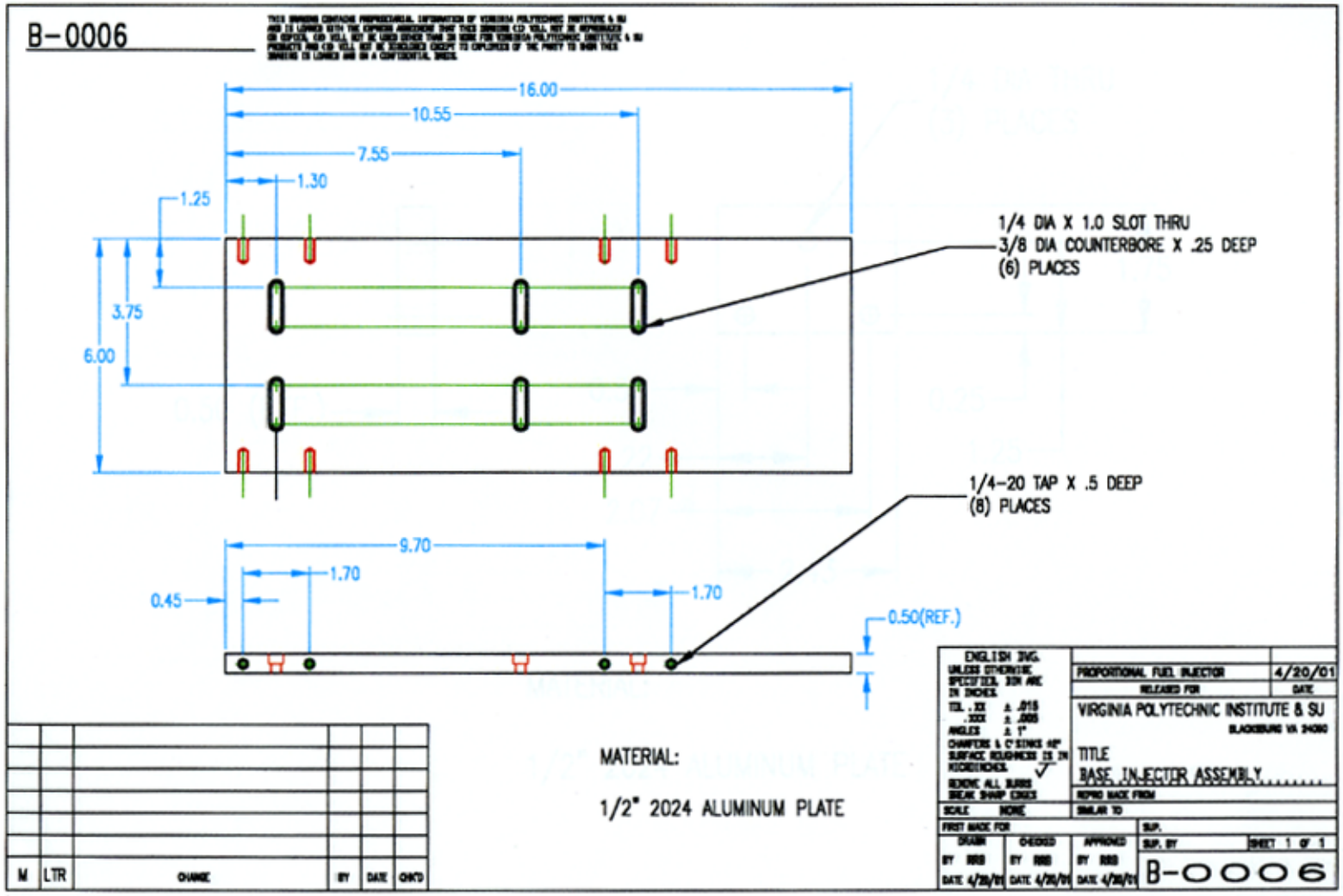
B-0006
16.00
10.55
7.55
1.30
1.25
3.75
6.00
1/4 DIA X 1.0 SLOT THRU
3/8 DIA COUNTERBORE X .25 DEEP
(6) PLACES
1/4-20 TAP X .5 DEEP
(8) PLACES
9.70
1.70
1.70
0.45
0.50(REF.)
MATERIAL:
1/2" 2024 ALUMINUM PLATE
PROPORTIONAL FUEL INJECTOR
4/20/01
VIRGINIA POLYTECHNIC INSTITUTE & SU
TITLE
BASE, INJECTOR ASSEMBLY
B-0006

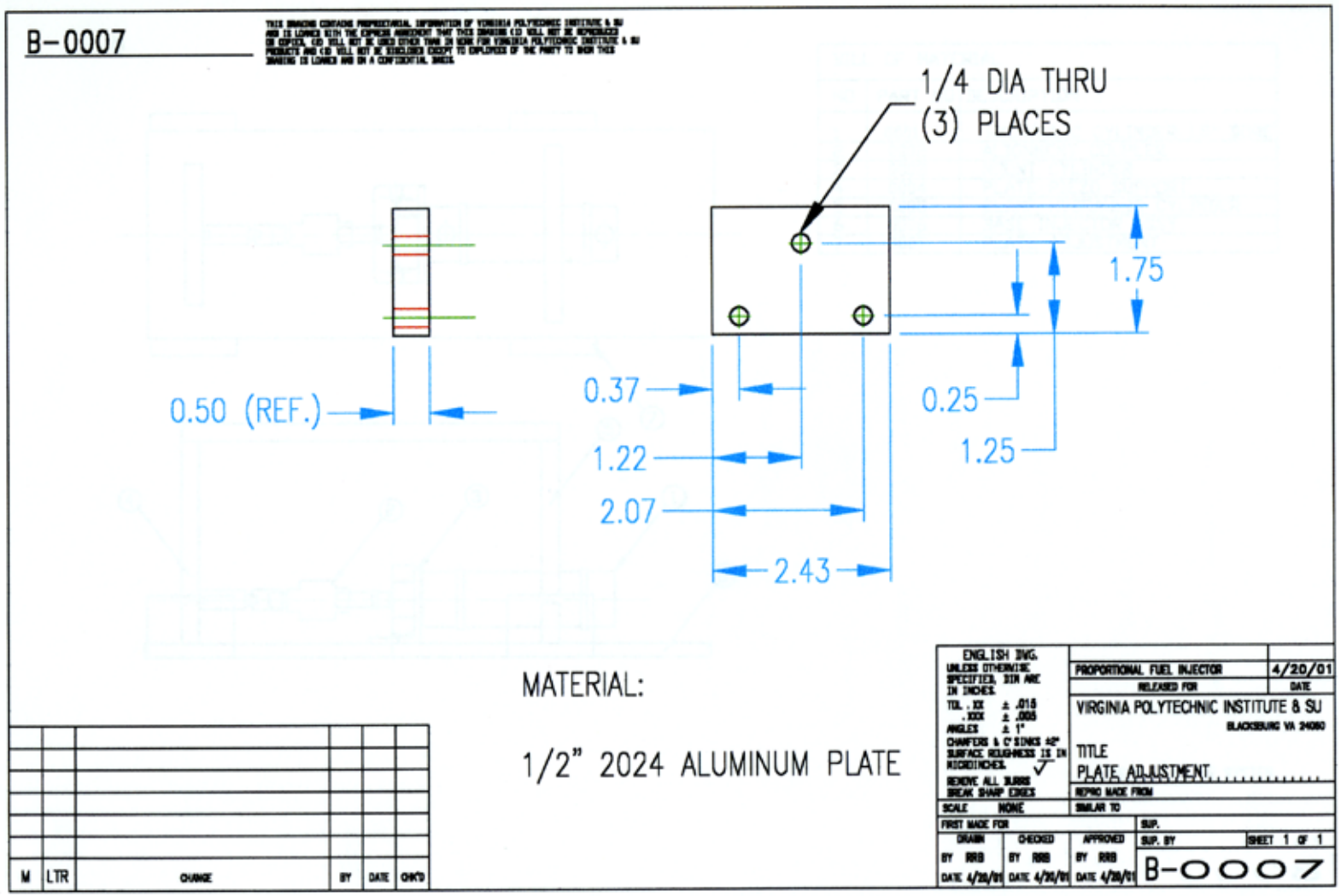
B-0007
1/4 DIA THRU
(3) PLACES
1.75
0.50 (REF.)
0.37
0.25
1.22
1.25
2.07
2.43
MATERIAL:
1/2" 2024 ALUMINUM PLATE
ENGLISH DWG.
PROPORTIONAL FUEL INJECTOR
4/20/01
VIRGINIA POLYTECHNIC INSTITUTE & SU
BLACKSBURG VA 24060
TITLE
PLATE ADJUSTMENT
SCALE NONE
SHEET 1 OF 1
B-0007
M LTR CHANGE BY DATE CHK'D

B-0008

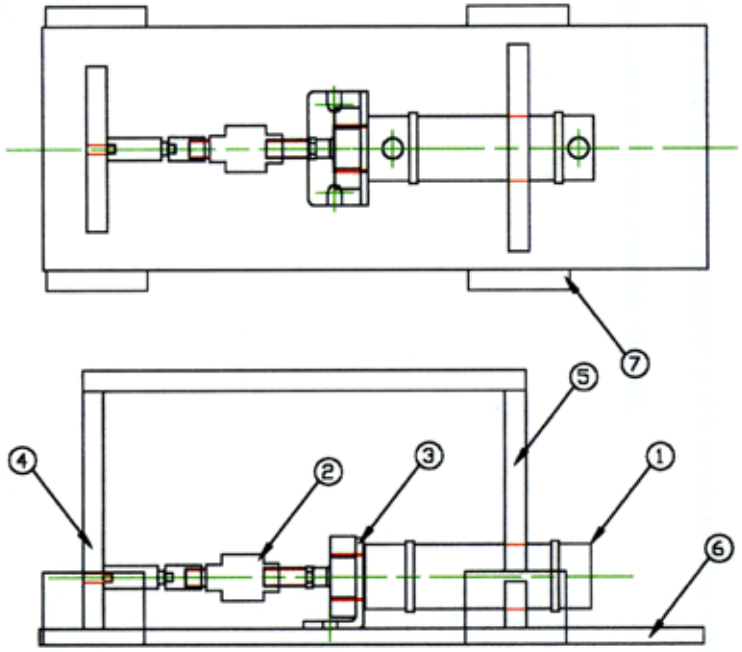

BILL OF MATERIAL		
NO	PART NO	DESCRIPTION
1	0001	HYDRAULIC CYLINDER 1.5" BORE
2	0002	ALIGNMENT COUPLER
3	0003	MOUNT CYLINDER
4	0004	PLATE PIEZO SUPPORT
5	0005	CLAMP HYDRAULIC CYLINDER
6	0006	BASE INJECTOR ASSY
7	0007	PLATE ADJUSTMENT

M	LTR	CHANGE	BY	DATE	CHK'D

ENGLISH DWG.
UNLESS OTHERWISE SPECIFIED, DIM ARE IN INCHES.
TOL. .XX ± .015
.XXX ± .005
ANGLES ± 1°
CHAMFERS & C'SINKS 82°
SURFACE ROUGHNESS 32 IN MICROINCHES ✓
REMOVE ALL BURRS
BREAK SHARP EDGES

SCALE NONE

FIRST MADE FOR

PROPORTIONAL FUEL INJECTOR — 4/26/01
RELEASED FOR — DATE

VIRGINIA POLYTECHNIC INSTITUTE & SU
BLACKSBURG VA 24060

TITLE
ASSEMBLY INJECTOR SYSTEM

REPRO MADE FROM

SIMILAR TO

SUP.

DRAWN	CHECKED	APPROVED	SUP. BY	SHEET 1 OF 1
BY RRB	BY RRB	BY RRB		
DATE 4/26/01	DATE 4/26/01	DATE 4/26/01	B-0008	

Vita

Ernie Lagimoniere was born on November 9, 1977 in Washington D.C. He lived in Huntingtown Maryland until the age of 17. After graduating from Northern High School in June 1995, he began his undergraduate degree at Virginia Tech in Mechanical Engineering. During his time at Virginia Tech he participated in the honors program as well as several academic and non-academic extracurricular activities. In May of 1999 Ernie graduated Magna Cum Laude with a B.S. degree in Mechanical Engineering. After his graduation he took a year sabbatical at his home in Maryland where he met his beautiful wife and was married in May 2000. Shortly after, Ernie entered into his graduate study at Virginia Tech. His graduate work involved the design, construction and characterization of a high bandwidth proportional fuel injection system for use in liquid fuel active combustion control. Fifteen months after beginning his graduate study he successfully defended his thesis. His future plans include beginning a career, purchasing a home and cherishing his family.